

Aus dem
Institut für Prophylaxe und Epidemiologie der Kreislaufkrankheiten
der Ludwig-Maximilians-Universität München
Campus Innenstadt
Direktor: Prof. Dr. Christian Weber

**Der Einfluss der neutrophilen Granulozyten und des zirkadianen
Rhythmus auf die Wundheilung nach einem Myokardinfarkt**

Dissertation
zum Erwerb des Doktorgrades der Medizin
an der Medizinischen Fakultät der
Ludwig-Maximilians-Universität zu München

vorgelegt von
Maximilian J. Schloss
aus Heidelberg, Baden-Württemberg, Deutschland

2018

Mit Genehmigung
der Medizinischen Fakultät der Universität München

Berichterstatterin: Prof. Dr. rer. nat. Sabine Steffens

Mitberichterstatter: Prof. Dr. rer. nat. Christoph Scheiermann
Prof. Dr. med. Stefan Endres
Prof. Dr. med. Christian Schulz

Mitbetreuung durch den
promovierten Mitarbeiter: Dr. Michael Horckmans (PhD)

Dekan: Prof. Dr. dent. med. Reinhard Hickel

Tag der mündlichen Prüfung: 17.05.2018

Eidesstattliche Versicherung

Schloss, Maximilian

Name, Vorname

Ich erkläre hiermit an Eides statt,
dass ich die vorliegende Dissertation mit dem Thema
Der Einfluss der neutrophilen Granulozyten und des zirkadianen Rhythmus auf die Wundheilung nach einem Myokardinfarkt

selbständig verfasst, mich außer der angegebenen keiner weiteren Hilfsmittel bedient und alle Erkenntnisse, die aus dem Schrifttum ganz oder annähernd übernommen sind, als solche kenntlich gemacht und nach ihrer Herkunft unter Bezeichnung der Fundstelle einzeln nachgewiesen habe.

Ich erkläre des Weiteren, dass die hier vorgelegte Dissertation nicht in gleicher oder in ähnlicher Form bei einer anderen Stelle zur Erlangung eines akademischen Grades eingereicht wurde.

München, den 22.05.2018

Ort, Datum

Unterschrift Doktorandin/Doktorand

Inhaltsverzeichnis

1. Abkürzungsverzeichnis	5
2. Publikationsliste	6
2.1 Veröffentlichungen der kumulativen Promotion	6
2.2 Weitere Veröffentlichungen	6
2.3 Wissenschaftliche Präsentationen der Ergebnisse der Dissertation	7
3. Einleitung	8
3.1 Neutrophile Granulozyten und ihre Rolle in der akuten Entzündung	8
3.2 Die Pathophysiologie des akuten Myokardinfarkts und die Rolle der neutrophilen Granulozyten	11
3.3 Der zirkadiane Rhythmus und sein Einfluss auf die Immunzellen-Homöostase	16
3.4 Der Einfluss des zirkadianen Rhythmus auf die Wundheilung nach Myokardinfarkt	19
4. Zusammenfassung	21
4.1 Zusammenfassung auf Deutsch	21
4.2 Zusammenfassung auf Englisch	22
5. Veröffentlichung I	24
<i>Neutrophils orchestrate post-myocardial infarction healing by polarizing macrophages towards a reparative phenotype.</i>	
6. Veröffentlichung II	49
<i>The time-of-day of myocardial infarction onset affects healing through oscillations in cardiac neutrophil recruitment.</i>	
7. Literaturverzeichnis	66
8. Danksagung	69

1. Abkürzungsverzeichnis (alphabetisch geordnet)

AAR	Area at risk
CCL	Chemokine ligand
CK-MB	Creatine kinase muscle-type
CXCL	Chemokine ligand
CXCR	Chemokine receptor
DNA	Deoxyribonucleic acid
G-CSF	Granulocyte colony stimulating factor
GMP	Granulocyte-macrophage progenitor
ICAM	Intercellular adhesion molecule
NGAL	Neutrophil gelatinase-associated lipocalin
NSC	Nucleus suprachiasmaticus
MERTK	Myeloid-epithelial-reproductive tyrosine kinase
MI	Myocardial infarction
MMP	Matrix metalloproteinase
ROS	Reactive oxygen species
TUNEL	TdT-mediated dUTP-biotin nick end labeling
VCAM	Vascular cell adhesion protein
ZT	Zeitgeber time

2. Publikationsliste

2.1 Veröffentlichungen der kumulativen Promotion:

Michael Horckmans, Larisa Ring, Johan Duchene, Donato Santovito, **Maximilian J Schloss**, Maik Drechsler, Christian Weber, Oliver Soehnlein, Sabine Steffens. *Neutrophils orchestrate post-myocardial infarction healing by polarizing macrophages towards a reparative phenotype.* **European Heart Journal.** Januar 2017; 38(3): 187-97.

Maximilian J Schloss, Michael Horckmans, Katrin Nitz, Johan Duchene, Maik Drechsler, Kiril Bidzhekov, Christoph Scheiermann, Christian Weber, Oliver Soehnlein, Sabine Steffens. *The time-of-day of myocardial infarction onset affects healing through oscillations in cardiac neutrophil recruitment.* **EMBO Molecular Medicine.** August 2016; 8(8): 937-48.

2.2 Weitere Veröffentlichungen:

Maximilian J Schloss, Michael Hilby, Katrin Nitz, Raquel Guillamat Prats, Bartolo Ferrero, Giovanna Leoni, Thorsten Kessler, Michael Horckmans, Bruno Luckow, Christian Weber, Johan Duchene, Sabine Steffens. *Ly6C^{high} monocytes oscillate in the heart during homeostasis and after myocardial infarction.* **Arteriosclerosis, Thrombosis, and Vascular Biology.** September 2017; 37(9): 1640-5.

Sabine Steffens, Carla Winter, **Maximilian J Schloss**, Andres Hidalgo, Christian Weber, Oliver Soehnlein. *Circadian control of inflammatory processes in atherosclerosis and its complications.* **Arteriosclerosis, Thrombosis, and Vascular Biology.** Juni 2017; 37(6): 1022-8. (Übersichtsarbeit)

Maximilian J Schloss,* Michael Horckmans,* Christian Weber, Sabine Steffens. *2-arachidonoylglycerol mobilizes myeloid cells via cannabinoid receptor CB2 and promotes their cardiac recruitment.* (*geteilte Erstautorenschaft; Manuskript in Revision)

2.3 Wissenschaftliche Präsentationen der Ergebnisse der Dissertation

- April 2017 Hatter Institute for Cardiovascular Research in Africa in Kapstadt, Südafrika
Does the time-of-day of ischemia onset affect myocardial infarction healing through oscillations in cardiac leukocyte recruitment?
(40-minütiger Vortrag im Journal Club)
- April 2016 82. Jahrestagung der Deutschen Gesellschaft für Kardiologie in Mannheim
2-arachidonolglycerol levels modulate cardiac neutrophil recruitment and healing after myocardial infarction.
(10-minütiger Vortrag in der Keynote Session)
- September 2015 3. Young Retreat des Deutschen Zentrums für Herz- und Kreislauftforschung in Potsdam
The time-of-day of ischemia onset affects myocardial infarction healing and heart function through oscillations in neutrophil mobilization.
(10-minütiger Vortrag)
- Juli 2015 Summer Meeting der Munich Heart Alliance in München
The time-of-day of ischemia onset affects myocardial infarction healing and heart function through oscillations in neutrophil mobilization.
(Poster Präsentation)
- Juni 2015 Gordon Research Conference, Atherosclerosis Meeting in Maine, USA
The time-of-day of ischemia onset affects myocardial infarction healing and heart function through oscillations in neutrophil mobilization.
(Poster Präsentation)
- April 2015 81. Jahrestagung der Deutschen Gesellschaft für Kardiologie in Mannheim
The Role of circadian rhythm in post-myocardial infarction healing.
(10-minütiger Vortrag)
- Februar 2015 Winter Meeting der Munich Heart Alliance in München
The Role of circadian rhythm in post-myocardial infarction healing.
(Poster Präsentation)

3. Einleitung

3.1 Neutrophile Granulozyten und ihre Rolle in der akuten Entzündung

Die Aufgabe des Immunsystems ist die Sicherstellung der Abwehr gegenüber Infektionen und die Initiierung von Wundheilungsprozessen (1). Grundsätzlich lässt sich das angeborene von dem erworbenen Immunsystem unterscheiden. Zu dem angeborenen Immunsystem gehören verschiedene Zellreihen wie neutrophile Granulozyten, Makrophagen, Monozyten und dendritische Zellen. Diese Zellen sind von Geburt an vollständig funktionsfähig; es sind die ersten Zellen, die auf eine Entzündung reagieren können. Davon abgrenzen ist das erworbene Immunsystem, welches aus B- und T-Lymphozyten besteht. Lymphozyten müssen einen komplexen Reifeprozess durchlaufen; sie sind erst bei wiederholtem Kontakt mit Pathogenen funktionsfähig und reagieren somit spezifisch auf pathogene Keime (2). Neuere Forschungen deuten darauf hin, dass es keine scharfe Abgrenzung zwischen den beiden Immunsystemen gibt, da zunehmende Evidenz für eine starke Interaktion und Interdependenz beider Systeme spricht (3).

Neutrophile Granulozyten machen beim Menschen 70% der Leukozyten im Blut aus und sind damit numerisch die häufigsten „Immunzellen“ im Blut. Bei der Maus sind die Lymphozyten die häufigsten Zellen im Blut, wohingegen Neutrophile mit 30% der Leukozyten die zweit häufigste Population darstellen. Die Lebenszeitspanne der Neutrophilen wird unter Homöostase auf etwa 6-8 Stunden geschätzt; damit gehören diese zu den Zellen mit der kürzesten Lebenszeit im menschlichen Körper. Durch ein Entzündungsgeschehen aktivierte Neutrophile haben eine längere Lebenszeit (4, 5). Neutrophile Granulozyten werden im Knochenmark gebildet und dort über einen Chemokin-regulierten Prozess in das Blut abgegeben. Unter Homöostase verweilen 98% der Neutrophilen (120 Millionen Zellen) im Knochenmark und lediglich 2% zirkulieren (<2,5 Millionen Zellen) im System (5, 6). Reife neutrophile Granulozyten befinden sich innerhalb des Knochenmarks in hämatopoetischen Inseln und sind durch das sinusoidale Endothel vom Blutfluss getrennt. Werden Neutrophile ins Blut mobilisiert, so müssen sie durch das sinusoidale Endothel in das Gefäßlumen migrieren. CXC-Motiv-Chemokinligand 12 (CXCL12) ist ein Chemokin, welches in hoher Konzentration im Knochenmark unreife Neutrophile zurückhält. Sein Rezeptor, CXC-Motiv-Chemokinrezeptor 4 (CXCR4), wird von reifen Neutrophilen nur wenig exprimiert, sodass diese leichter ins Blut migrieren können (7). Alte Neutrophile, die sich über Stunden in der Zirkulation befinden, regulieren CXCR4 hoch und wandern somit wieder in das Knochenmark zurück, wo sie von lokalen Makrophagen eliminiert werden (7).

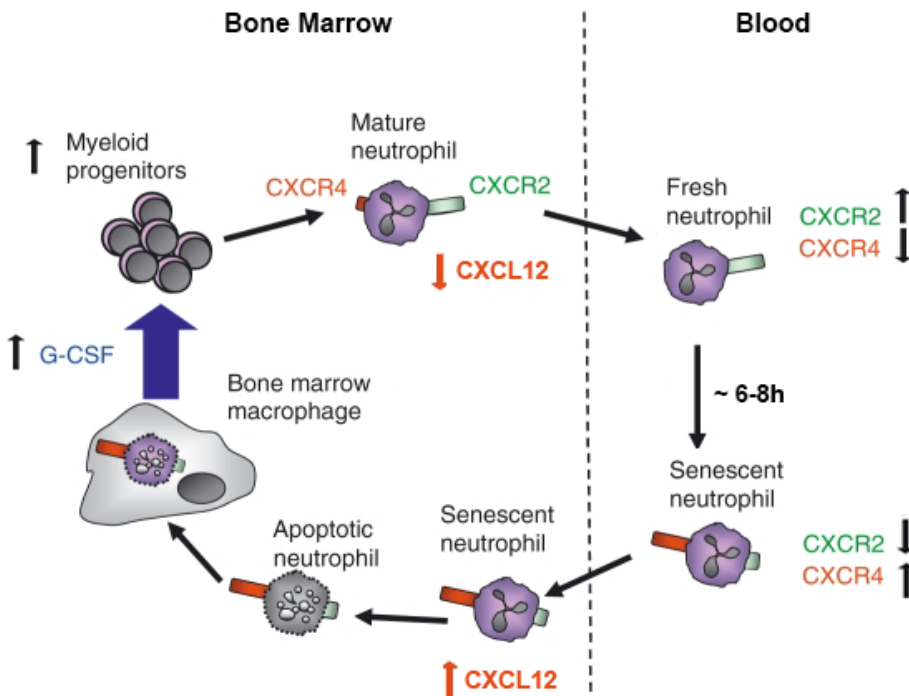


Abbildung 3.1.1: Produktion und Eliminierung von neutrophilen Granulozyten im Knochenmark unter Homöostase. G-CSF stimuliert die Produktion von Neutrophilen im Knochenmark. Niedrige CXCL12 Konzentrationen im Knochenmark und eine hohe CXCR2 Expression auf jungen Neutrophilen erleichtern deren Mobilisation aus dem Knochenmark in das Blut. Reife, im Blut zirkulierende Neutrophile erhöhen ihre CXCR4 Expression und migrieren somit leichter ins Knochenmark zurück, wo sie von Makrophagen eliminiert werden. Diese Makrophagen produzieren wiederum G-CSF und damit beginnt der Kreislauf von Neuem. Überarbeitete Abbildung (5).

Das Knochenmark ist eine stets einsatzbereite Neutrophilen-Reserve, die im Falle einer Infektion mobilisiert werden kann. Dies führt dazu, dass sich die Neutrophilenzahlen im Blut innerhalb von Stunden verzehnfachen können. Kommt es zu einer Entzündung in einem Gewebe, so werden Chemokine und Zytokine ins Blut ausgeschüttet: G-CSF senkt im Knochenmark die CXCL12 Konzentration, wodurch Neutrophile leichter mobilisiert werden können. Zusätzlich stimuliert G-CSF die Granulopoese, sodass Neutrophile nachproduziert werden. CXCL1, CXCL2 und CXCL5 werden von Zellen, die sich im entzündeten Gewebe befinden, in das Plasma ausgeschüttet, wodurch ein chemotaktischer Gradient zwischen dem Blut und dem Knochenmark aufgebaut wird. Neutrophile Granulozyten folgen dem Ort der höheren *Chemokinkonzentration* und migrieren durch sinusoidale Endothel in das Blut. Der Rezeptor für Neutrophilen-mobilisierende Chemokine CXCL1, CXCL2 und CXCL5 ist der CXC-Motiv-Chemokinrezeptor 2 (CXCR2), welcher auf der Zelloberfläche der Granulozyten exprimiert ist und über intrazelluläre Signaltransduktionskaskaden mittels Gi-Proteinen seine

Funktion vermittelt. Die Zahl der Chemokinrezeptoren ist für die oben beschriebene Mobilisierung aus dem Knochenmark und die Rekrutierung hin zu einem inflammatorischen Geschehen entscheidend (8).

Die zentrale Aufgabe der neutrophilen Granulozyten ist die Verteidigung des Organismus gegenüber Mikroorganismen. Dafür stehen den neutrophilen Granulozyten zwei Mechanismen zur Verfügung: 1. die Phagozytose des Mikroorganismus und 2. die Sekretion von antimikrobiotischen Granula wie Myeloperoxidase, Defensine und Lysosine. Im Prozess der Verteidigung gegen Mikroorganismen kommt es zu einem Kollateralschaden des Wirts in Form einer Gewebeschädigung (9, 10). Damit dieser möglichst gering gehalten wird, ist eine engmaschige Kontrolle über diesen Vorgang essentiell, und der menschliche Körper hat dafür ausgefeilte Kontrollmechanismen entwickelt: Er reguliert den kontrollierten Zelltod, die sogenannte Apoptose, und nimmt Einfluss auf die Rekrutierung und Produktion weiterer inflammatorischer Zellen über Chemokin- und Zytokin-Kaskaden (5). Greifen diese Kontrollmechanismen nicht, kommt es zu einer übertriebenen inflammatorischen Reaktion des Körpers, die eine massive Schädigung des Wirts zu Folge haben kann. Neben der mikrobiellen Infektion gibt es noch die sterile Inflammation. Diese beschreibt eine Situation, in der der Stimulus der inflammatorischen Reaktion steriler Natur, also nicht infektiös, ist. Ein klinisch relevantes Beispiel hierfür wäre der akute Myokardinfarkt.

Lange nach der Entdeckung der neutrophilen Granulozyten galten diese als eher unspezifisch und primitiv in ihrem Verhalten. In den letzten Jahren hat ihnen die Forschung jedoch ein immer komplexeres Verhalten zugesprochen. In diesem Kontext ist beispielsweise die Fähigkeit der Neutrophilen zu erwähnen, „neutrophile extrazelluläre Fallen“ zu bilden, die aus extrazellulären DNA-Fasern bestehen und dort Pathogene binden können (11, 12).

Des Weiteren wurde festgestellt, dass neutrophile Granulozyten weitere Immunzellen wie Monozyten, Makrophagen, dendritische Zellen und Lymphozyten über eigens produzierte und sekretierte Chemokine und Zytokine rekrutieren können (13). Aus experimentellen Studien ist bekannt, dass neutrophile Granulozyten den Weg für klassische Monozyten ebnen, indem sie Chemokine wie CC-chemokine ligand 2 (CCL2), CCL3 und CCL19/20 ins Blut ausschütten und damit Monozyten aus dem Knochenmark und der Milz mobilisieren (14). Im Entzündungsherd, dem Ort der höchsten Chemokinkonzentration, angekommen, differenzieren sich die Monozyten zu Makrophagen. Welche Rolle die neutrophilen Granulozyten bei diesem Differenzierungsprozess spielen ist bislang unklar.

3.2 Die Pathophysiologie des akuten Myokardinfarktes und die Rolle der neutrophilen Granulozyten

Ein Myokardinfarkt ist definiert als akute Minderversorgung des Myokards mit Blut und den darin befindlichen Nährstoffen. Der häufigste Grund für eine Einschränkung der Myokarddurchblutung sind präformierte arteriosklerotische Koronararterien (15). In diesen pathologisch veränderten Gefäßwänden können sich arteriosklerotische Plaques lösen, was zur Folge hat, dass gerinnungsinduzierende Faktoren Kontakt mit dem Blut erhalten. Dadurch bilden sich an der Läsionsstelle Blutgerinnsel, die das Gefäßlumen akut verstopfen können (16). In dem vom Blutfluss abgetrennten Myokardbereich entsteht ein Mangel an Sauerstoff und Nährstoffen, der zum Absterben von Kardiomyozyten führt. Um diesen irreversiblen Schaden möglichst gering zu halten, ist innerhalb der Myokardinfarkttherapie eine rasche Wiederherstellung des Blutflusses mittels perkutaner Koronarintervention entscheidend.

Das Absterben des Herzmuskelgewebes löst eine Entzündungsreaktion mit einer phasischen Rekrutierung von Immunzellen in das Herz aus: Neutrophile Granulozyten sind die ersten inflammatorischen Zellen, die wenige Stunden nach einem Myokardinfarkt aus dem Knochenmark ins Blut mobilisiert und von dort ins Herz rekrutiert werden. Etwa 24 Stunden nach einem Myokardinfarkt erreichen die Neutrophilen-Zahlen ihr Maximum und sind auch 48 Stunden danach noch in erhöhter Zahl im Herz zu finden. Am dritten bis fünften Tag nach einem Infarkt ist die Einwanderung der Monozyten am höchsten. Diese differenzieren sich nach ihrer Einwanderung zu Makrophagen (17). Nach sieben Tagen sind hauptsächlich Lymphozyten im Herz zu finden (18, 19).

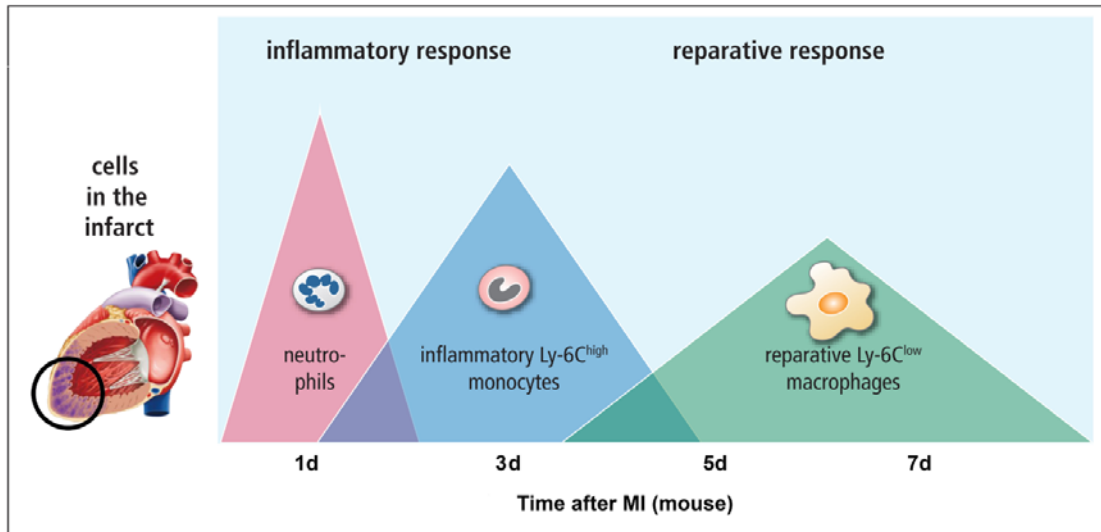


Abbildung 3.2.1: Phasische Rekrutierung von Immunzellen nach einem Myokardinfarkt im Mausmodell.

Während der inflammatorischen Phase in den ersten zwei Tagen nach einem Myokardinfarkt (MI) werden hauptsächlich neutrophile Granulozyten in das Herz rekrutiert. Ab dem dritten Tag beginnt die Reparaturphase, in der inflammatorische Monozyten (Ly6C^{high} monocytes) ins Herz rekrutiert werden und sich dort zu nicht-inflammatorischen Makrophagen (Ly6C^{low} macrophages) differenzieren. Überarbeitete Abbildung (20, 21).

Sobald ischämische Kardiomyozyten absterben, werden von lokalen Makrophagen und Kardiomyozyten Chemokine und Zytokine (wie z.B. CXCL1, CXCL2 und CXCL5) ins Plasma sekretiert (22, 23). CXCL1, CXCL2 und CXCL5 sind die Liganden für den Chemokinrezeptor CXCR2 auf Neutrophilen, der die Mobilisierung aus dem Knochenmark und die Migration in das Herz ermöglicht. Die Regulierung dieses Prozesses wird durch die CXCR2 Expressionsstärke ermöglicht, die im Falle einer Entzündung ansteigen kann (24). Im ischämischen Herzen haben neutrophile Granulozyten eine wichtige Funktion in der Beseitigung apoptotischer Kardiomyozyten, indem sie diese phagozytieren. Des Weiteren schütten sie Enzyme wie Matrix-Metalloproteasen (MMP) und radikale Sauerstoffmoleküle (ROS) aus, die lokal die Entzündung verstärken (25). Über sekretierte Zytokine und Chemokine locken sie weitere Leukozyten, wie z.B. klassische Monozyten, ins Herz.

Der nicht durchblutete Myokardbereich, der nach der Okklusion des Koronargefäßes von der Ischämie betroffen ist, nennt sich „area at risk“ (AAR). Der Infarktbereich breitet sich innerhalb von Stunden in der AAR aus; das Ausmaß, zu welchem Anteil die AAR Infarktnarbe wird, hängt von der Qualität der Kompensationsmechanismen (Eindämmung der Entzündung, Kollateralenfluss, kardialer Metabolismus etc.) ab. Pathophysiologisch wird das Infarktgewebe nach einer Woche zu einer fibrotischen Narbe umgebaut und neue Gefäße wachsen vom Randbereich in die Narbe ein.

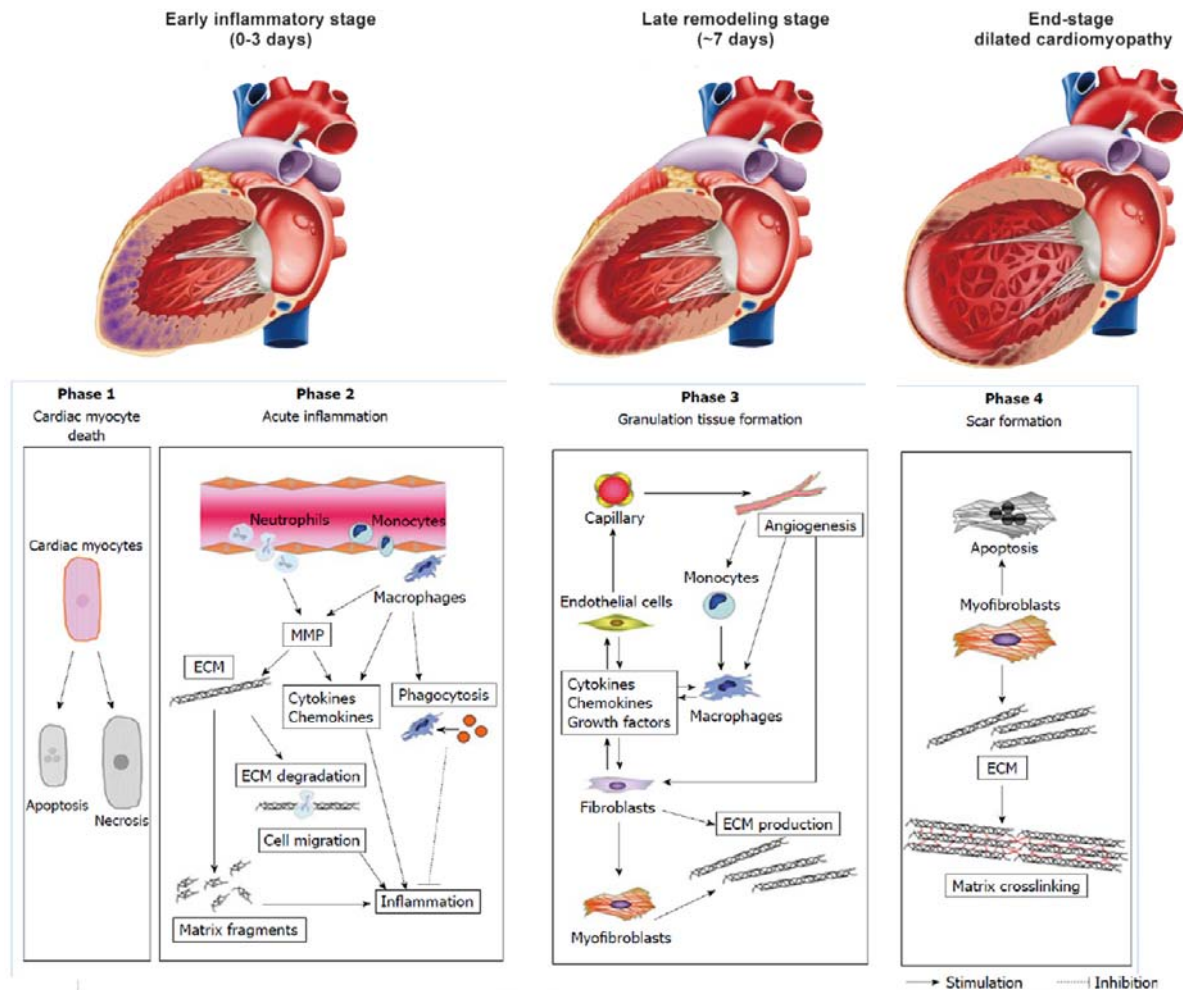


Abbildung 3.2.2: Pathophysiologie des akuten Myokardinfarktes. 24 Stunden nach Myokardinfarkt gehen ischämische Kardiomyozyten in Apoptose oder Nekrose. Dies löst in den ersten 72 Stunden eine Entzündungsreaktion aus, in der Neutrophile und Monozyten die Entzündung amplifizieren, indem sie Matrixmetalloproteine (MMP), Zytokine und Chemokine ausschütten. Nach etwa einer Woche wachsen Gefäße vom Randbereich des Infarktes in das Zentrum ein (Angiogenese). Myofibroblasten produzieren eine extrazelluläre Matrix (ECM), aus der eine fibrotische Narbe entsteht. Überarbeitete Abbildung (21, 25).

Eine ausgewogene Balance aus Entzündungsinduktion und Entzündungshemmung ist notwendig, um eine adäquate Wundheilung zu gewährleisten. Eine erhöhte Zahl an neutrophilen Granulozyten im Blut von Patienten mit einem Myokardinfarkt führt zu einer mangelhaften Wundheilung mit Komplikationen wie Herzinsuffizienz und Herzrupturen (26). In Anwesenheit einer extremen Anzahl an Neutrophilen produzieren Kardiomyozyten und Fibroblasten mehr Kollagen, sodass sich die Infarktnarbe vergrößert. Eine größere Infarktnarbe schränkt die Herzfunktion ein. Dadurch entsteht ein erhöhter intraventrikulärer Druck, der das Risiko einer Herzruptur bedingt.

The diagram shows a horizontal gradient from orange on the left to red on the right, representing increasing myofibroblast density. Below this gradient, there is a table with four columns corresponding to different levels of density.

	Myofibroblast density		
Scar properties	Weak Poorly structured Expansive	Strong Flexible Contracted	Strong Rigid Contracted
Short term consequences	Ventricular dilatation Ventricular wall thinning Systolic dysfunction Cardiac rupture	Well managed	Myocardial stiffness Systolic dysfunction Diastolic dysfunction
Longer term consequences	LV hypertrophy Reactive fibrosis Reduced cardiac output Arrhythmia Heart Failure	Well managed	LV hypertrophy Reactive fibrosis Reduced cardiac output Arrhythmia Heart Failure

Abbildung 3.2.3: Die Beschaffenheit der fibrotischen Narbe nach einem Myokardinfarkt beeinflusst die Herzfunktion und Komplikationsrate. Eine zu geringe Dichte an Myofibroblasten nach einem Myokardinfarkt führt zu einer unzureichenden Vernarbung des Infarktareals, die eine ventrikuläre Dilatation verursacht und das Risiko von Herzrupturen erhöht. Demgegenüber führt eine pathologisch erhöhte Dichte an dicken Kollagenfasern im Narbenbereich zu einem steifen Myokard mit eingeschränkter systolischer und diastolischer Herzfunktion (27).

Diese Ergebnisse deuten darauf hin, dass die ersten Stunden nach einem Myokardinfarkt entscheidend für das Ausmaß der Ausdehnung des Infarktbereichs und die Tage später stattfindende Wundheilung sind. Auf Grund dieser Problematik ist eine positive Beeinflussung der Inflammationsreaktion nach einem Myokardinfarkt, welche den Entzündungsschaden minimieren könnte, Ziel der kardiovaskulären Forschung. Unspezifische immunmodulatorische Therapien, wie etwa die Kortisontherapie nach einem akuten Myokardinfarkt, haben sich nicht durchsetzen können (28). Jedoch führte in experimentellen Studien eine spezifische Reduktion der Neutrophilen nach einem Myokardinfarkt zu einer besseren Wundheilung und Herzfunktion (29, 30).

Wir haben uns in der ersten Studie auf drei Hauptfragen konzentriert: 1. Welche Rolle spielen Neutrophile im Wundheilungsprozess nach akutem Myokardinfarkt? 2. Welchen Einfluss haben neutrophile Granulozyten auf die Rekrutierung von Monozyten in diesem Kontext? 3. Wie beeinflussen Neutrophile die lokale Makrophagen-Proliferation und deren Differenzierung in unterschiedliche Makrophagen-Subtypen? Um diese Fragen zu beantworten, haben wir neutrophile Granulozyten über einen spezifischen Antikörper in der Maus depletiert und mittels eines experimentellen Myokardinfarktmodells die Entzündungs-

und Wundheilungsprozesse nach einem induzierten Myokardinfarkt erforscht. Es zeigte sich, dass Neutrophilen-depletierte Mäuse im Vergleich zu ihren Isotyp-Kontrollen nach Infarkt eine eingeschränkte Wundheilung mit größerer Infarktnarbe und schlechterer Herzfunktion hatten. Depletierte Mäuse rekrutierten weniger inflammatorische Monozyten ($\text{Ly6C}^{\text{high}}$ Monozyten) ins infarzierte Herz. Zugleich befanden sich eine höhere Anzahl an Makrophagen im infarzierten Herzen, was hauptsächlich durch eine vermehrte lokale Proliferation bedingt war. Mechanistisch fanden wir heraus, dass Neutrophile die Expression des Phagozytose-Rezeptors MERTK (myeloid-epithelial-reproductive tyrosine kinase) auf der Makrophagenoberfläche erhöhten, sodass Neutrophilen-depletierte Mäuse eine größere Anzahl apoptotischer Zellen im Infarktbereich zeigten. Das von Neutrophilen sekretierte NGAL (neutrophil gelatinase-associated lipocalin) hatte bei diesem Prozess einen wesentlichen Einfluss, indem es die Differenzierung von Makrophagen mit reparativen Eigenschaften begünstigte. Diese durch NGAL induzierten reparativen Makrophagen waren besser in der Lage, apoptotische Zellen mittels Phagozytose abzubauen (31).

Zusammenfassend lässt sich festhalten, dass unsere Veröffentlichung einen bedeutenden Beitrag zum besseren Verständnis der komplexen Mitwirkung von neutrophilen Granulozyten an der systemischen und lokalen Entzündung nach Myokardinfarkt leistet. Darüber hinaus zeigt unsere Studie, dass eine vollständige Depletion von Neutrophilen zu einer eingeschränkten Wundheilung führt, sodass antiinflammatorische Therapieansätze mit Vorsicht eingesetzt werden sollten.

In der ersten Studie wirkte ich als Koautor bei der Entwicklung und Gestaltung des Projektes mit. Ich stand unterstützend bei der Durchführung von Versuchen (histologische Daten in Figure 3 A-H; Multiplex-Messungen in Figure 2 D-F und Figure 4 F-H) und bei der Diskussion der Ergebnisse zur Verfügung. Das Manuskript wurde von mir gegengelesen und vom Erst- sowie Letztautor in die endgültige Fassung gebracht.

3.3 Der zirkadiane Rhythmus und sein Einfluss auf die Immunzellen-Homöostase

Fast alle lebenden Organismen haben im Laufe der Evolution einen zirkadianen Rhythmus entwickelt, um sich an die Herausforderungen der Umwelt anzupassen. Das Wort zirkadian (lateinisch *circa* „ringsum“, *dies* „Tag“) weist auf einen Kreislauf hin, der sich fortwährend wiederholt. In den meisten Organismen ist dies ein 24-Stunden währender Kreislauf, der an die Umwelt angepasst werden kann. Die zirkadianen Rhythmen werden einerseits von Umweltfaktoren, den sogenannten Zeitgeber-Faktoren wie Licht, Nahrung, Temperatur und Umweltbedingungen, synchronisiert; andererseits gibt es biologische Rhythmen, die unabhängig von diesen Zeitgeber-Faktoren auf Zellebene existieren. Zirkadiane Rhythmen beeinflussen das Leben von Organismen maßgeblich, in dem sie aktive Phasen und Ruhephasen vorschreiben. Auf kleinster Ebene werden diese zirkadianen Rhythmen über molekulare Mechanismen reguliert, indem eine Vielzahl von Genen tageszeitpunktabhängig exprimiert wird (32-34).

Das Steuerungssystem des zirkadianen Rhythmus ist komplex: Als übergeordnete Instanz nimmt der *nucleus suprachiasmaticus* (NSC) über den retinohypothalamischen Trakt Licht auf. Das Licht wird auf neuronaler Ebene in ein elektrisches Signal umgewandelt und der Organismus wird entsprechend synchronisiert. Fast jede Zelle hat einen eigenen Rhythmus, der vom NSC moduliert werden kann (32). Die genauen Mechanismen, mit Hilfe derer der NSC dies ermöglicht, sind noch nicht vollständig geklärt. Man geht davon aus, dass humorale und neuronale Systeme dabei eine Schlüsselrolle spielen (35).

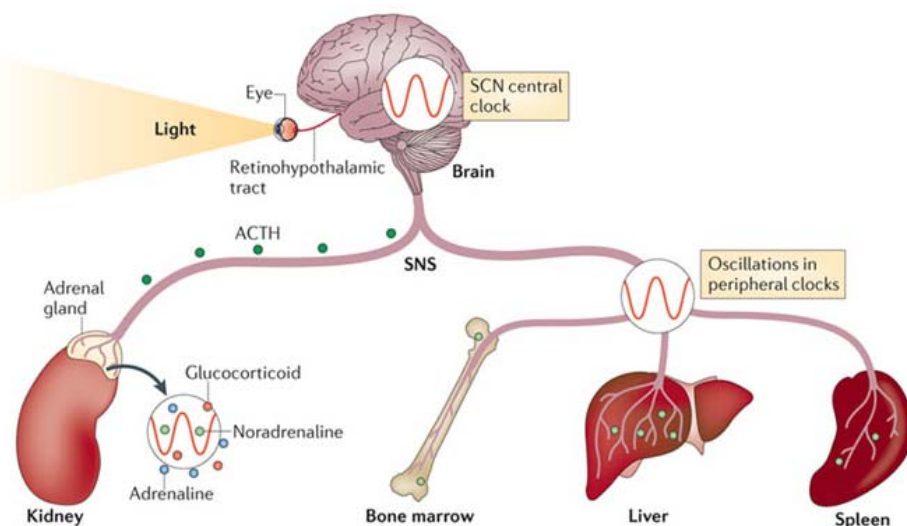


Abbildung 3.3.1: Das Steuerungssystem des zirkadianen Rhythmus. Der *nucleus suprachiasmaticus* (NSC) nimmt über den retinohypothalamischen Trakt Licht auf. Das Licht wird auf neuronaler Ebene verschaltet und der Organismus wird über humorale und nervale Mechanismen synchronisiert. Überarbeitete Abbildung (36).

Die Grundlagenforschung der letzten Jahre hat den Einfluss des zirkadianen Rhythmus auf verschiedene Organsysteme, wie z.B. das Immunsystem, untersucht. Es wurde gezeigt, dass die Hypophyse adrenokortikotrope Hormone und die Nebenniere Cortison sowie Katecholamine tageszeitabhängig ins Blut sekretieren (37). Wesentliche immunologische Schlüsselmoleküle wie beispielweise der Glukokortikoidrezeptor, pro- und antiinflammatorische Chemokine und der Toll-like-Rezeptor oszillieren im Tagesverlauf (38, 39). Silver et al. konnten in einem Mausmodell zeigen, dass der Toll-like-Rezeptor 9 auf verschiedenen Immunzellen und in der Milz zum Beginn der Aktivphase der Mäuse hochreguliert wird und deshalb eine Sepsis-Induktion zu dieser Tageszeit eine erhöhte Entzündungsreaktion zur Folge hat. Durch solche zirkadianen Schwankungen wird die inflammatorische Homöostase des Körpers in erheblichem Maße beeinflusst. Somit kann unser Organismus je nach Tageszeitpunkt unterschiedlich gut mit Infektionen umgehen (40, 41).

Wenngleich der biologische Rhythmus vom Licht gesteuert wird, ist es entscheidend, ob ein Lebewesen in der Lichtphase (Beginn der Lichtphase ZT0) oder in der Dunkelphase (Beginn der Dunkelphase zu ZT12) aktiv ist. Die „Zeitgeber Time“ (ZT) beschreibt die Stunden nach Lichtbeginn, wobei ZT0 dem Beginn der Hellphase entspricht. Sowohl beim Menschen als auch bei der Maus oszillieren Leukozytenzahlen im Blut: Bei Menschen, welche ihre Aktivphase in der Lichtphase haben, sind die Leukozytenzahlen im Blut abends gegen 20:30 Uhr am höchsten (42, 43). Nagetiere sind in der Dunkelphase aktiv und der Höhepunkt ihrer Leukozytenzahlen im Blut ist um ZT5 und der Tiefpunkt um ZT13 (35). Scheiermann et al. konnten im Mausmodell Oszillierungen von Leukozyten im Knochenmark und Skelettmuskel zeigen, bei denen die Leukozyten ihren Höhepunkt zum Zeitpunkt ZT13 und ihren Tiefpunkt zum Zeitpunkt ZT5 hatten, also genau gegensätzlich zu den Blut-Oszillierungen (35). Die Oszillierungen entstehen über eine vom Tagezeitpunkt abhängige beta-adrenerge nervale Innervation der Gewebe, welche lokale Adhäsionsmoleküle je nach Tageszeit hoch- bzw. herunterregulieren. Beispielsweise wurden im Knochenmark VCAM1 und CXCL12 und im Skelettmuskel ICAM-1 und CCL2 tageszeitpunktabhängig reguliert. Man kann deshalb annehmen, dass jedes Organ tageszeitpunktabhängig durch eine individuelle Regulation von bestimmten Molekülen spezifische Leukozyten anlocken kann.

Aus diesen Erkenntnissen entstand die Vorstellung, dass Leukozyten im Verlauf von 24 Stunden vom Blut ins Gewebe und wieder zurück wandern. Einen Beweis für diese Hypothese gibt es nicht, da es technisch schwierig ist, einzelne Zellen über einen längeren

Zeitraum in ihrem Weg durch verschiedene Organe zu verfolgen. Einige Autoren erklären den Grund für die Oszillierungen damit, dass sich das Immunsystem im Laufe der Evolution dem zirkadianen Umweltrhythmus angepasst hat, bei dem die Wahrscheinlichkeit einer Verletzung und Infektion des Körpers in der Aktivphase sehr viel wahrscheinlicher ist als in der Dunkelphase (44). Die hohen Leukozytenzahlen im Gewebe in der Aktivphase machen den Wirt abwehrfähiger gegen mögliche Infektionen. Ein weiterer nennenswerter Aspekt des zirkadianen Rhythmus ist, dass es für den Körper ökonomischer ist, bei begrenzten metabolischen Ressourcen den Tag in Phasen der immunologischen Bereitschaft und in Phasen der Ruhe einzuteilen (45).

Es ist bislang nicht geklärt, welche Leukozyten-Subpopulationen und welche weiteren Organe an diesen Oszillierungen Anteil haben. In unserer zweiten Studie haben wir die Frage untersucht, ob neutrophile Granulozyten im Blut, Knochenmark und Herzen oszillieren und welche Faktoren diese Oszillierungen in dem jeweiligen Organ ermöglichen. Wir haben erstmals zeigen können, dass das Herz ein immunologisch dynamisches Organ ist, in dem Adhäsionmoleküle, Chemokine und Neutrophilenzahlen zirkadian oszillieren. Des Weiteren haben wir Vorarbeiten bestätigen können, nach welchen zirkadianen Mechanismen die Produktion von Vorläuferzellen und die Mobilisierung von neutrophilen Granulozyten aus dem Knochenmark beeinflussen (46).

3.4 Der Einfluss des zirkadianen Rhythmus auf die Wundheilung nach Myokardinfarkt

Es ist bekannt, dass viele kardiovaskuläre Parameter wie der Blutdruck, die Herzfrequenz und die Aktivität des Gerinnungssystems von der Tageszeit beeinflusst werden (47, 48). Aus klinischen Studien wissen wir, dass sich kardiovaskuläre Erkrankungen wie der Myokardinfarkt und der Schlaganfall vermehrt in den frühen Morgenstunden ereignen (47, 49, 50). Einige Studien zeigen, dass Patienten mit einem Myokardinfarkt in den Morgenstunden, verglichen mit einem Symptombeginn in den Abendstunden, an einem größeren Infarkt, gemessen an CK-MB Enzymmessungen, leiden (51-53). Der Grund für diesen tageszeitpunktabhängigen Zusammenhang ist nicht vollständig geklärt. Es gibt einige Arbeiten aus der Grundlagenforschung, die zeigen, dass die Anfälligkeit gegenüber einer Infektion und das Ausmaß der inflammatorischen Antwort vom Tageszeitpunkt der Exposition abhängen (54-56). Durgan et al. konnte im Mausmodell zeigen, dass bei einer myokardialen Ischämie mit darauffolgender Reperfusion zu Beginn der Aktivphase (ZT12) eine größere Anzahl von Neutrophilen in das Herz einwandert als bei ZT0 operierten Tieren. Dies führt bei ZT12 operierten Mäusen zu größeren Infarkten mit vermehrter Fibrose und einer schlechteren Herzfunktion verglichen mit ZT0 operierten Mäusen (57). Es stellt sich die Frage, ob dabei tageszeitpunktabhängige Regulationen der Immunfunktion eine Rolle spielen. Es ist auch zu klären, ob es sich lediglich um quantitative Effekte bezüglich der Leukozytenrekrutierung oder auch um qualitative Unterschiede bezüglich der zellulären Funktionsfähigkeit handelt. Solche qualitativen Unterschiede in der zirkadianen Aktivität von Zellen könnten zum Beispiel durch eine Hochregulierung von Chemokinrezeptoren bewirkt werden, welche Leukozyten tageszeitabhängig empfänglicher für eine Zellaktivierung sowie -migration macht.

In der zweiten Veröffentlichung sind wir dieser Frage nachgegangen. Wir konnten die Hypothese der Vorarbeiten bestätigen, dass ein Myokardinfarkt in der Maus ein vom Tageszeitpunkt abhängiges Outcome zeigt. Des Weiteren haben wir zugrunde liegende Mechanismen der tageszeitpunktabhängigen Neutrophilen-Mobilisation identifiziert: Neutrophile Granulozyten im Blut erhöhen ihre CXCR2 Oberflächenexpression zu Beginn der Aktivphase (ZT13), sodass sie leichter ins Herz migrieren können. Eine pharmakologische Inhibition von CXCR2 reduzierte die Neutrophilen-Zahlen im Herzen gezielt in ZT13 operierten Mäusen und bestätigte die Wichtigkeit des Rezeptors in der tageszeitpunktabhängigen Neutrophilen-Rekrutierung. Des Weiteren zeigten wir, dass die Neutrophilen-Produktion im Knochenmark und deren Mobilisierung durch CXCL12 und G-

CSF zirkadian gesteuert ist (58). Diese Erkenntnisse lassen die Weitläufigkeit erahnen, mit der der zirkadiane Rhythmus auf den Körper und seine Immunzell-Homöostase wirkt.

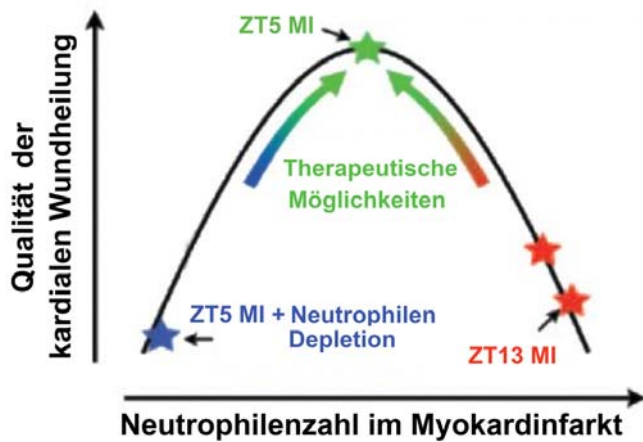


Abbildung 3.4.1: Das Ausmaß der Entzündung nach Myokardinfarkt beeinflusst die Qualität der kardialen Wundheilung. Wir stellen die Hypothese auf, dass ein Myokardinfarkt zur Mittagszeit (ZT5) durch eine adäquate inflammatorische Antwort eine qualitativ hochwertigere Wundheilung ermöglicht. Ist die inflammatorische Antwort übertrieben (Myokardinfarkte zu Beginn der Aktivphase (ZT13)) oder zu sehr reduziert (Neutrophilen-depletierte Mäuse) ist die Qualität der Wundheilung eingeschränkt. Überarbeitete Abbildung (20).

In der zweiten Veröffentlichung wurden die Versuchsvorbereitungen, Datenerhebungen sowie Auswertungen eigenständig von mir durchgeführt. Das Manuskript wurde zunächst von mir verfasst und anschließend durch Frau Professor Dr. Sabine Steffens revidiert und in gemeinsamer Arbeit in seine endgültige Fassung gebracht. Die Graphen, Abbildungen und Schemata habe ich selbstständig erstellt und überarbeitet. Die statistische Auswertung erfolgte eigenständig durch mich. Koautoren standen unterstützend bei speziellen Fragestellungen, bei der Durchführung von Versuchen und für die intellektuelle Diskussion zur Verfügung.

4. Zusammenfassung

4.1 Zusammenfassung auf Deutsch

Kardiovaskuläre Erkrankungen und insbesondere der akute Myokardinfarkt sind die häufigste Todesursache in der entwickelten Welt. Das Überleben von Patienten mit einem akuten Myokardinfarkt wird wesentlich durch eine adäquat balancierte Inflammationsreaktion auf den Infarkt beeinflusst (59). So führte eine exzessive Neutrophilenzahl im Blut von Myokardinfarktpatienten zu einer mangelhaften kardialen Wundheilung und folglich zu einer eingeschränkten Herzfunktion (26). Lange bestand die Vorstellung, dass neutrophile Granulozyten im ischämischen Myokard zwar für eine frühe Phagozytose von absterbenden Kardiomyozyten notwendig sind, darüber hinaus aber wesentlich zur einer destruktiven Inflammationsamplifizierung beitragen. Ziel der ersten Veröffentlichung war es zu klären, ob sich neutrophile Granulozyten nicht auch fördernd auf die kardiale Wundheilung nach Myokardinfarkt auswirken.

In der ersten Studie konnten wir zeigen, dass neutrophile Granulozyten neben den bereits bekannten Aufgaben auch eine entscheidende Rolle bei der Eindämmung der Inflammationsreaktion nach Myokardinfarkt spielen und damit eine protektive Wirkung auf das Myokard haben. Neutrophil-depletierte Mäuse hatten im Vergleich zu ihren Isotyp-Kontrollen signifikant höhere inflammatorische Makrophagenzahlen jedoch eine geringere Zahl von reparativen Makrophagen sowie mehr apoptotische Zellen im ischämischen Myokard. Dies konnten wir damit erklären, dass neutrophile Granulozyten NGAL (neutrophil gelatinase-associated lipocalin) sezernierten, welches im Herzen nach Myokardinfarkt die Umwandlung von inflammatorischen zu reparativen Makrophagen bewirkte. In Neutrophil-depletierten Mäusen kam es verglichen mit Isotyp-Kontrollen nach Myokardinfarkt zu einer amplifizierten Entzündung und folglich zu einer größeren fibrotischen Infarktnarbe und einer eingeschränkten Herzfunktion.

Interessanterweise deuten klinische Studien darauf hin, dass das Überleben von Patienten mit akutem Myokardinfarkt von der Tageszeit ihres Symptombeginns abhängt. Ziel der zweiten Veröffentlichung war es, die dahinterstehenden Mechanismen zu klären.

In der zweiten Studie konnten wir zeigen, dass das Herz ein immunologisch dynamisches Organ ist, in dem Adhäsionsmoleküle, Chemokin- und Zytokinexpressionen sowie Neutrophilen-Zahlen zirkadian oszillieren. Dies gilt auch für das Knochenmark, in dem die Neutrophilen-Produktion und -Mobilisierung ebenfalls von der Tageszeit abhängt. Unter nicht

ischämischen Bedingungen zeigten neutrophile Granulozyten zu Beginn der Aktivphase (ZT13) eine höhere Neigung zur Myokardinfiltation als ZT5 operierte Mäuse, welche wir auf eine Hochregulierung ihres CXCR2 zurückführten. Bei einem Myokardinfarkt zum ZT13 Zeitpunkt konnten folglich mehr CXCR2^{high} Neutrophile vom Blut ins Herz migrieren als zum ZT5 Zeitpunkt, was zu einer extremen Akkumulation von Neutrophilen im Herzen führte. Gleichzeitig konnte ein pharmakologischer CXCR2 Inhibitor nur zum ZT13 Zeitpunkt die kardiale Neutrophilen-Migration verhindern. Ein Myokardinfarkt zu Beginn der Aktivphase resultierte in einer übertriebenen Entzündungsreaktion mit größeren Infarkten und beeinträchtigter Wundheilung; letztere führte zu einer größeren fibrotischen Narbe mit schlechterer Herzfunktion. Eine Reduzierung der Neutrophilenzahl durch einen pharmakologischen CXCR2-Inhibitor oder einen Ly6G-Antikörper bei Myokardinfarkten am Beginn der Aktivphase hatte einen schützenden Effekt und führte folglich zu kleineren Infarkten und einer besseren Herzfunktion.

Unsere Daten bieten einen Erklärungsansatz für die schlechtere Überlebensrate von Patienten, die einen Herzinfarkt in den frühen Morgenstunden erleiden. Eine Reduktion der von Neutrophilen verursachten Inflammation nach Myokardinfarkt könnte das Überleben dieser Patienten verbessern. Dabei ist die richtige Dosierung der antiinflammatorischen Therapie entscheidend, da neutrophile Granulozyten zwar einen potentiellen Schaden verursachen, aber auch eine essenzielle reparative Funktion in der kardialen Wundheilung wahrnehmen können.

4.2 Zusammenfassung auf Englisch

Cardiovascular diseases and especially acute myocardial infarction are the leading causes of death in the developed world. The clinical outcome of patients with myocardial infarction strongly depends on an adequately balanced post-myocardial infarction inflammation (59). Excessive neutrophil counts in the blood of patients with myocardial infarction impair cardiac healing and lead to decreased heart functions (26). Consequently, neutrophils were initially thought to play an important role in phagocytizing dead cardiomyocytes. In addition, they were considered to amplify post-infarct inflammation in a crucial way. The objective of the first study was to determine whether neutrophils might also play a beneficial role in myocardial infarction healing.

In the first study, we confirmed that neutrophils play an important role in resolving post-

myocardial infarction inflammation. Compared to Isotype-controls, neutrophil-depleted mice subjected to myocardial infarction showed significantly higher numbers of inflammatory macrophages, but fewer reparative macrophages and thus a higher number of apoptotic cells in the infarcted myocardium. We identified neutrophil gelatinase-associated lipocalin (NGAL) in the neutrophil secretome as a key inducer of macrophage polarisation towards a reparative phenotype with a high capacity to engulf apoptotic cells. Consequently, neutrophil depletion after myocardial infarction resulted in an amplified inflammatory state within the ischemic myocardium and thereby lead to increased fibrosis, lower cardiac function and progressive heart failure.

Recent research has suggested that the outcome after myocardial infarction is time-of-day dependent, as clinical studies show a correlation between the infarct size and the time-of-day of the ischemia onset. The objective of the second study was to clarify the mechanisms behind this nexus.

In the second study, we found the heart to be an immunologically dynamic organ with circadian fluctuations of adhesion molecules and chemokine expression leading to circadian oscillations of cardiac neutrophil counts. In addition, we observed that neutrophil production and retention in the bone marrow are time-of-day dependent and that circulating neutrophils at the beginning of the active phase had a higher capacity to migrate into the myocardium than at ZT5 due to upregulated CXCR2 expression. We, therefore, concluded that myocardial infarction during the peak of CXCR2 expression on blood neutrophils facilitated cardiac neutrophil accumulation and thereby promoted an exaggerated inflammatory response. Mice operated at ZT13 suffered from a larger infarct size, increased fibrosis and a lower heart function compared to ZT5 operated mice. Reducing neutrophil counts by injecting a pharmacological CXCR2 antagonist or a Ly6G antibody prevented excessive neutrophil driven cardiac damage only in mice subjected to myocardial infarction during the active phase.

Our findings provide a mechanistic explanation for the worse outcomes in patients with myocardial infarction occurring during the sleep-to-wake transition period. Limiting exaggerated neutrophil-mediated inflammation in these patients might improve their clinical outcome after myocardial infarction. However, therapeutic strategies to reduce acute neutrophil-driven inflammation after myocardial infarction should be carefully balanced as they might interfere with the cardiac wound healing process, in which a certain neutrophil count is beneficial.

5. Veröffentlichung I

Michael Horckmans, Larisa Ring, Johan Duchene, Donato Santovito, **Maximilian J Schloss**, Maik Drechsler, Christian Weber, Oliver Soehnlein, Sabine Steffens.

Neutrophils orchestrate post-myocardial infarction healing by polarizing macrophages towards a reparative phenotype.

European Heart Journal. Januar 2017; 38(3): 187-97.

Die Originalarbeit unterlag einem Review-Verfahren. Der Impact-Faktor lag 2016 bei 20.213 Punkten.

In der ersten Studie wirkte ich als Koautor bei der Entwicklung und Gestaltung des Projektes mit. Ich stand unterstützend bei der Durchführung von Versuchen (histologische Daten in Figure 3 A-H; Multiplex-Messungen in Figure 2 D-F und Figure 4 F-H) und bei der Diskussion der Ergebnisse zur Verfügung. Das Manuskript wurde von mir gegengelesen und vom Erst- sowie Letztautor in die endgültige Fassung gebracht.

Neutrophils orchestrate post-myocardial infarction healing by polarizing macrophages towards a reparative phenotype

Michael Horckmans¹, Larisa Ring¹, Johan Duchene¹, Donato Santovito^{1,2}, Maximilian J. Schloss¹, Maik Drechsler^{1,3,4}, Christian Weber^{1,3}, Oliver Soehnlein^{1,3,4}, and Sabine Steffens^{1,3*}

¹Institute for Cardiovascular Prevention (IPEK), Ludwig-Maximilians-University (LMU) Munich, Pettenkoferstr. 9, 80336 Munich, Germany; ²European Center of Excellence on Atherosclerosis, Hypertension and Dyslipidemia, G. d'Annunzio University, Chieti, Italy; ³German Centre for Cardiovascular Research (DZHK), Partner Site Munich Heart Alliance, Munich, Germany; and ⁴Department of Pathology, Amsterdam Medical Center (AMC), Amsterdam, The Netherlands

Received 21 May 2015; revised 13 November 2015; accepted 4 January 2016; online publish-ahead-of-print 2 February 2016

See page 198 for the editorial comment on this article (doi:10.1093/eurheartj/ehw085)

Aims

Acute myocardial infarction (MI) is the leading cause of mortality worldwide. Anti-inflammatory strategies to reduce neutrophil-driven acute post-MI injury have been shown to limit acute cardiac tissue damage. On the other hand, whether neutrophils are required for resolving post-MI inflammation and repair is unknown.

Methods and results

We show that neutrophil-depleted mice subjected to MI had worsened cardiac function, increased fibrosis, and progressively developed heart failure. Flow cytometry of blood, lymphoid organs and digested hearts revealed reduced numbers of Ly6C^{high} monocytes in infarcts of neutrophil-depleted mice, whereas the number of macrophages increased, which was paralleled by reduced splenic Ly6C^{high} monocyte mobilization but enhanced proliferation of cardiac macrophages. Macrophage subtype analysis revealed reduced cardiac expression of M1 markers, whereas M2 markers were increased in neutrophil-depleted mice. Surprisingly, we found reduced expression of phagocytosis receptor myeloid-epithelial-reproductive tyrosine kinase, a marker of reparative M2c macrophages which mediate clearance of apoptotic cells. In agreement with this finding, neutrophil-depleted mice had increased numbers of TUNEL-positive cells within infarcts. We identified neutrophil gelatinase-associated lipocalin (NGAL) in the neutrophil secretome as a key inducer of macrophages with high capacity to engulf apoptotic cells. The cardiac macrophage phenotype in neutrophil-depleted mice was restored by administration of neutrophil secretome or NGAL.

Conclusion

Neutrophils are crucially involved in cardiac repair after MI by polarizing macrophages towards a reparative phenotype. Therapeutic strategies to reduce acute neutrophil-driven inflammation after MI should be carefully balanced as they might interfere with the healing response and cardiac remodelling.

Keywords

Neutrophils • Myocardial infarction healing • Adverse remodelling • Macrophages • Efferocytosis • Lipocalin

Translational perspective

Neutrophils are generally considered to play a detrimental role after post-myocardial infarction (MI) revascularization, but their role in myocardial ischaemia by itself has not been fully elucidated. Here, we provide novel evidence that neutrophils, despite being short-living innate immune responders, could contribute to improve cardiac healing and outcomes by influencing macrophage polarization towards a 'reparative' phenotype, via neutrophil gelatinase-associated lipocalin release. A better knowledge of the role of neutrophils in MI healing could help predicting the net results of neutrophil-targeted therapies in MI.

* Corresponding author. Tel: +49 89 4400 54674, Fax: +49 89 4400 54676, Email: sabine.steffens@med.uni-muenchen.de

Published on behalf of the European Society of Cardiology. All rights reserved. © The Author 2016. For permissions please email: journals.permissions@oup.com.

Introduction

Myocardial infarction (MI) induces an inflammatory response which is required for the induction of cardiac repair processes. Various cell types, including neutrophils and macrophages, are involved at different stages of infarct healing, ultimately leading to scar formation and adaptive remodelling to preserve cardiac function.¹ Attracted by cell debris, danger-associated molecular patterns and cytokines of activated neighbouring cells, neutrophils massively infiltrate the infarct area in the first few hours following onset of ischemia.¹ They generate high levels of reactive oxygen species and secrete proteases, which exacerbates local vascular and tissue injury.² Subsequently, monocyte-derived macrophages are recruited to the heart to remove debris and apoptotic neutrophils, which leads to activation of reparative pathways necessary for scar formation.^{1,3} Macrophages in the ischaemic myocardium exhibit high plasticity and are involved in both inflammatory as well as reparative processes. In the context of post-MI inflammation resolution, pro-inflammatory M1 macrophages are thought to undergo local conversion to M2 resolution-mediating macrophages.⁴

The crucial importance for efficient clearance of cell debris in resolving post-MI inflammation has been highlighted in mice with genetic deficiency of myeloid-epithelial-reproductive tyrosine kinase (MertK). Insufficient clearance of apoptotic cells by MertK-deficient macrophages led to delayed inflammation resolution after MI, adverse remodelling, and decreased cardiac function.⁵ Hence, reprogramming macrophages in the heart to a reparative state seems to be an attractive therapeutic strategy to improve infarct repair, e.g. as previously reported by systemic administration of phosphatidylserine-decorated liposomes.⁶ In this regard, further studies are warranted to better understand the signalling pathways and local regulators in the cardiac microenvironment promoting resolution of inflammation and macrophage differentiation to a reparative phenotype.

Less is known about the role of neutrophils in post-MI healing. High neutrophil counts are considered as predictor of adverse clinical outcomes and mortality in patients with acute coronary syndromes,^{7,8} and their contribution in the acute inflammatory phase after MI is generally considered detrimental. However, in acute inflammation, neutrophils are not only vital for the clearance of pathogens or debris, but also for the resolution of inflammation and return to tissue homeostasis.⁹ Macrophages engulfing apoptotic neutrophils activate an anti-inflammatory response by inhibiting pro-inflammatory cytokines and inducing the production of interleukin (IL)-10, transforming growth factor (TGF)- β and pro-resolving lipid mediators.¹⁰ Consequently, anti-inflammatory strategies reducing neutrophil influx in order to limit acute post-ischaemic tissue injury might also inhibit the subsequent healing response. In the present study, we therefore aimed to clarify the contribution of neutrophils in post-MI healing.

Methods

An expanded version is provided in Supplementary material online, Methods.

Animal experiments

Female 10- to 12-week-old C57BL/6 mice were used in this study. Myocardial infarction was induced by permanent ligation of the left anterior

descending coronary artery (LAD). In additional experiments, mice were subjected to transient LAD occlusion for 45 min followed by reperfusion. Neutrophil depletion was performed by intraperitoneal (i.p.) injection of monoclonal antibody clone 1A8 (50 µg; Figure 1A). Control mice received corresponding isotype i.p. injections. In some experiments, mice received intramyocardial injections of neutrophil supernatant in the ischaemic LAD territory.¹¹ Control animals received intramyocardial injections of vehicle (saline). In other experiments, recombinant murine neutrophil gelatinase-associated lipocalin (NGAL) (100 µg) or vehicle (saline) was injected i.p. after 1, 3, and 4 days LAD ligation. We performed echocardiography, quantification of infarct size, histology, flow cytometry, real-time PCR, western blot, multiplex, and ELISA as described in Supplementary material online. All animal experiments were approved by the local ethical committee.

Macrophage polarization

Murine bone marrow-derived macrophages (BMM) were left untreated or converted to M1 macrophages by stimulation with IFN- γ (10 ng/mL for 72 h). M2a or M2c were obtained by a 72 h treatment with IL-4 (20 ng/mL) or dexamethasone (20 nM), respectively. To assess the effect of neutrophil secretome or recombinant proteins on macrophage polarization, BMM were polarized in the presence of 100 µL of neutrophil supernatant or with recombinant mouse NGAL (100 ng/mL), lactoferrin (10 µg/mL), Cramp (1 µg/mL), neutrophil elastase (5 µM), or myeloperoxidase (MPO, 5 µM). Human monocytes were isolated from blood of healthy donors and macrophages were differentiated from monocytes by culturing for 6 days in the presence of recombinant human macrophage colony-stimulating factor (50 ng/mL). Human macrophages were polarized as described above.

Western blot

MertK in heart or cell lysates was detected with anti-MertK antibody (R&D Systems) followed by anti-goat-horseradish peroxidase as secondary antibody.

Neutrophil gelatinase-associated lipocalin immunoprecipitation

Protein G-conjugated magnetic beads were incubated with goat polyclonal anti-NGAL antibody (R&D Systems) or normal goat IgG as negative control. The antibody-conjugated beads were incubated with 500 µL of conditioned medium obtained from activated mouse neutrophils, magnetically separated and supernatants collected for subsequent treatment of macrophages.

Efferocytosis

Macrophages were co-cultured with apoptotic mouse cardiomyocytes (stained with calcein AM) at 37°C for 60 min. Phagocytosis efficiency (%) was quantified by flow cytometry and calculated as calcein positive divided by the total number of macrophages.

Statistical analysis

All data are expressed as mean \pm SD, and statistical analysis was performed with Prism Software (version 6; GraphPad, CA, USA). Endpoint comparisons between 2 groups were performed using unpaired 2-tailed Student's *t*-test. For multiple comparisons, false discovery rate according to Benjamini–Hochberg was applied to control type I false positive errors, and FDR was set to 0.05. For parallel repeated-measures studies, 2-way ANOVA was used with Bonferroni *post hoc* evaluation to determine the significance for individual time points. A 2-tailed *P* < 0.05 was considered as significant.

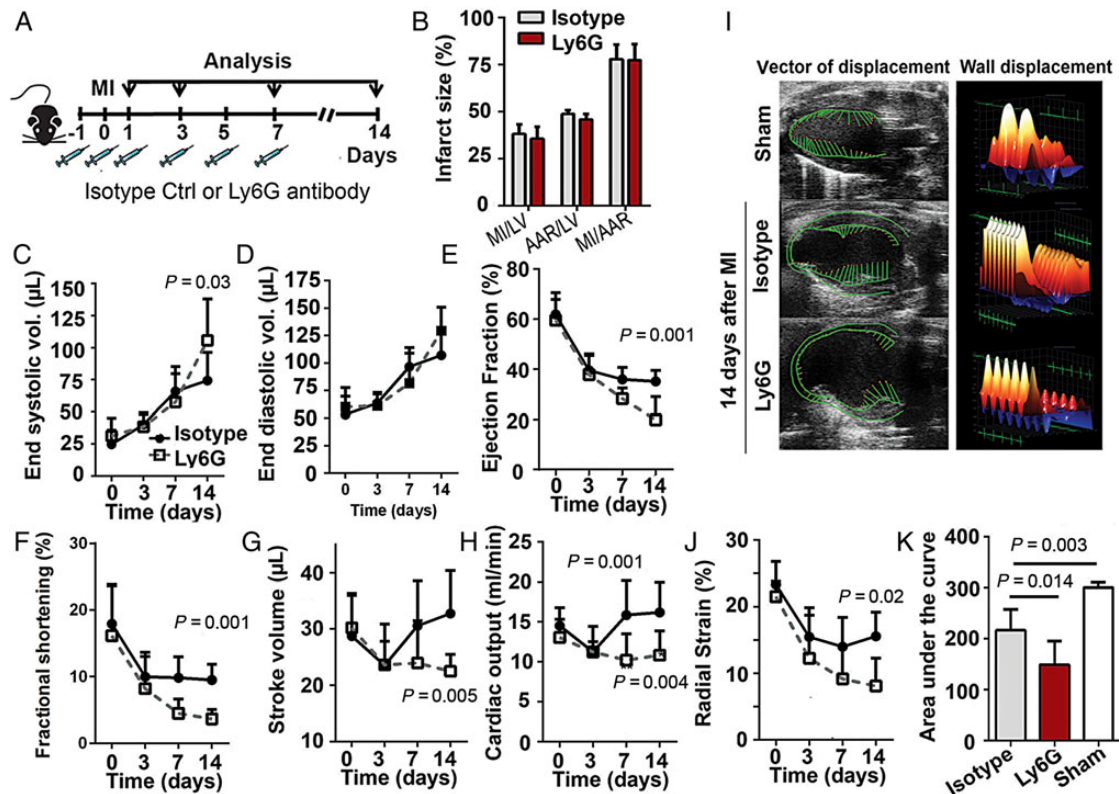


Figure 1 Neutrophil depletion does not affect infarct size but progressively worsens cardiac function. (A) Experimental protocol for treatment with neutrophil-depleting antibody (Ly6G) or isotype. (B) Quantification of ratios between infarct size (myocardial infarction), area at risk, and left ventricular area, 24 h after myocardial infarction. (C–H) Quantification of functional parameters after sham operation (Day 0) or 3, 7, 14 days after myocardial infarction. (I) Vector diagrams showing the direction and magnitude of myocardial contraction at midsystole. Three-dimensional regional wall displacement illustrations, showing contraction (positive values, yellow–red) or relaxation (negative values, blue) of consecutive cardiac cycle results. (J) Global averages of radial strain and (K) measurement of the area under the curve of radial strain. Data are mean \pm SD from 8 mice/group.

Results

Neutrophil depletion worsens cardiac function and promotes heart failure

Depletion with anti-Ly6G resulted in significant reduction of circulating neutrophil counts, whereas blood monocytes were unaffected at steady state (Supplementary material online, Figure S1). In agreement with previous observations after prolonged ischaemia,¹² we found no difference in infarct size between control and neutrophil-depleted mice 24 h post-infarction (Figure 1B). However, 7–14 days after infarction, neutrophil depletion led to worsening of heart function. Characteristic features of neutrophil depletion were larger end-systolic left ventricular dimensions, a significant reduction of left ventricular ejection fraction and cardiac output (Figure 1C–H and Supplementary material online, Table S1).

In support of reduced global contractility, infarcted hearts of neutrophil-depleted mice had pronounced hypokinesia of left ventricular walls (Figure 1I). The radial strain was significantly more decreased in infarcted hearts of depleted animals compared with controls (Figure 1J and K). Worsening of global contractility might

lead to heart failure (HF). In support of this hypothesis, neutrophil-depleted mice had up-regulated cytokine and chemokine levels associated with HF^{13–15} 7 days post-MI (Figure 2A–F). Moreover, the kidneys had macroscopic lesions and increased expression of galectin-3, a marker of kidney injury (Figure 2G and H)¹⁶ as well as increased plasma levels of creatinine (Figure 2I).

Neutrophil depletion promotes excessive fibrosis

Histological analysis of the myocardium revealed an increased percentage of α -smooth muscle actin-positive myofibroblasts 7 days post-MI in neutrophil-depleted mice (Figure 3A and B), which was confirmed at the mRNA level (Figure 3C). The number of CD31-stained microvessels in healing infarcts of control and neutrophil-depleted mice was comparable (Figure 3D). Consistent with a higher amount of cells promoting fibrosis, the collagen content, in particular of thicker type I collagen fibres, was higher in infarcts of depleted mice (Figure 3E–H). These findings suggest that depletion of neutrophils leads to excessive fibrosis that might explain the progressive worsening of cardiac function.

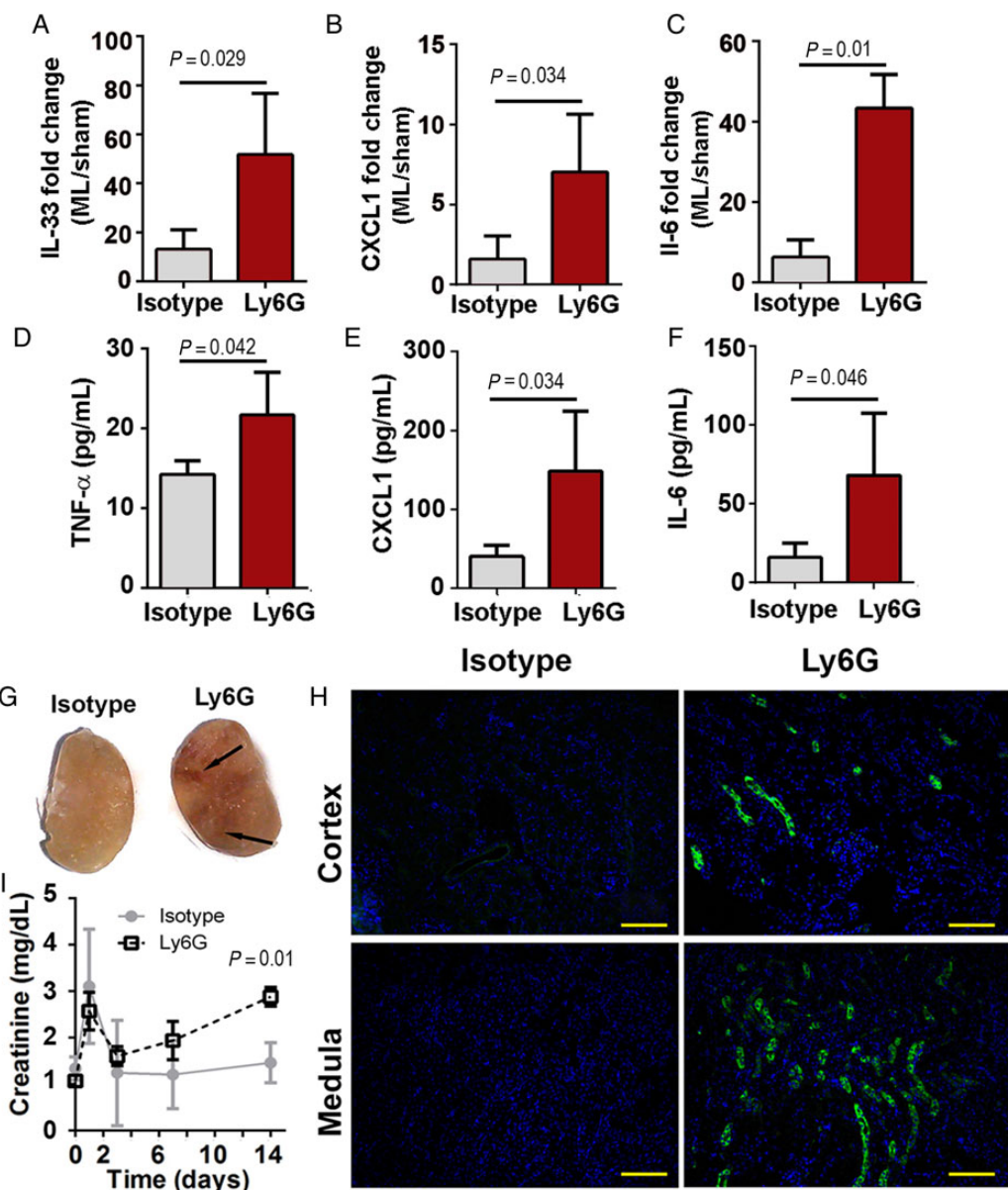


Figure 2 Neutrophil depletion leads to up-regulation of markers for heart failure. (A–C) Quantification of cardiac mRNA expression in isotype-treated and neutrophil-depleted (Ly6G) mice 7 days after myocardial infarction. (D–F) Plasma levels 7 days after MI. (G) Macroscopic view of the kidney 5 days after myocardial infarction. Arrows indicate macroscopic lesions observed in neutrophil-depleted mice. (H) Representative galectin-3 immunostaining 5 days after myocardial infarction. (I) Plasma creatinine levels before and 1, 3, 7, 14 days post-myocardial infarction. Data are mean \pm SD from 3–4 mice/group.

Neutrophil depletion modulates cardiac monocyte and macrophage profiles

Unfavourable repair in the absence of neutrophils might be a consequence of impaired resolution of inflammation due to insufficient monocyte recruitment or activation of reparative macrophages. We therefore analysed leucocyte profiles in hearts and lymphoid organs. As expected, treatment with depleting antibody Ly6G potently reduced cardiac neutrophil counts (Figure 4A and B). We detected an overall reduction of blood leukocytes in

neutrophil-depleted mice up to 7 days after MI (Supplementary material online, Figure S1), probably due to reduced neutrophil-mediated inflammation. Flow cytometric analysis of digested hearts revealed less Ly6C^{hi} monocytes 3 days post-infarction, whereas the number of macrophages was increased at day 3 to 7 post-infarction (Figure 4C and D).

In response to MI, monocytes are mobilized from the bone marrow and spleen into the blood stream and subsequently recruited into the ischaemic myocardium.¹⁷ In agreement with reduced recruitment of monocytes into infarcts of neutrophil-depleted mice,

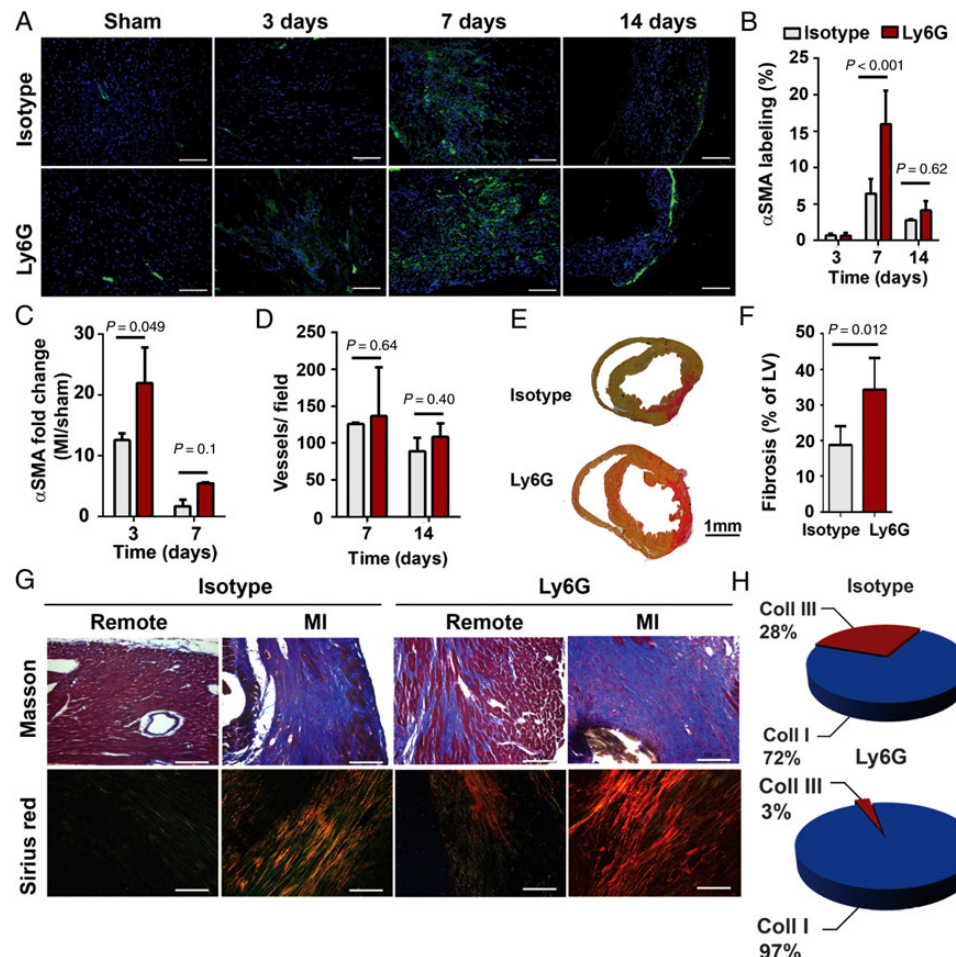


Figure 3 Neutrophil depletion increases cardiac fibrosis. (A) Myofibroblasts within infarct areas identified by α -smooth muscle actin labelling (green) and 4',6-diamidino-2-phenylindole staining of nuclei (blue) in hearts from neutrophil-depleted (Ly6G) or isotype-treated mice. Scale bar, 50 μ m; $\times 20$ magnification. (B) Quantification of α -smooth muscle actin staining as ratio between stained and total area of myocardium within randomly selected fields. (C) Quantification of α -smooth muscle actin mRNA levels, represented as fold change compared with sham-operated hearts. (D) Quantification of CD31-stained microvessels within infarct areas of randomly selected fields. (E and G) Representative collagen staining with Sirius red and Masson trichrome (collagen in blue) at day 7 after infarction. Images were taken at $\times 2.5$ magnification (whole hearts, Sirius red) and $\times 20$ magnification of infarct area and remote zone (scale bar, 100 μ m). (F) Quantification of fibrosis as ratio between collagen-stained area and total area of the left ventricle (LV). (H) Relative content of type I and III collagen fibres within infarcts. The graphs show mean \pm SD from 5 mice/group.

the spleens contained higher numbers of the Ly6G^{hi} subset (Figure 4E). The bone marrow mobilization of monocytes was not different between depleted and control group (data not shown). In support of reduced splenic monocyte mobilization, we found decreased plasma levels of chemokines involved in monocyte recruitment^{1,18} one day post-MI (Figure 4F).

Neutrophil depletion promotes local macrophage proliferation

To explain the increased number of macrophages in the heart, we may speculate that the microenvironment in the absence of neutrophil-driven inflammation supports an expansion by local proliferation. In support of this hypothesis, we found decreased

plasma levels of pro-inflammatory cytokine levels IL-1 β , IL-12, TNF- α , and IFN- γ in neutrophil-depleted mice (Figure 4G). Conversely, plasma levels of IL-4, a cytokine that induces macrophage proliferation and M2 polarization,^{19,20} were increased (Figure 4H). Moreover, the flow cytometric analysis revealed a higher number of proliferating macrophages, evidenced by higher percentage of KI-67-positive macrophages in G1 and G2/S/M phase, whereas the percentage in G0 decreased in infarcted hearts of neutrophil-depleted mice (Figure 4I and J). Conversely, we determined a lower percentage of monocytes in G1 with concomitant increase of monocytes in the G0 phase (Figure 4K). Therefore, our data suggest that neutrophils are crucial regulators of the microenvironment driving polarization and proliferation of macrophages involved in cardiac repair.

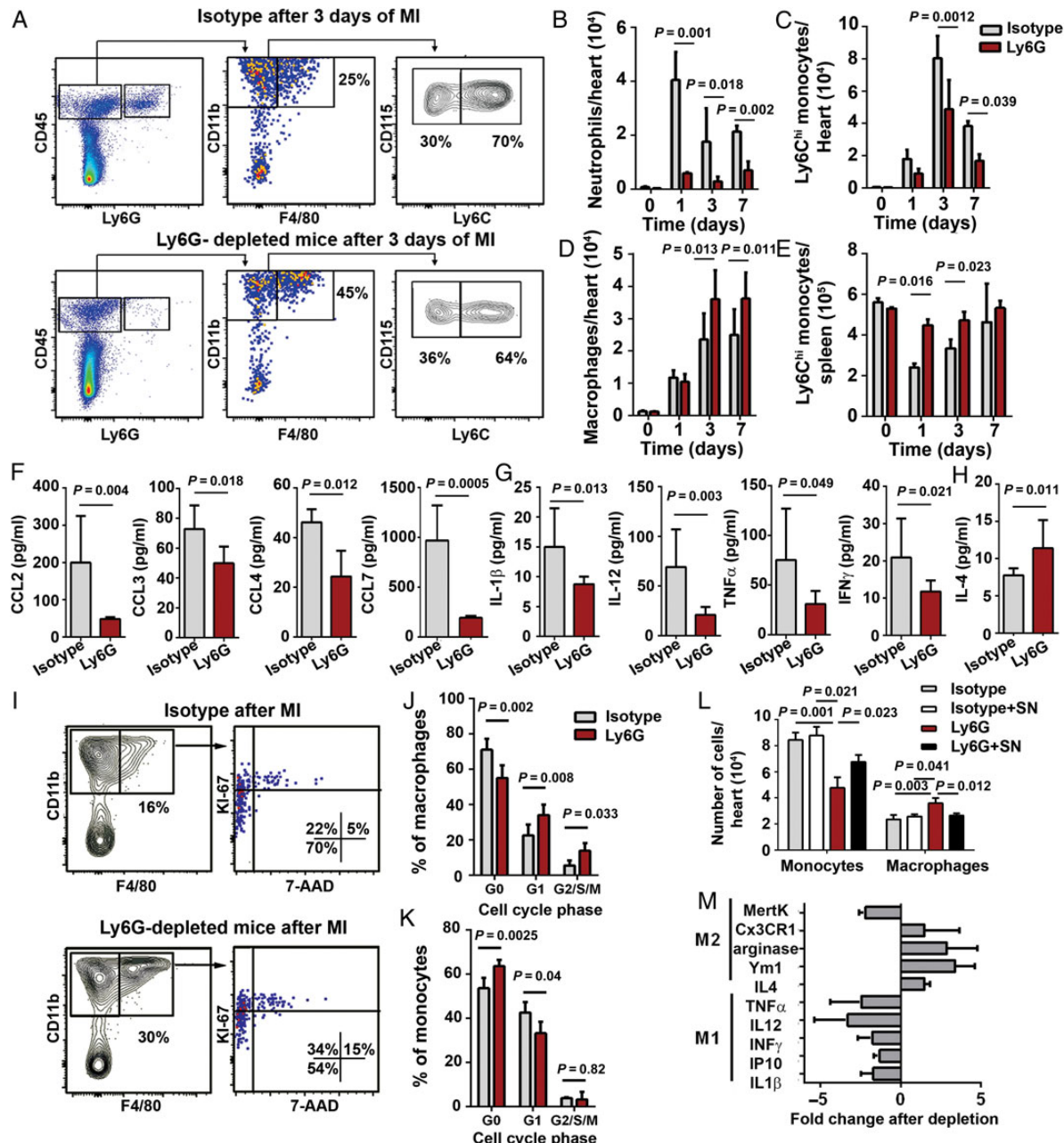


Figure 4 Neutrophil depletion modulates cardiac monocyte/macrophage profiles, splenic mobilization, and local proliferation. (A–D) Representative FACS plots and quantification of neutrophils, Ly6C^{high} monocytes and macrophages in digested hearts of neutrophil-depleted (Ly6G) or isotype-treated mice at baseline (0) or 1–7 days after myocardial infarction. (E) Quantification of Ly6C^{high} monocytes in the spleen. (F) Plasma levels of chemokines involved in monocyte recruitment 24 h after myocardial infarction. Plasma levels of (G) pro- and (H) anti-inflammatory cytokines 24 h after MI. (I–K) Quantification of proliferating (KI67 positive) Ly6C^{high} monocytes and macrophages in the heart 3 days after myocardial infarction, based on flow cytometric cell cycle analysis using 7-AAD for nuclear DNA staining. (I) Representative dot plots with quadrants to identify cells in G0 (lower left), G1 (upper left), and G2/S/M (upper right) phase. (L) Quantification of Ly6C^{high} monocytes and macrophages in the heart 3 days after myocardial infarction with or without intramyocardial injection of neutrophil supernatant. (M) Cardiac mRNA expression levels of M1 and M2 markers, normalized to hypoxanthine phosphoribosyltransferase (fold change compared with isotype group, $P < 0.05$ for all represented factors). (B–H) Data are mean \pm SD from 8 (J and K) 5 or (L and M) 3 mice/group.

The neutrophil secretome changes cardiac monocyte and macrophage profiles

To strengthen this finding, we asked whether neutrophil supernatant was sufficient to restore the cardiac macrophage profile. Indeed, local administration of neutrophil supernatant into infarcted hearts of neutrophil-depleted mice partially reversed the phenotype by increasing the number of Ly6C^{hi} monocytes, while macrophage numbers decreased (Figure 4L).

Neutrophil depletion affects macrophage polarization

Polarized macrophages are generally referred to as M1 and M2 macrophages.²¹ M1 macrophages are found in the early stages after MI injury and play a key role in acute inflammation, followed by reparative M2 macrophages that mediate resolution of inflammation.⁴ We characterized the transcriptional profile in Ly6G depleted vs. control hearts 7 days post-MI and found a significant down-regulation of M1 markers (IL-12, TNF α , IFN γ , IP-10, IL1 β) and up-regulation of M2 signature markers (CX3CR1, arginase, YM1, IL-4) compared with controls (Figure 4M). Surprisingly, expression of macrophage marker MertK, a phagocytosis receptor mainly expressed by M2c macrophages,^{22,23} was decreased (Figure 4M).

The neutrophil secretome promotes macrophage polarization towards M2c

We hypothesized that factors released by neutrophils might promote an M2c phenotype with enhanced ability to phagocytose dead cardiomyocytes. To verify this possibility, we tested the influence of neutrophil supernatant on murine macrophage polarization. We confirmed that MertK was mainly expressed by *in vitro* polarized M2c macrophages, whereas M1 and M2a macrophages expressed only low levels of MertK (Figure 5A and B). Addition of neutrophil supernatant induced MertK expression in M2a macrophages, indicating a polarization from M2a toward M2c (Figure 5A and B). To test a potential relevance for humans, we incubated human primary macrophages with human neutrophil supernatant and found a comparable induction of MertK expression in M2a polarized macrophages (Figure 5C and D).

Neutrophil-derived neutrophil gelatinase-associated lipocalin promotes macrophage polarization towards M2c

We further screened the effect of various recombinant neutrophil-related proteins on macrophage polarization. Strikingly, the effect of neutrophil supernatant on MertK expression was reproduced by incubating *in vitro* polarized murine macrophages with recombinant NGAL (Figure 5A and B). To validate this finding, we performed immunodepletion of NGAL in neutrophil supernatant, which blunted the M2c-polarizing effect (Figure 5A and B). No change in macrophage polarization from M2a to M2c was observed when cells were treated with other neutrophil-released proteins, i.e. recombinant Cramp, lactoferrin, neutrophil elastase, or MPO (Supplementary material online, Figure S2).

In agreement with our *in vitro* data, we found reduced cardiac protein levels of the M2c marker MertK in hearts of neutrophil-depleted mice (Figure 5E and F). Neutrophil gelatinase-associated lipocalin plasma levels were up-regulated 1–3 days after MI, but were significantly lower in neutrophil-depleted mice (Figure 5G), indicating neutrophils to be an important source for NGAL expression after MI. Systemic administration of NGAL in neutrophil-depleted mice not only restored normal plasma levels (Supplementary material online, Figure S4) but also cardiac protein levels of MertK (Figure 5E and F). This effect was confirmed by flow cytometric analysis of digested hearts, revealing a lower percentage of MertK^{hi} expressing macrophages in neutrophil-depleted hearts, while their percentage was restored when injecting NGAL (Figure 5H and I).

M2c polarization is required for apoptotic cell clearance

An important role of M2c macrophages is the clearance of apoptotic cells (efferocytosis),²² which is of crucial importance for wound healing after MI.⁵ To assess the role of neutrophil-derived NGAL on efferocytosis capacity, we treated *in vitro* polarized macrophages with neutrophil supernatant or NGAL. After incubation with apoptotic cardiomyocytes, we observed a higher efficiency of M2c to phagocytose apoptotic cells compared with M1 and M2a macrophages (Figure 5J and K), as previously reported.²² The efferocytosis capacity of M2a was increased after incubation with neutrophil supernatant or NGAL, which is in agreement with the up-regulation of phagocytosis receptor MertK expression (Figure 5A and B). To test the hypothesis that neutrophil depletion leads to a defect of dying cardiomyocyte clearance in neutrophil-depleted infarcts, we performed histological analysis and found an accumulation of apoptotic cells in infarcts of mice treated with depleting antibody (Figure 5L and M).

Neutrophil depletion affects macrophage MertK expression after ischaemia reperfusion

Finally, to verify whether the effect of neutrophils in regulating MertK expression is also detectable in reperfused hearts, we subjected mice to transient ischaemia and reperfusion. The flow cytometric analysis confirmed a strong reduction of cardiac neutrophil counts in Ly6G-treated mice. Similar to the effect after permanent ligation, reperfused hearts of neutrophil-depleted mice had less Ly6C^{hi} monocytes 3 days post-infarction, but the number of macrophages was not significantly changed (Figure 6A and B). The latter effect might be explained by a reduction of infarct size ($28 \pm 5\%$) that we observed after neutrophil depletion in the reperfusion model (data not shown). Strikingly, the number of MertK^{hi} expressing macrophages was significantly lower in neutrophil-depleted reperfused hearts (Figure 6C), which was confirmed by western blot analysis in heart lysates (Figure 6D and E).

Discussion

Acute MI leads to death of a large number of cardiomyocytes, which induces an inflammatory process in order to remove the damaged

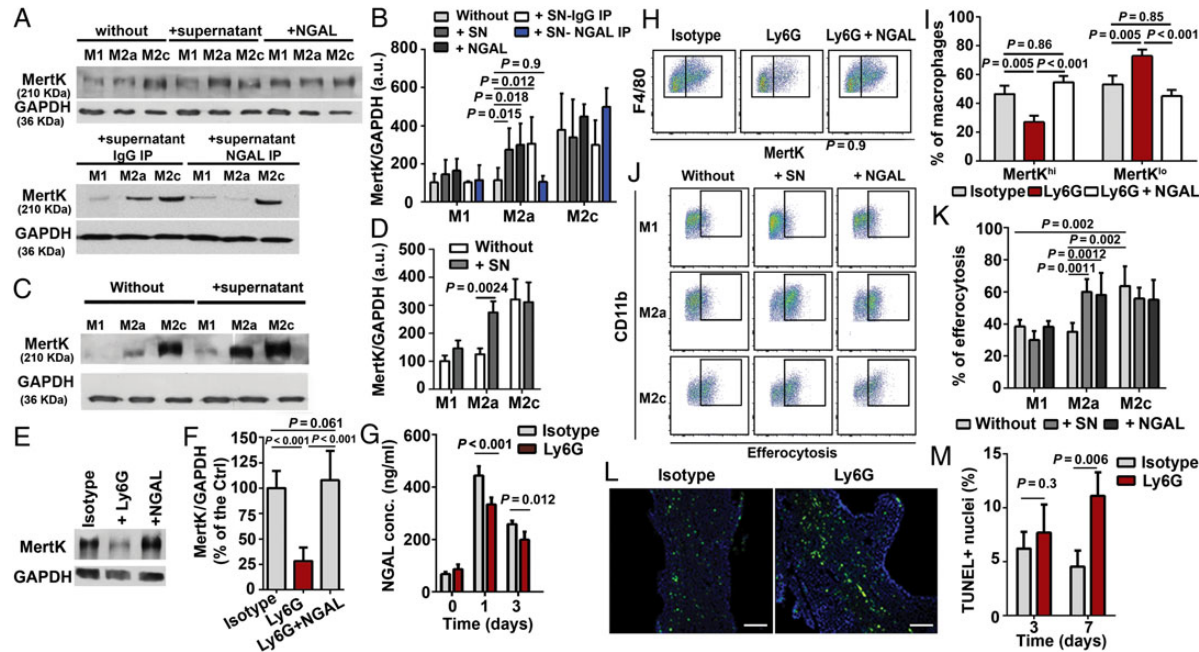


Figure 5 Neutrophils regulate macrophage polarization and efferocytosis. (A and B) Detection of MertK and GAPDH by western blot in murine bone marrow-derived macrophages. Upper blot: bone marrow-derived macrophages were polarized with IFN- γ (M1), IL-4 (M2a), or dexamethasone (M2c) alone or in the presence of neutrophil supernatant or recombinant murine neutrophil gelatinase-associated lipocalin (100 ng/mL). Lower blot: bone marrow-derived macrophages were polarized in the presence of neutrophil supernatant immunoprecipitated with anti-IgG or anti-neutrophil gelatinase-associated lipocalin. (B) Quantification of MertK band density, normalized to GAPDH, shown as arbitrary units. (C and D) Detection of MertK and GAPDH in polarized human macrophages incubated with human neutrophil supernatant ($n = 2$ donors). (E and F) Detection of MertK and GAPDH by western blot in hearts of isotype-treated, neutrophil-depleted (Ly6G), or Ly6G-treated mice co-injected with neutrophil gelatinase-associated lipocalin, 7 days after myocardial infarction. (F) Quantification of MertK band density, normalized to GAPDH and shown as relative expression compared with isotype. (G) Plasma levels of neutrophil gelatinase-associated lipocalin at baseline or after myocardial infarction. (H and I) Flow cytometric quantification of M2c (MertK^{hi}) and M2a macrophages (MertK^{lo}) in hearts of isotype-, Ly6G-, or Ly6G-treated mice co-injected with neutrophil gelatinase-associated lipocalin 5 days after myocardial infarction. (J and K) Efferocytosis of fluorescence-labelled apoptotic cardiomyocytes was measured by flow cytometry, after co-incubation of apoptotic cardiomyocytes with polarized bone marrow-derived macrophages. Polarization was performed in the presence or absence of neutrophil supernatant or recombinant mouse neutrophil gelatinase-associated lipocalin (100 ng/mL). (L) Representative TUNEL staining in infarcts of isotype or Ly6G-treated mice, 7 days after myocardial infarction. Scale bar, 200 μ m; $\times 5$ magnification. (M) Quantification of TUNEL-positive apoptotic cells per field of view. Data are mean \pm SD from (B, F, I, and K) three experiments and donor mice, (G) 8, or (M) 5 mice/group.

tissue. In acute inflammation, neutrophils are not only vital for clearing the wound from pathogens or debris but also for the resolution of inflammation and return to tissue homeostasis.⁹ In the context of MI, however, neutrophils are generally considered detrimental. They are recruited few hours after onset of MI and contribute to acute tissue injury, whereas their role in infarct healing has been largely neglected so far. Here, we provide evidence that neutrophils are required for resolving post-MI inflammation and cardiac healing. We show that neutrophil-depleted mice subjected to MI had worsened cardiac function, increased fibrosis, and a progressive increase in biomarkers associated with HF. This was accompanied by reduced cardiac expression of phagocytosis receptor MertK by macrophages and a worsened capacity to clear apoptotic cardiomyocytes.

The clearance of dead cardiomyocytes and inflammatory neutrophils is orchestrated by macrophages which are thought to derive from recruited Ly6C^{hi} monocytes.^{3,4} After an acute inflammatory phase mainly driven by pro-inflammatory macrophages, these cells

are replaced by reparative macrophages which facilitate wound healing and regeneration by promoting myofibroblast accumulation, collagen deposition, and angiogenesis. Wan and co-workers convincingly demonstrated that accurate clearance of dead cells is a prerequisite for favourable MI healing, whereas failed resolution promotes unfavourable cardiac remodelling which may ultimately result in HF.^{5,24} In agreement with this study, our data suggest that inefficient removal of dead cells due to impaired macrophage phenotypic shift in the absence of neutrophil secretome leads to a dysregulated healing response, excessive fibrosis, and progressive loss of ventricular function.

While sufficient myofibroblast density is important for replacing dead cardiac muscle by a robust scar, excessive myofibroblast numbers or inappropriate composition of collagen fibres in the infarcted ventricle might lead to myocardial stiffness,²⁵ contractile dysfunction, and progression of HF.^{26–28} In support of the hypothesis that neutrophil depletion may lead to HF, we found an up-regulation

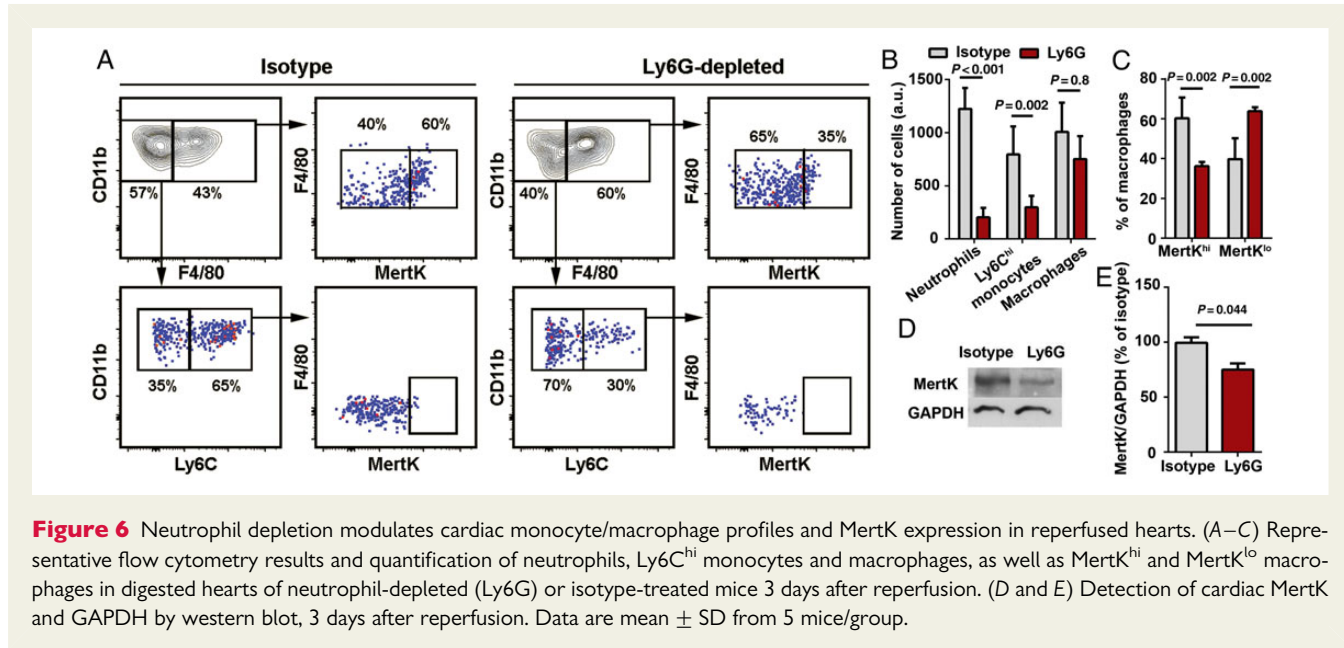


Figure 6 Neutrophil depletion modulates cardiac monocyte/macrophage profiles and MertK expression in reperfused hearts. (A–C) Representative flow cytometry results and quantification of neutrophils, Ly6C^{hi} monocytes and macrophages, as well as MertK^{hi} and MertK^{lo} macrophages in digested hearts of neutrophil-depleted (Ly6G) or isotype-treated mice 3 days after reperfusion. (D and E) Detection of cardiac MertK and GAPDH by western blot, 3 days after reperfusion. Data are mean \pm SD from 5 mice/group.

of cardiac and systemic markers associated with HF.^{14,29} Cardio-renal syndrome may occur as a result of cardiac dysfunction and hypoperfusion of the kidney leading to medullary ischaemia.³⁰ Indeed, we detected signs of acute kidney injury, which by itself is a prognostic factor associated with adverse outcome.¹⁶

We identified NGAL in the neutrophil secretome as a key inducer of macrophages with high efferocytosis capacity. Neutrophil gelatinase-associated lipocalin is released by activated neutrophils from specific granules, but also from other cells including macrophages, ischaemic cardiomyocytes, or injured kidney epithelial cells in acute renal injury.^{31–33} In the setting of *Streptococcus pneumoniae* infection, it was recently shown that NGAL skewed activated alveolar macrophages to a resolving phenotype expressing high levels of IL-10.³⁴ In skeletal muscle injury, the macrophages involved in muscle regeneration have been characterized as M2c macrophages that exhibit anti-inflammatory properties by releasing TGF- β and by neutralizing pro-inflammatory M1 macrophages.³⁵ In post-MI repair, M2c marker MertK-expressing macrophages play a crucial role in the clearance of cell debris.⁵

Our findings that neutrophils could contribute to improve cardiac healing and the outcome by influencing macrophage polarization are somewhat surprising, given that they are generally considered to play a detrimental role after post-MI revascularization. In fact, elevated circulating neutrophil counts or plasma levels of their released factors, including NGAL, are associated with poor prognosis and mortality in MI patients.^{7,36} We may speculate that a certain number of neutrophils and secretion products are required in the local cardiac microenvironment to promote reparative macrophage polarization. However, there might be a threshold level where the acute tissue damaging effects of neutrophils outweigh their resolving properties during MI healing. This is supported by clinical data reporting that associations between blood neutrophil counts and clinical outcomes are mainly evident in patients with neutrophilia (neutrophil counts $> 65\%$)³⁷ or in the highest tertile,^{38,39} respectively.

Our study has several limitations: First, the mouse model of permanent LAD occlusion, although widely used to study post-MI repair and remodelling, may have limited predictive value for human pathophysiology. Nevertheless, it is a valuable tool to dissect the function of, e.g. specific-cell populations and molecular pathways involved in post-MI healing, which provides the basis for more defined therapeutic approaches. In view of potential relevance for humans, it is promising that we could confirm the effect of neutrophil depletion on macrophage MertK expression in the ischaemia-reperfusion model, and we were also able to show the polarizing effect of human neutrophil secretome in human primary macrophages. In the future, additional studies with clinically more relevant large animal models are warranted before extrapolating a potential significance of our findings for humans. Second, we cannot exclude that additional factors other than NGAL might contribute to the polarizing effects of the neutrophil secretome on macrophages. Nevertheless, we identified NGAL as a key regulator of macrophage reprogramming both *in vitro* and *in vivo*. Finally, it is conceivable that neutrophil-derived factors might promote autocrine release of factors by the macrophages themselves that might facilitate their own phenotypic switch.³⁴ In the future, a better knowledge of the molecular regulators involved in macrophage reprogramming will help to answer these unresolved questions.

In conclusion, our data suggest that neutrophils participate in MI repair in a mouse model through the secretion of NGAL, thereby skewing macrophages towards a resolving phenotype which mediates efficient clearance of cell debris. This is a prerequisite for regulated fibrosis, scar formation and favourable cardiac remodelling.⁵ Our findings therefore have important clinical implications. Beyond their established pro-inflammatory role in acute post-MI injury, we identify neutrophils as pivotal modulators of the healing response after MI and consequently cardiac repair and function. This novel role for neutrophils should be taken in account when designing and applying ‘aggressive’ anti-neutrophil treatments in the setting of MI.

Authors' contributions

M.H. and D.S. performed statistical analysis. S.S., O.S., and C.W. handled funding and supervision. M.H., L.R., D.S., and M.S. acquired the data. S.S., O.S., and M.H. conceived and designed the research. S.S. drafted the manuscript. M.H., J.D., O.S., M.D., and D.S. made critical revision of the manuscript for key intellectual content.

Supplementary material

Supplementary material is available at *European Heart Journal* online.

Acknowledgements

The authors thank Cornelia Seidl for excellent technical assistance.

Funding

This work was supported in part by the Deutsche Forschungsgemeinschaft (STE-1053/3-1 to S.S., SO876/6-1, SFB1123 TP A6 and B5 to O.S., and SFB 1123 TP A1 to C.W.), the Netherlands Organisation for Scientific Research (VIDI project 91712303 to O.S.), and the European Research Council (ERC AdG °249929 to C.W.).

Conflict of interest: none declared.

References

- Frangogiannis NG. Regulation of the inflammatory response in cardiac repair. *Circ Res* 2012; **110**:159–173.
- Ma Y, Yabluchanskiy A, Lindsey ML. Neutrophil roles in left ventricular remodeling following myocardial infarction. *Fibrogenesis Tissue Repair* 2013; **6**:11.
- Dutta P, Nahrendorf M. Monocytes in myocardial infarction. *Arterioscler Thromb Vasc Biol* 2015; **35**:1066–1070.
- Nahrendorf M, Swirski FK. Monocyte and macrophage heterogeneity in the heart. *Circ Res* 2013; **112**:1624–1633.
- Wan E, Yeap XY, Dehn S, Terry R, Novak M, Zhang S, Iwata S, Han X, Homma S, Drosatos K, Lomasney JW, Engman DM, Miller SD, Vaughan DE, Morrow JP, Kishore R, Thorp EB. Enhanced efferocytosis of apoptotic cardiomyocytes through myeloid–epithelial–reproductive tyrosine kinase links acute inflammation resolution to cardiac repair after infarction. *Circ Res* 2013; **113**:1004–1012.
- Harel-Adar T, Ben Mordechai T, Amsalem Y, Feinberg MS, Leor J, Cohen S. Modulation of cardiac macrophages by phosphatidylserine-presenting liposomes improves infarct repair. *Proc Natl Acad Sci USA* 2011; **108**:1827–1832.
- Chia S, Nagurney JT, Brown DF, Raffel OC, Bamberg F, Senatore F, Wackers FJ, Jang IK. Association of leukocyte and neutrophil counts with infarct size, left ventricular function and outcomes after percutaneous coronary intervention for ST-elevation myocardial infarction. *Am J Cardiol* 2009; **103**:333–337.
- Guasti L, Dentali F, Castiglioni L, Maroni L, Marino F, Squizzato A, Ageno W, Gianni M, Gaudio G, Grandi AM, Cosentino M, Venco A. Neutrophils and clinical outcomes in patients with acute coronary syndromes and/or cardiac revascularisation. A systematic review on more than 34,000 subjects. *Thromb Haemost* 2011; **106**:591–599.
- Ortega-Gomez A, Perretti M, Soehnlein O. Resolution of inflammation: an integrated view. *EMBO Mol Med* 2013; **5**:661–674.
- Soehnlein O, Lindbom L. Phagocyte partnership during the onset and resolution of inflammation. *Nat Rev Immunol* 2010; **10**:427–439.
- Virag JAI, Lust RM. Coronary Artery Ligation and Intramyocardial Injection in a Murine Model of Infarction. *J Vis Exp* 2011; **52**:2581.
- Jolly SR, Kane WJ, Hook BG, Abrams GD, Kunkel SL, Lucchesi BR. Reduction of myocardial infarct size by neutrophil depletion: effect of duration of occlusion. *Am Heart J* 1986; **112**:682–690.
- Kakkar R, Lee RT. The IL-33/ST2 pathway: therapeutic target and novel biomarker. *Nat Rev Drug Discov* 2008; **7**:827–840.
- Deswal A, Petersen NJ, Feldman AM, Young JB, White BG, Mann DL. Cytokines and cytokine receptors in advanced heart failure: an analysis of the cytokine database from the Vesnarinone trial (VEST). *Circulation* 2001; **103**:2055–2059.
- Damas JK, Gullestad L, Ueland T, Solum NO, Simonsen S, Froland SS, Aukrust P. CXC-chemokines, a new group of cytokines in congestive heart failure – possible role of platelets and monocytes. *Cardiovasc Res* 2000; **45**:428–436.
- Hsu CY, Chertow GM, McCulloch CE, Fan D, Ordonez JD, Go AS. Nonrecovery of kidney function and death after acute on chronic renal failure. *Clin J Am Soc Nephrol* 2009; **4**:891–898.
- Swirski FK, Nahrendorf M, Etzrodt M, Wildgruber M, Cortez-Retamozo V, Panizzi P, Figueiredo JL, Kohler RH, Chudnovskiy A, Waterman P, Aikawa E, Mempel TR, Libby P, Weissleder R, Pittet MJ. Identification of splenic reservoir monocytes and their deployment to inflammatory sites. *Science* 2009; **325**:612–616.
- Mantovani A, Sica A, Sozzani S, Allavena P, Vecchi A, Locati M. The chemokine system in diverse forms of macrophage activation and polarization. *Trends Immunol* 2004; **25**:677–686.
- Jenkins SJ, Ruckerl D, Thomas GD, Hewitson JP, Duncan S, Brombacher F, Maizels RM, Hume DA, Allen JE. IL-4 directly signals tissue-resident macrophages to proliferate beyond homeostatic levels controlled by CSF-1. *J Exp Med* 2013; **210**:2477–2491.
- Mantovani A, Sozzani S, Locati M, Allavena P, Sica A. Macrophage polarization: tumor-associated macrophages as a paradigm for polarized M2 mononuclear phagocytes. *Trends Immunol* 2002; **23**:549–555.
- Mosser DM, Edwards JP. Exploring the full spectrum of macrophage activation. *Nat Rev Immunol* 2008; **8**:958–969.
- Zizzo G, Hilliard BA, Monestier M, Cohen PL. Efficient clearance of early apoptotic cells by human macrophages requires M2c polarization and MerTK induction. *J Immunol* 2012; **189**:3508–3520.
- Ohlsson SS, Lingé CP, Gullstrand B, Lood C, Johansson A, Ohlsson S, Lundqvist A, Bengtsson AA, Carlsson F, Hellmark T. Serum from patients with systemic vasculitis induces alternatively activated macrophage M2c polarization. *Clin Immunol* 2014; **152**:10–19.
- Heymans S, Luttun A, Nuyens D, Theilmeier G, Creemers E, Moons L, Dyspersin GD, Cleutjens JP, Shipley M, Angellilo A, Levi M, Nube O, Baker A, Keshet E, Lupu F, Herbert JM, Smits JF, Shapiro SD, Baes M, Borgers M, Collen D, Daemen MJ, Carmeliet P. Inhibition of plasminogen activators or matrix metalloproteinases prevents cardiac rupture but impairs therapeutic angiogenesis and causes cardiac failure. *Nat Med* 1999; **5**:1135–1142.
- Davis J, Molkentin JD. Myofibroblasts: trust your heart and let fate decide. *J Mol Cell Cardiol* 2014; **70**:9–18.
- Kehat I, Molkentin JD. Molecular pathways underlying cardiac remodeling during pathophysiological stimulation. *Circulation* 2010; **122**:2727–2735.
- Chaturvedi RR, Herron T, Simmons R, Shore D, Kumar P, Sethia B, Chua F, Vassiliadis E, Kentish JC. Passive stiffness of myocardium from congenital heart disease and implications for diastole. *Circulation* 2010; **121**:979–988.
- Zhang KW, French B, May Khan A, Plappert T, Fang JC, Sweitzer NK, Borlaug BA, Chirinos JA, St John Sutton M, Cappola TP, Ky B. Strain improves risk prediction beyond ejection fraction in chronic systolic heart failure. *J Am Heart Assoc* 2014; **3**:e000550.
- Rauchhaus M, Doehner W, Francis DP, Davos C, Kemp M, Liebenthal C, Niebauer J, Hooper J, Volk HD, Coats AJ, Anker SD. Plasma cytokine parameters and mortality in patients with chronic heart failure. *Circulation* 2000; **102**:3060–3067.
- Ronco C, Haapo M, House AA, Anavekar N, Bellomo R. Cardiorenal syndrome. *J Am Coll Cardiol* 2008; **52**:1527–1539.
- Yndestad A, Landro L, Ueland T, Dahl CP, Flo TH, Vinge LE, Espvik T, Froland SS, Husberg C, Christensen G, Dickstein K, Kjekshus J, Oie E, Gullestad L, Aukrust P. Increased systemic and myocardial expression of neutrophil gelatinase-associated lipocalin in clinical and experimental heart failure. *Eur Heart J* 2009; **30**:1229–1236.
- Hemdahl AL, Gabrielsen A, Zhu C, Eriksson P, Hedin U, Kastrup J, Thoren P, Hansson GK. Expression of neutrophil gelatinase-associated lipocalin in atherosclerosis and myocardial infarction. *Arterioscler Thromb Vasc Biol* 2006; **26**:136–142.
- Mishra J, Dent C, Tarabishi R, Mitsnefes MM, Ma Q, Kelly C, Ruff SM, Zahedi K, Shao M, Bean J, Mori K, Barasch J, Devarajan P. Neutrophil gelatinase-associated lipocalin (NGAL) as a biomarker for acute renal injury after cardiac surgery. *Lancet* 2005; **365**:1231–1238.
- Warszawska JM, Gawish R, Sharif O, Sigel S, Doninger B, Lakovits K, Mesteri I, Nairz M, Boon L, Spiel A, Fuhrmann V, Strobl B, Muller M, Schenk P, Weiss G, Knapp S. Lipocalin 2 deactivates macrophages and worsens pneumococcal pneumonia outcomes. *J Clin Invest* 2013; **123**:3363–3372.
- Arnold L, Henry A, Poron F, Baba-Amer Y, van Rooijen N, Plonquet A, Gherardi RK, Chazaud B. Inflammatory monocytes recruited after skeletal muscle injury switch into antiinflammatory macrophages to support myogenesis. *J Exp Med* 2007; **204**:1057–1069.

36. Lindberg S, Pedersen SH, Mogelvang R, Jensen JS, Flyvbjerg A, Galatius S, Magnusson NE. Prognostic utility of neutrophil gelatinase-associated lipocalin in predicting mortality and cardiovascular events in patients with ST-segment elevation myocardial infarction treated with primary percutaneous coronary intervention. *J Am Coll Cardiol* 2012;60:339–345.
37. Kyne L, Hausdorff JM, Knight E, Dukas L, Azhar G, Wei JY. Neutrophilia and congestive heart failure after acute myocardial infarction. *Am Heart J* 2000;139:94–100.
38. Arruda-Olson AM, Reeder GS, Bell MR, Weston SA, Roger VL. Neutrophilia predicts death and heart failure after myocardial infarction: a community-based study. *Circ Cardiovasc Qual Outcomes* 2009;2:656–662.
39. Zhang S, Wan Z, Zhang Y, Fan Y, Gu W, Li F, Meng L, Zeng X, Han D, Li X. Neutrophil count improves the GRACE risk score prediction of clinical outcomes in patients with ST-elevation myocardial infarction. *Atherosclerosis* 2015;241:723–728.

SUPPLEMENTARY DATA

Neutrophils orchestrate post-myocardial infarction healing by polarizing macrophages towards a reparative phenotype

Horckmans Michael, Ring Larisa, Duchene Johan, Santovito Donato, Schloss Maximilian,
Drechsler Maik, Weber Christian, Söhnlein Oliver, Steffens Sabine

Supplementary methods

Animal experiments

Female 10-12 week old C57BL/6J mice were purchased from Janvier Labs, France. Myocardial infarction (MI) was induced by permanent ligation of the left anterior descending coronary artery (LAD). Mice were anesthetized with midazolam (5 mg/kg), medetomidin (0.5mg/kg) and fentanyl (0.05 mg/kg), intubated and ventilated with a MiniVent mouse ventilator (Harvard Apparatus, Holliston, MA). A left thoracotomy was performed in the 4th left intercostal space, and the pericardium was incised. MI was induced by permanent ligation of the LAD proximal to its bifurcation from the main stem with monofilament nylon 8-0 sutures (Ethicon, Somerville, USA). In selective experiments, a transient LAD occlusion for 45 min followed by reperfusion was performed. A small piece of polyethylene tubing was used to secure the ligature without damaging the artery. After 45 min of ischemia, the LAD coronary artery occlusion was released and reperfusion occurred. Reperfusion was confirmed by visible restoration of color to the ischemic tissue. The chest wall and skin were closed with 5-0 nylon sutures (Ethicon, Sommerville, NJ). After surgery, naloxone (1,2mg/kg), flumazenil (0,5mg/kg) and atipamezol (2,5mg/kg) were injected to reverse the effect of anesthesia. Post-operative analgesia (buprenorphine; 0,1mg/kg) was given for the first 12h after surgery. Sham-operated animals were submitted to the same surgical protocol as described but without LAD occlusion. Neutrophil depletion was performed by intraperitoneal injection (i.p.) of monoclonal antibody clone 1A8 (50

μ g; BioXcell) at day -1, 0, 1, 3, 5 and 7 days of LAD ligation. Control mice received corresponding isotype (clone RG7/11.1; BioXcell) i.p. injections. In some experiments, mice received intramyocardial injections (in total 100 μ l through 5 injections of 20 μ l each) of neutrophil supernatant in the ischemic LAD territory using a 30-G Hamilton syringe.¹ Control animals received intramyocardial injections of vehicle (saline). To verify the cardiac injection method, control injections of calcein AM (Life science, Munich, Germany) into the myocardium were performed, confirming diffusion of the fluorescent dye within the area of interest (*Figure S3*). In other experiments, recombinant murine NGAL (100 μ g; R&D, Abingdon, United Kingdom) or vehicle (saline) was injected i.p. 1, 3 and 4 days after LAD ligation. The plasma levels of NGAL after injection of the recombinant protein were measured by ELISA, confirming that the plasma levels after injection were in the physiological range (*Figure S4*). Sample size for in vivo experiments was calculated in order to provide a statistical power >85% for an alpha <0.05 in detecting a population effect size > 0.8. Calculations were performed based on baseline distribution of study outcomes in control mice at steady state by using the G*Power software.² All animal experiments were approved by the local ethical committee (protocol 55.2-1-54-2532-176-13) and comply with institutional and national guidelines for the care and use of laboratory animals.

Echocardiography

Transthoracic echocardiography was performed on mildly anesthetized spontaneously breathing mice (sedated by inhalation of 1% isoflurane, 1L/min oxygen), using a Vevo 2100 High Resolution Imaging system equipped with a 40 MHz transducer (Visualsonics, Toronto, Canada). The mice were placed on a heated ECG platform. Left parasternal long axis view and left mid-papillary, apical and basal short axis views were acquired. End-diastolic volume, end-

systolic volume and ejection fraction were evaluated on the left parasternal long axis view. Long-axis B-mode images were recorded for longitudinal and radial strain analysis using the VevoStrain software following a recently published protocol.³

Quantification of infarct size

Hearts were perfused and harvested 24h after LAD ligation and sectioned into 4 equal transverse slices. The slices were incubated in 2% triphenyltetrazolium chloride (TTC) solution (Sigma-Aldrich, Munich, Germany) at 37°C for 15 min and fixed overnight in 4% formol at 4°C. Images were taken at 2x magnification, and quantification of viable (red) and infarct areas (white) was performed with Image J software.

Histology

Paraffin cross-sections (4 μ m) of infarcted hearts were cut, fixed in Bouin solution (Sigma-Aldrich) and stained with Masson trichrome (Sigma-Aldrich). Fibrosis was quantified as the relative area of blue staining (collagen) compared to the left ventricle surface, as an average of five sections per heart at the level of the papillary muscle, using Image J software. For Sirius red staining of collagen, sections were incubated with 0.1% Sirius red (Sigma-Aldrich) in saturated picric acid for 90 min. Sections were rinsed twice with 0.01 N HCl for 1 min and then immersed in water. After dehydration with ethanol for 30 seconds and cover-slipping, the sections were photographed with identical exposure settings under ordinary polychromatic or polarized light microscopy. Total collagen content was evaluated under polychromatic light. Interstitial collagen subtypes were evaluated using polarized light illumination; under this condition thicker type I collagen fibers appeared orange or red, whereas thinner type III collagen fibers were yellow or green. Quantifications were performed with LAS software (Leica). For

quantification of myofibroblasts and endothelial cells (microvessels), sections were stained with antibodies against smooth muscle actin (α SMA, Sigma-Aldrich) or CD31 (BD Biosciences, Heidelberg, Germany), respectively. Myofibroblast and microvessel density were quantified using Image J software by examining 10 fields per section at 20x magnification, in a blinded fashion. Apoptotic cells were stained with Tdt-mediated dUTP nick end labeling method (DeadEndTM Fluorometric TUNEL System, Promega). Sections were counterstained with Hoechst to visualize the entire population of cell nuclei within each myocardial section. Apoptotic cells were determined as ratio of TUNEL-positive to total amount of number of nuclei in 10 fields per section at 20x magnification, using Image J software. Paraffine longitudinal sections (4 μ m) of kidneys were stained with anti-galectin 3 antibody (clone M3/38, Biozol, Eching, Germany), a marker of kidney injury,⁴ and representative images were taken from the cortex and the medulla of kidneys. For all histological examinations, at least 3 sections per mouse were analyzed.

Flow cytometry

Hearts were harvested, perfused with saline to remove peripheral cells, minced with fine scissors, and digested with collagenase I (450U/ml), collagenase XI (125U/ml), hyaluronidase type I-s (60U/ml) and DNase (60U/ml) (Sigma-Aldrich and Worthington Biochemical Corporation, Lakewood, USA) at 37°C for one hour. The spleen was triturated through 100 μ m nylon mesh strainer and centrifuged at 15 minutes at 500 x g, 4°C. The resulting single cell suspensions were rinsed, resuspended in PBS/BSA 1% and incubated with antibodies CD45(clone 30F11), CD11b (clone M1/70), Ly6C (clone HK1.4), Ly6G (clone 1A8), F4/80 (clone BM8), KI-67 (clone SolA15) (all from BioLegend, San Diego, CA, USA) and MertK (AF591, R&D). Nuclear DNA staining with 7-aminoactinomycin D (7-AAD, Life Technologies)

was performed after fixation and permeabilization with an intracellular staining buffer set (eBioscience). Data were acquired on a FACS Canto II (BD Biosciences), and analysis was performed with FlowJo software (Ashland, USA).

Macrophage isolation and polarization

For bone marrow-derived macrophage (BMM) isolation, cells were flushed from femurs and tibia of mice and subjected to red blood cell lysis using ammonium chloride. Cells were plated onto petri dishes and cultured in DMEM medium with 10% fetal bovine serum, 1% penicillin-streptomycin and 20% L929 cell-conditioned medium (as a source for M-CSF) for 7 days, with a complete change of medium every 2–3 days. Macrophages were left untreated or converted to M1 macrophages by stimulation with IFN- γ (10 ng/ml, R&D, for 72 h). M2a or M2c were obtained by a 72h treatment with IL-4 (20 ng/ml, Cedarlane Labs, Burlington, ON, Canada) or dexamethasone (20 nM, Sigma-Aldrich), respectively.

To assess the role of neutrophil secretome or recombinant proteins in the polarization of macrophages, cells were incubated with 100 μ l of neutrophil supernatant (obtained from 10^7 neutrophils/ml) or with recombinant mouse NGAL (100 ng/ml, BioLegend), lactoferrin (10 μ g/ml, Sigma-Aldrich), Cramp (1 μ g/ml, Innovagen, Lund, Sweden), neutrophil elastase (5 μ M, R&D) or myeloperoxidase (5 μ M, R&D). For human macrophage isolation, monocytes were recovered from blood of healthy donors on a Ficoll (Lymphoprep Axis-Schield) density gradient and erythrocytes were lysed by ammonium chloride. Monocytes were resuspended at the density of 10^6 cells/ml, and seeded in six-well plates in RPMI 1640 medium (Invitrogen) supplemented with 10% heat-inactivated FBS (Invitrogen). Macrophages were differentiated from monocytes by culturing for 6 days in the presence of recombinant human M-CSF (50 ng/ml, Peprotech, London, UK). Human M1 macrophages were polarized by incubating for 48h with IFN γ (20

ng/ml, R&D). For M2a and M2c polarization, macrophages were exposed for 48h to IL-4 (20 ng/ml; R&D) or dexamethasone (20 nM, Sigma-Aldrich), respectively.

Neutrophil supernatant

For neutrophil isolation, cells were flushed from femurs and tibia of mice and separated by Percoll gradient. After red cell lysis with ammonium chloride, neutrophils were stimulated for 30 min at 37°C with fibrinogen-coated beads at a density of 10^7 cells/ml, and supernatants were subsequently harvested by centrifugation. Human neutrophils were recovered from blood of healthy donors on a Ficoll (Lymphoprep, Axis-Schield) density gradient and erythrocytes were lysed by ammonium chloride. Neutrophils were resuspended at a density of 10^7 cells/ml and stimulated with fibrinogen-coated beads as described above.

Western blot

Hearts or macrophages were lysed for 10 min on ice in 200 μ l RIPA lysis buffer (50 mM Tris, 150 mM NaCl, 1% Triton X-100, 0.5% sodium deoxycholate, 0.1% SDS, pH 8.0) containing protease inhibitor cocktail (Roche Diagnostics, Penzberg , Germany). Lysates were mixed 5:1 with 5x Laemmli buffer (0.625 M Tris-HCl, 10% SDS (w/v), 50% glycerine, under reducing conditions with 25% DTT, bromophenol blue, pH 6.8) and incubated for 5 min at 70 C. The membrane was blocked for 1h at room temperature (RT) with blocking buffer consisting of 5% (w/v) non-fat dry milk in TBST (50 mM Tris-buffered saline, 150 mM NaCl, 0.05% Tween 20, pH 7.5). MertK was detected with anti-MertK antibody (AF591, 1:1000, R&D) followed by anti-goat-HRP (1:5000, Cell Signalling, Danvers, MA, USA) as secondary antibody. Incubation with antibodies was carried out in 0.5% (w/v) non-fat dry milk in TBST overnight (primary

antibody) or for 1h (secondary antibody) at RT. Visualization was accomplished using Chemiluminescence Reagent Plus (Roche Diagnostics) and X-ray films (Hyperfilms ECL, GE Healthcare, Munich, Germany).

NGAL immunoprecipitation

Under sterile conditions, 1.8 mg of protein G-conjugated magnetic beads (Dynabeads®, Life Technologies) were incubated with 14.4 µg of goat polyclonal anti-NGAL antibody (AF1857, R&D System) or 14.4 µg of normal goat IgG (Santa Cruz Biotechnology), used as negative control. Then, the antibody-conjugated beads were incubated overnight at 4°C with 500 µL of conditioned medium obtained from activated mouse neutrophils as described above. After incubation, the samples were placed on the magnet for 1 min and the supernatants were collected for the subsequent treatment of macrophages. The bead-antibody-antigen complexes were washed 3 times, and resuspended in 100 µL of washing buffer. Efficiency of immunoprecipitation was tested by Western blot (*Figure S5*). Briefly, 15 µL of conditioned medium (input sample), NGAL- and normal IgG-immunoprecipitated complexes (output samples), and immunodepleted supernatants (wash samples) were separated on SDS-PAGE and then transferred on PVDF membrane. After blocking in 10% non-fat milk for 3 hours, the membranes were incubated overnight at 4°C with 0.2 µg/mL anti-NGAL primary antibody (AF1857, R&D System). Blots were incubated with HRP-conjugated donkey anti-goat as secondary antibody diluted 1:2000 (Santa Cruz Biotechnologies) for 30 min before detection.

Quantitative real time PCR

Whole RNA from lysed hearts (TissueLyser LT, Qiagen) or cells was extracted (RNeasy mini kit, Qiagen) and reverse transcribed (PrimeScript™ RT reagent kit, Clontech). Real-time

PCR was performed with the 7900HT Sequence Detection System (Applied Biosystems) using the KAPA PROBE FAST Universal qPCR kit (Peqlab, Erlangen, Germany) and predesigned primer and probe mix (TaqMan® Gene Expression Assays, Life Technologies). Messenger RNA expression of markers of interest was normalized to HPRT, and the fold induction was calculated by the comparative C_t method.

Efferocytosis

Adult mouse cardiomyocytes from 10-week-old mice were isolated using collagenase I (450U/ml) digestion. Single cell suspensions were plated on tissue culture-treated dishes for 1h. Then, non-adherent cardiomyocytes were collected and stained with calcein AM (Life Science, Munich, Germany). For the induction of apoptosis, cardiomyocytes were exposed to UV irradiation for 10 min, followed by incubation at 37°C for 2 h. For phagocytosis, macrophages were co-cultured with apoptotic cardiomyocytes at 37°C for 60 minutes, then washed thoroughly with PBS to remove nonengulfed apoptotic cells. Phagocytosis efficiency (%) was quantified by flow cytometry and subsequent calculation of calcein-positive macrophages divided by the total number of macrophages.

ELISA

Plasma NGAL levels were measured by enzyme-linked immunosorbent assay (ELISA, DuoSet, R&D systems). Plasma chemokines and cytokines were measured with ProcartaPlex™ Multiplex Immunoassay (eBioscience).

Creatinine measurement

Plasma creatinine levels were measured by a commercially available colorimetric assay kit (Abcam).

Statistical analysis

All data are expressed as mean \pm SD, and statistical analysis was performed with Prism Software (version 6; GraphPad, CA). Endpoint comparisons between 2 groups were performed using unpaired 2-tailed Student's *t* test. For multiple comparisons, false discovery rate according Benjamini-Hochberg was applied to control for type I false positive errors, FDR was set to 0.05. For parallel repeated-measures studies, 2-way ANOVA was used with Bonferroni post-hoc evaluation to determine the significance for individual time points. A 2-tailed $P < 0.05$ was considered as significant.

References

1. Virag JAI, Lust RM. Coronary Artery Ligation and Intramyocardial Injection in a Murine Model of Infarction. *Journal of Visualized Experiments : JoVE* 2011(52):2581.
2. Faul F, Erdfelder E, Buchner A, Lang AG. Statistical power analyses using G*Power 3.1: tests for correlation and regression analyses. *Behav Res Methods* 2009;41(4):1149-60.
3. Bauer M, Cheng S, Jain M, Ngoy S, Theodoropoulos C, Trujillo A, Lin FC, Liao R. Echocardiographic speckle-tracking based strain imaging for rapid cardiovascular phenotyping in mice. *Circ Res* 2011;108(8):908-16.
4. Nishiyama J, Kobayashi S, Ishida A, Nakabayashi I, Tajima O, Miura S, Katayama M, Nogami H. Up-regulation of galectin-3 in acute renal failure of the rat. *Am J Pathol* 2000;157(3):815-23.

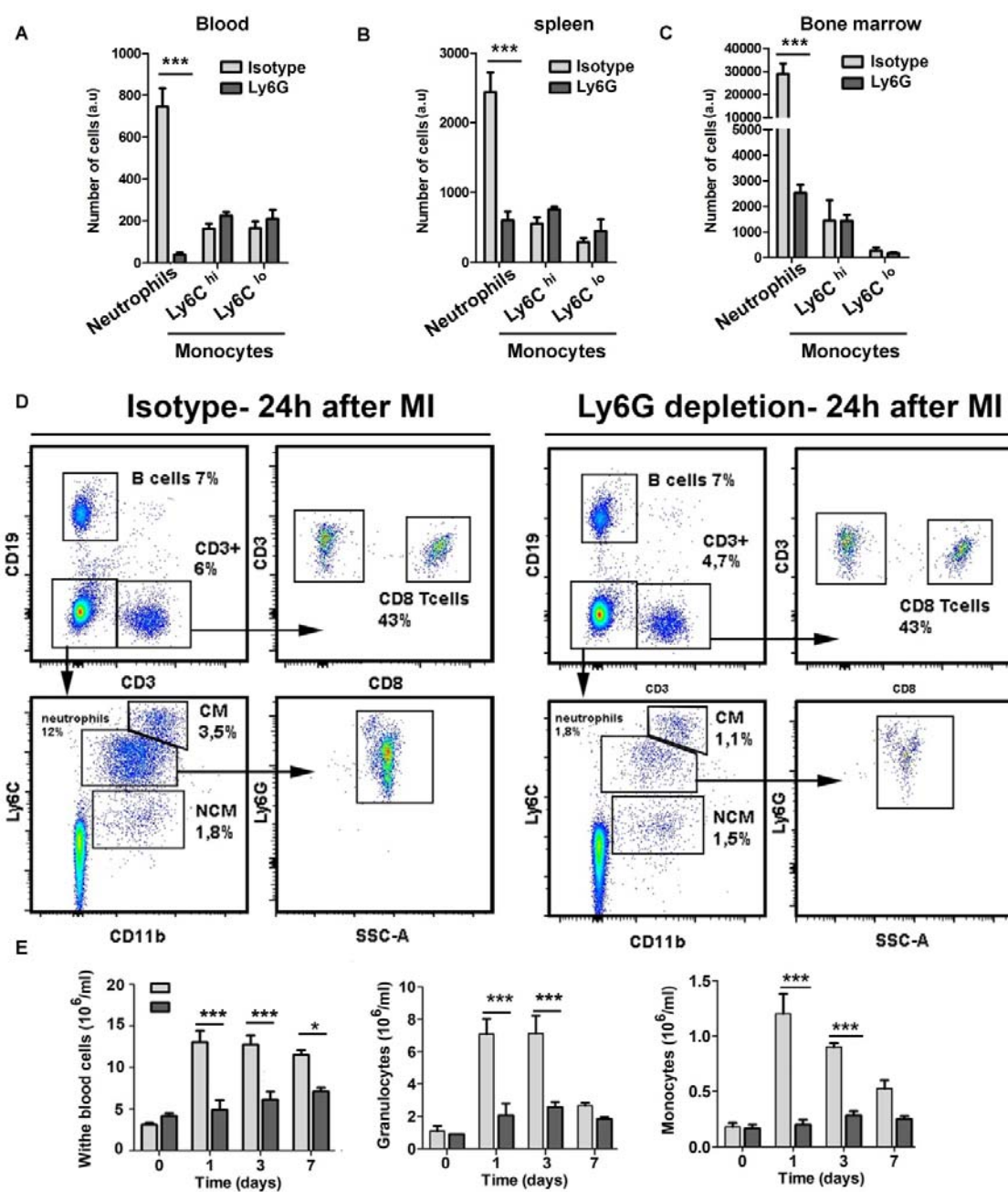
Supplementary data

Supplementary Table

		day 0		day 3		day 7		day 14		
Parameters		(mm)	Isotype	Ly6G	Isotype	Ly6G	Isotype	Ly6G	Isotype	Ly6G
IVSs		1,18± 0,152	1,16±0,18	1,12±0,09	1,03±0,06	1,20±0,09	1,01±0,05	1,21±0,05	1,07±0,1	
IVSd		0,71±0,08	0,77±0,08	0,75±0,07	0,70±0,03	0,83±0,08	0,70±0,06	0,82±0,04	0,87±0,1	
LVPWs		0,99 ± 0,06	1,07 ± 0,12	1,09 ± 0,06	1,20 ± 0,1	1,38 ± 0,13	1,43 ± 0,17	1,23 ± 0,06	1,38 ± 0,07	
LVPWd		0,88 ± 0,09	0,97 ± 0,1	1,03 ± 0,05	1,04 ± 0,07	1,32 ± 0,14	1,23 ± 0,10	0,91 ± 0,06	1,05 ± 0,05	

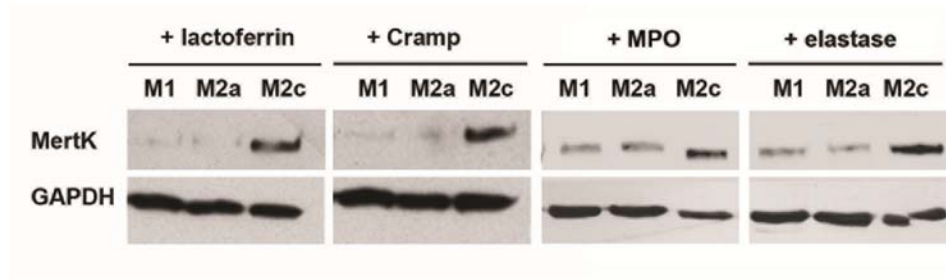
Supplementary Table S1: Structural echocardiography parameters of isotype and Ly6G-treated mice. Values are mean ± s.e.m. (n=8); IVSs, systolic inter ventricular septum thickness; IVSd, diastolic inter ventricular septum thickness; LVPWd, diastolic left ventricular posterior wall thickness; LVPWs, systolic left ventricular posterior wall thickness.

Supplementary Figures

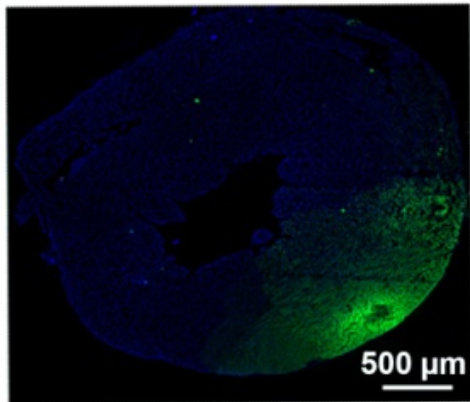


Supplementary Figure S1: Circulating leukocytes in neutrophil-depleted mice under steady state and after myocardial infarction. (A-C) Flow cytometric analysis of granulocytes, Ly6C^{hi} and Ly6C^{lo} monocytes in the blood, spleen and bone marrow of neutrophil-depleted (Ly6G) or isotype-treated mice under steady state, measured 5 days after injection at day -1, 0, 1, 3, 5 before harvest (n = 3 mice per group). (D) Gating strategy used for the quantification of neutrophils and

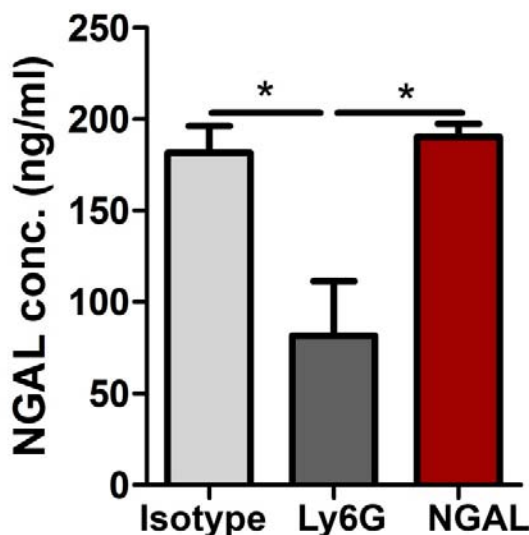
monocytes in blood after myocardial infarction. CM, classical monocytes (Ly6C^{hi}); NCM, non-classical monocytes (Ly6C^{lo}) (**E**) Blood counts of white blood cells, granulocytes and monocytes in neutrophil-depleted (Ly6G) or isotype-treated mice were measured with blood counter (scil Vet abc) at indicated time points after MI (n = 8 mice per group). *P < 0.05, ***P < 0.001 versus isotype as determined by two-way ANOVA with Bonferroni post test.



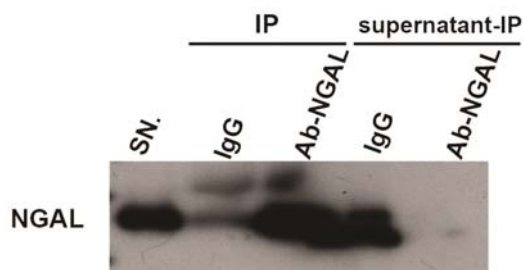
Supplementary Figure S2: Lactoferrin, Cramp, myeloperoxidase (MPO), and neutrophil elastase do not affect macrophage polarization. Representative Western blot of MertK expressed in bone marrow-derived murine macrophages. Macrophages were polarized with INF γ (M1), IL-4 (M2a) or dexamethasone (M2c), respectively, in presence of recombinant lactoferrin (10 μ g/ml), Cramp (1 μ g/ml), MPO (5 μ M), or neutrophil elastase (5 μ M).



Supplementary Figure S3 Validation of cardiac injection method. Local diffusion of injected green fluorescent calcein within the left ventricle around injection sites.



Supplementary Figure S4 Plasma levels of NGAL in neutrophil-depleted mice subjected to MI, after injection of recombinant NGAL, compared to the plasma levels in non-depleted mice (IgG) and depleted (Ly6G) mice, measured 1 day after MI. (For comparison, part of the data shown in Fig. 5G are represented on this graph.) Data are mean \pm SEM, n=3-8 mice per group.



Supplementary Figure S5 Immunodepletion of NGAL. Representative Western blot for the detection of NGAL in murine neutrophil supernatant without immunoprecipitation (SN) or in immunoprecipitated fraction (IP) and supernatant after IP. The IP was performed with IgG as negative control or anti-NGAL antibody (Ab-IgG).

6. Veröffentlichung II

Maximilian J Schloss, Michael Horckmans, Katrin Nitz, Johan Duchene, Maik Drechsler, Kiril Bidzhekov, Christoph Scheiermann, Christian Weber, Oliver Soehnlein, Sabine Steffens.

The time-of-day of myocardial infarction onset affects healing through oscillations in cardiac neutrophil recruitment.

EMBO Molecular Medicine. August 2016; 8(8): 937-48.

Die Originalarbeit unterlag einem Review-Verfahren. Der Impact-Faktor lag 2016 bei 9.249 Punkten.

In der zweiten Veröffentlichung wurden die Versuchsvorbereitungen, Datenerhebungen sowie Auswertungen eigenständig von mir durchgeführt. Das Manuskript wurde zunächst von mir verfasst und anschließend durch Frau Professor Sabine Steffens revidiert und in gemeinsamer Arbeit in seine endgültige Fassung gebracht. Die Graphen, Abbildungen und Schemata habe ich selbstständig erstellt und überarbeitet. Die statistische Auswertung erfolgte eigenständig durch mich. Koautoren standen unterstützend bei speziellen Fragestellungen, bei der Durchführung von Versuchen und für die intellektuelle Diskussion zur Verfügung.

The time-of-day of myocardial infarction onset affects healing through oscillations in cardiac neutrophil recruitment

Maximilian J Schloss¹, Michael Horckmans¹, Katrin Nitz^{1,2}, Johan Duchene¹, Maik Drechsler^{1,3,4}, Kiril Bidzhekov¹, Christoph Scheiermann⁵, Christian Weber^{1,3,6}, Oliver Soehnlein^{1,3,4} & Sabine Steffens^{1,3,*}

Abstract

Myocardial infarction (MI) is the leading cause of death in Western countries. Epidemiological studies show acute MI to be more prevalent in the morning and to be associated with a poorer outcome in terms of mortality and recovery. The mechanisms behind this association are not fully understood. Here, we report that circadian oscillations of neutrophil recruitment to the heart determine infarct size, healing, and cardiac function after MI. Preferential cardiac neutrophil recruitment during the active phase (Zeitgeber time, ZT13) was paralleled by enhanced myeloid progenitor production, increased circulating numbers of CXCR2^{hi} neutrophils as well as upregulated cardiac adhesion molecule and chemokine expression. MI at ZT13 resulted in significantly higher cardiac neutrophil infiltration compared to ZT5, which was inhibited by CXCR2 antagonism or neutrophil-specific CXCR2 knockout. Limiting exaggerated neutrophilic inflammation at this time point significantly reduced the infarct size and improved cardiac function.

Keywords circadian rhythm; fibrosis; myocardial infarction healing; neutrophils; progenitors

Subject Categories Cardiovascular System; Immunology

DOI 10.15252/emmm.201506083 | Received 20 November 2015 | Revised 21 April 2016 | Accepted 26 April 2016

Introduction

The incidence of cardiovascular events, such as MI, ischemic stroke, and arrhythmias, exhibits time-of-day dependency in humans, peaking around the sleep-to-wake transition period (Muller *et al*, 1987a,b; Chen & Yang, 2015). The underlying mechanisms for this time-of-day

dependency are thought to involve circadian fluctuations of glucocorticoids and catecholamines, blood pressure, heart rate, blood viscosity, and platelet reactivity, thereby predisposing for plaque rupture and thrombus formation (Tofler *et al*, 1987; Chen & Yang, 2015). In addition to the increased prevalence of MI in the morning, experimental and clinical evidence suggests that the outcome after MI exhibits a similar time-of-day dependency. A circadian variation of infarct size has first been described in a mouse model of ischemia/reperfusion, showing significantly larger infarct size, fibrosis, and adverse remodeling after ischemia onset at the sleep-to-wake transition period (Durgan *et al*, 2010). Likewise, several clinical studies reported a correlation between infarct size assessed by peak creatine kinase and the time-of-day of ischemia onset (Suarez-Barrientos *et al*, 2011; Fournier *et al*, 2012; Reiter *et al*, 2012).

In recent years, circadian oscillations of immune cell functions and circulating mediators (e.g. hematopoietic stem cells, glucocorticoids) have emerged (Scheiermann *et al*, 2013). Circulating leukocytes oscillate between blood and peripheral tissue, peaking in mice at ZT5 (where ZT0 refers to lights on and ZT12 to lights off) in the blood and at ZT13 in muscle tissue and bone marrow (Scheiermann *et al*, 2012). In humans, which have an opposing sleep–wake cycle, blood neutrophils oscillate throughout the day with an amplitude of $0.31 \text{ } 10^9/\text{l}$ and a high point around 8:30 pm (Sennels *et al*, 2011). These fluctuations in immune cell trafficking into tissues coincide with sensitivity to acute inflammatory stimuli, being highest at the beginning of the active phase (Scheiermann *et al*, 2013). Whether these oscillations in immune cell activity occur in the heart after an infarction and which consequences this would have on myocardial healing is unknown.

High numbers of circulating neutrophils are generally considered detrimental for post-MI outcome (Kyne *et al*, 2000; Chia *et al*, 2009). Neutrophils massively infiltrate the ischemic myocardium within the first 24 h post-MI, especially when reopening of the

¹ Institute for Cardiovascular Prevention (IPEK), Ludwig-Maximilians-University (LMU) Munich, Munich, Germany

² Max Delbrück Center for Molecular Medicine in the Helmholtz Association, Berlin, Germany

³ German Centre for Cardiovascular Research (DZHK), partner site Munich Heart Alliance, Munich, Germany

⁴ Department of Pathology, Amsterdam Medical Center (AMC), Amsterdam, The Netherlands

⁵ Walter-Brendel-Center of Experimental Medicine, Ludwig-Maximilians-University (LMU) Munich, Munich, Germany

⁶ Department of Biochemistry, Cardiovascular Research Institute Maastricht (CARIM), Maastricht University, Maastricht, The Netherlands

*Corresponding author. Tel: +49 89 4400 54674; E-mail: sabine.steffens@med.uni-muenchen.de

occluded coronary artery is achieved (Frangogiannis, 2012). Depleting neutrophils during the reperfusion phase limited acute tissue injury in experimental models (Romson *et al.*, 1983; Litt *et al.*, 1989). Nevertheless, despite their detrimental role during the acute post-ischemic inflammatory role, a limited number of neutrophils might be important for coordinated resolution of post-MI inflammation and repair (Frangogiannis, 2012). This is supported by our own recent findings that neutrophil depletion in a mouse model of permanent LAD occlusion negatively affects cardiac healing after MI (when induced during the acrophase of neutrophils in the blood, ZT5; Horckmans *et al.*, 2016).

In the present study, we raised the question whether the magnitude of neutrophil-driven inflammatory response and quality of the healing response in a murine MI scenario is influenced by circadian oscillations of neutrophil recruitment to the heart. We found that the migration of neutrophils to the heart preferentially occurs during the active phase (ZT13). MI at this time point resulted in significantly higher cardiac neutrophil infiltration, in a CXCR2-dependent manner. Consequently, an ischemic event occurring during the active phase resulted in an exaggerated neutrophilic inflammation and worsened cardiac repair. Limiting neutrophil counts at this time point reduced the infarct size and improved cardiac function. Our findings suggest that the time-of-day of ischemia onset is a critical determinant when considering anti-inflammatory treatments for improving MI outcome.

Results

Circadian oscillations of neutrophils in the mouse heart under steady state

We first investigated whether a rhythmic recruitment of neutrophils to the cardiac muscle occurs, as previously reported for skeletal muscle (Scheiermann *et al.*, 2012). The analysis of blood counts in resting WT mice confirmed a peak of blood granulocyte counts at ZT5 and lowest levels around ZT13 (Fig 1A). The flow cytometric analysis of digested hearts revealed more than twofold higher neutrophil counts in the myocardium at ZT13 compared to ZT5 (Fig 1B). We also performed immunohistological staining which revealed the presence of a limited number of neutrophils in the healthy myocardium, with markedly more cells at ZT13 compared to ZT5 (Fig 1C). In support of enhanced adhesion and subsequent extravasation of neutrophils into the cardiac tissue, cardiac ICAM-1 and VCAM-1 adhesion molecule mRNA expression increased during the active phase (ZT13-17; Fig 1D), which was paralleled by enhanced mRNA levels of chemokines mediating neutrophil chemotaxis, that is, CXCL1, CXCL2, CXCL5, CCL3, and CCL5 (Fig 1D). Analysis of the corresponding chemokine receptor for CXCL1, CXCL2, and CXCL5 on circulating and cardiac neutrophils, CXCR2, revealed an increased expression level in both compartments at ZT13 (Fig 1E).

Increased cardiac neutrophil infiltration after MI during active phase is associated with enhanced myelopoiesis and neutrophil mobilization

We next investigated whether onset of MI during the peak of cardiac neutrophil counts would lead to increased neutrophil recruitment.

Indeed, mice subjected to LAD occlusion at ZT13 had higher neutrophil counts in the heart 12–24 h post-MI compared to ZT5 infarcts (Fig 2A). Of note, 12 h post-MI induced at ZT13 is the time point when oscillating neutrophil counts in tissues are lowest under steady-state condition. Neutrophils were mobilized from the bone marrow, resulting in a significant decrease in neutrophil counts in femurs 12–24 h post-MI, which was much more dramatic in ZT13-infarcted mice (Fig 2B). In line with enhanced cardiac infiltration after ZT13 MI, blood counts of granulocytes tended to be lower in mice with ZT13 MI compared to ZT5 MI (12–24 h post-MI), albeit the differences were not significant (Fig 2C). To confirm the relevance of circadian time and light for the reported effects on cardiac neutrophil recruitment, we entrained mice to an inverted light cycle. Under these conditions, we found a similar increase in cardiac neutrophil recruitment and enhanced bone marrow mobilization 24 h after ZT13 MI compared to ZT5 MI (Fig 2D).

To better understand the mechanisms of neutrophil mobilization, we further assessed progenitor numbers in the bone marrow. We found higher baseline granulocyte-monocyte progenitor (GMP) counts in the bone marrow at ZT13 compared to ZT5, which were even higher 24 h after MI (Fig 2E). In agreement with published data (Mendez-Ferrer *et al.*, 2008), bone marrow levels of the retention signal CXCL12 decreased from ZT5 to ZT13; however, there was no further reduction in the bone marrow of ZT13-operated mice (Fig 2F). We therefore reasoned that enhanced neutrophil mobilization after MI at ZT13 might be triggered by enhanced circulating levels of neutrophil chemoattractants. We found a remarkable upregulation of TNF- α , CXCL1, CXCL2, CCL3, CCL5, and G-CSF levels in the plasma of ZT13- versus ZT5-operated mice 24 h post-MI (Fig 2G). Of note, no difference in chemokine and cytokine plasma levels between ZT5 and ZT13 was found without infarction, and there was no induction of CXCL5 plasma levels after MI.

MI during active phase leads to larger infarcts and reduced cardiac function

In support of the concept that exaggerated neutrophil presence in ZT13-infarcted hearts results in increased cardiac damage, mice subjected to LAD occlusion at ZT13 resulted in larger infarcts compared to mice with ZT5 MI (Fig 3A). The morphometric analysis was confirmed by elevated plasma levels of troponin I (Fig 3B) and higher numbers of dead cardiomyocytes after ZT13 MI (Fig 3C). A similar increase in troponin I levels was observed in infarcted mice with shifted light cycle (Appendix Fig S1). The mortality rate after ZT13 MI was significantly higher than after ZT5 MI, with increased incidence of ventricular rupture in this group (Fig 3D).

In agreement with larger infarcts, ZT13 infarcts had more myofibroblasts 7 days after MI (Fig 3E and Appendix Fig S2A), resulting in an increased area of fibrosis (Fig 3F). However, the anterior wall thickness was significantly reduced in ZT13 infarcts. More detailed analysis of the collagen composition revealed lower density of thicker collagen type I fibers in ZT13 infarcts (Fig 3G and Appendix Fig S2B). Thus, insufficient stabilization of the infarct scar might contribute to the increased incidence of ventricular rupture after ZT13 MI. Mice with ZT13 infarcts also had significantly lower ejection fractions at day 3 to day 14 compared to mice subjected to MI at ZT5, as well as significant increase in the left ventricular end-diastolic and end-systolic volume (Fig 3H).

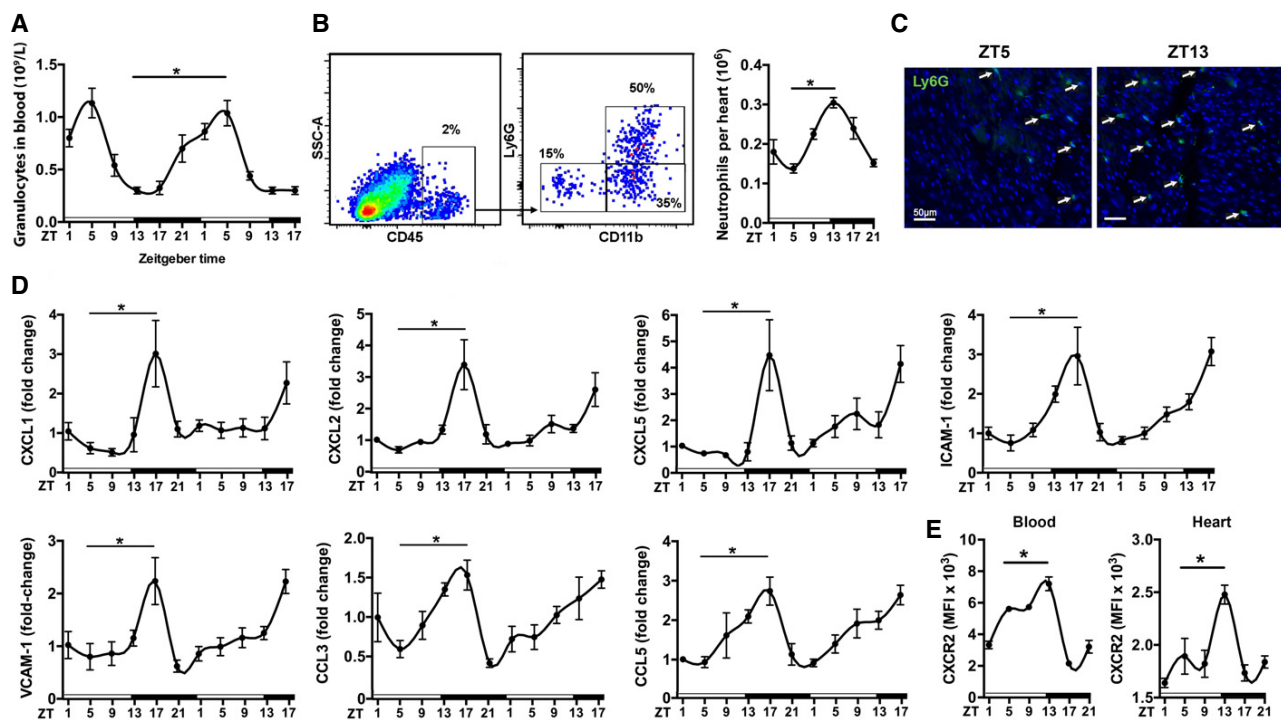


Figure 1. Circadian oscillations of neutrophils, adhesion molecules, and chemokines in the mouse heart at steady state.

- A Baseline blood counts of granulocytes. One-way ANOVA; $n = 8$ mice per ZT; $*P = 0.0001$ ZT5 versus ZT13.
- B Flow cytometric quantification of neutrophils in digested hearts. The representative dot plots show the gating strategy for cardiac neutrophils ($\text{CD45}^+\text{Ly6G}^+\text{CD11b}^+$) at ZT5. One-way ANOVA; $n = 5$ mice per ZT; $*P = 0.0001$ ZT5 versus ZT13.
- C Representative immunostainings for neutrophils in the myocardium (left ventricle), identified as Ly6G positive ($20\times$ magnification).
- D Cardiac mRNA expression levels normalized to HPRT. One-way ANOVA; $n = 5$ mice per ZT; ZT5 versus ZT17: $*P = 0.0064$ (CXCL1), $*P = 0.0007$ (CXCL2), $*P = 0.0007$ (CXCL5), $*P = 0.0001$ (ICAM-1), $*P = 0.0009$ (VCAM-1), $*P = 0.0181$ (CCL3), $*P = 0.0360$ (CCL5).
- E Mean fluorescence intensity (MFI) of CXCR2 expression by neutrophils in blood and heart. One-way ANOVA; $n = 3$ mice for ZT1, ZT17, ZT21 and $n = 5$ for ZT5, ZT9, ZT13; ZT5 versus ZT13: $*P = 0.0425$ (blood), $*P = 0.0078$ (heart).

Data information: All data are expressed as mean \pm SEM.

Reduction in neutrophil-mediated inflammation during active phase preserves cardiac function after MI

To confirm that the larger infarct size and decreased cardiac function after ZT13 MI are mainly driven by an exaggerated neutrophilic inflammatory response, we investigated whether systemic reduction in neutrophils would limit this process. Mice subjected to MI at ZT13 received neutrophil-depleting Ly6G antibody (Fig 4A), resulting in a significant reduction in cardiac neutrophils (Fig 4B), approximately to the levels observed at ZT5 reported in Fig 3, and lower plasma levels of pro-inflammatory cytokine TNF- α 24 h after MI (Fig 4C). Mice with ZT13 MI receiving anti-Ly6G had significantly smaller infarcts and lower plasma troponin I levels compared to isotype-treated controls, whereas anti-Ly6G treatment of mice with ZT5 MI had no effect (Fig 4D). This is in agreement with our recently published data (Horckmans *et al*, 2016). Moreover, ZT13 infarcts of Ly6G-treated mice had less fibrosis and thicker left ventricular anterior wall (Fig 4E) with significantly more collagen type I fibers (Fig 4F), and a higher ejection fraction as well as less ventricular dilatation (Fig 4G).

Enhanced cardiac neutrophil recruitment during the active phase is CXCR2 dependent

To further explore the underlying mechanisms of circadian neutrophil recruitment to the myocardium, we focused on CXCR2, as its expression levels coincided with the peak of neutrophils in the heart (Fig 1E). There is emerging evidence that circulating neutrophils are heterogeneous, due to aging and replenishment from the bone marrow (Casanova-Acebes *et al*, 2013). Previous *in vitro* findings have suggested that aged neutrophils exhibit reduced chemotactic activity and ability to respond to inflammatory stimuli (Whyte *et al*, 1993). Similar to the oscillations at baseline, we found significantly higher percentage of CXCR2^{hi}-expressing neutrophils in the blood of mice subjected to MI at ZT13 compared to ZT5 MI, with highest levels 8 h after ZT13 MI (Fig 5A). All cardiac neutrophils were CXCR2 positive regardless of the time point of LAD occlusion (measured 12 h post-MI at ZT5 versus ZT13); however, the level of CXCR2 surface expression was much higher at ZT13 compared to ZT5 (Fig 5B). In order to clarify the causal relationship between time-of-day-dependent changes in CXCR2 expression levels on circulating neutrophils and their recruitment to the ischemic

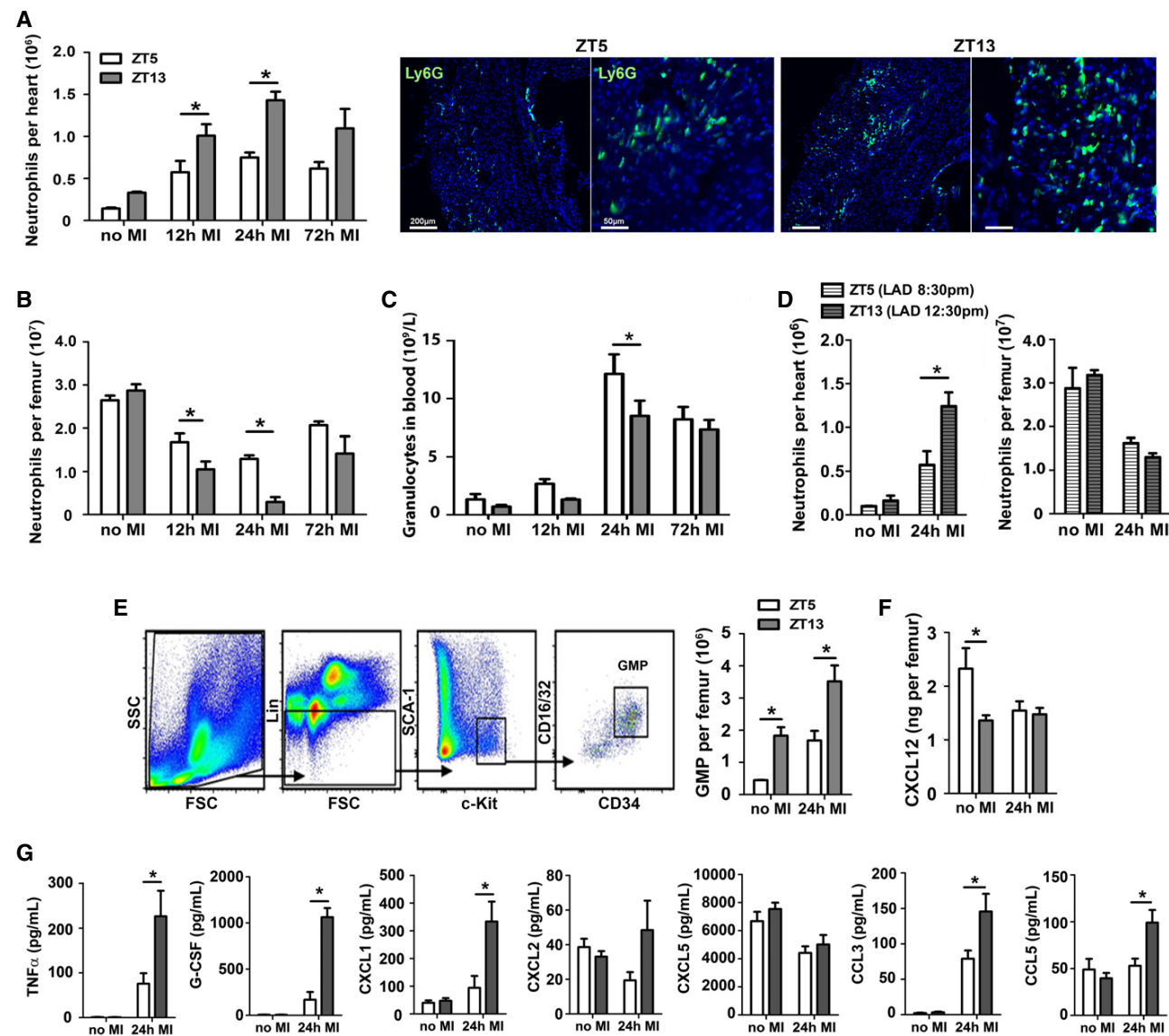
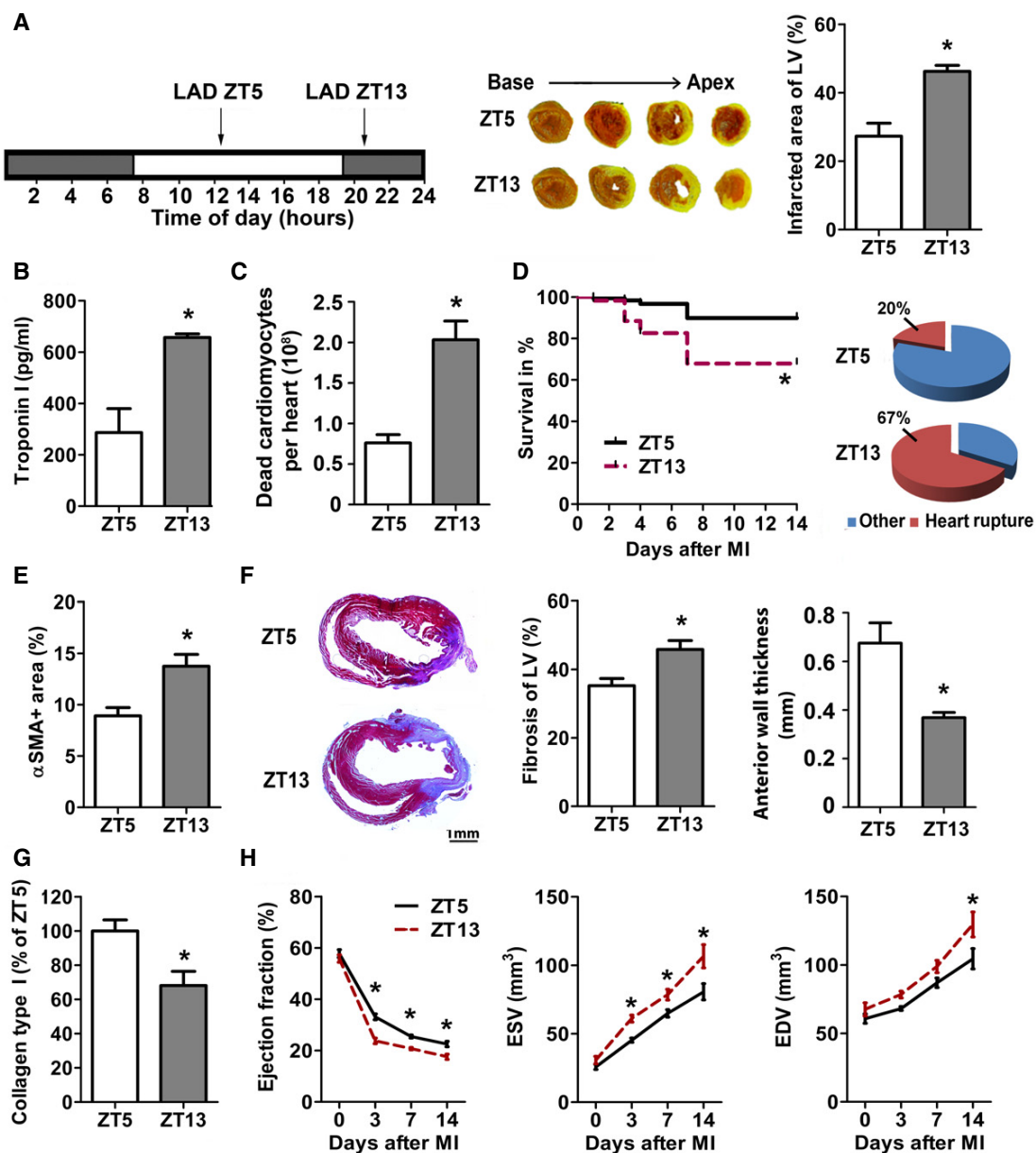


Figure 2. Inflammatory response after MI during active (ZT13) or resting phase (ZT5).

- A Flow cytometric analysis of neutrophils in hearts and representative immunostainings for neutrophils in the infarct area, identified as Ly6G positive (5 \times and 20 \times magnifications). Two-way ANOVA followed by Bonferroni *post hoc* test; $n = 5$ mice for no MI, $n = 5$ for 12 h post-MI, $n = 3$ for 24 h post-MI, and $n = 3$ for 72 h post-MI in both ZT groups; ZT5 versus ZT13: * $P = 0.0161$ (12 h MI), * $P = 0.003$ (24 h MI).
- B Flow cytometric analysis of neutrophils in bone marrow. Two-way ANOVA followed by Bonferroni *post hoc* test; $n = 5$ mice for no MI, $n = 5$ for 12 h post-MI, $n = 4$ for 24 h post-MI, and $n = 4$ for 72 h post-MI in both ZT groups; ZT5 versus ZT13: * $P = 0.0471$ (12 h MI), * $P = 0.0035$ (24 h MI).
- C Blood counts of granulocytes. Two-way ANOVA followed by Bonferroni *post hoc* test; $n = 9$ mice for no MI, $n = 10$ for 12 h post-MI, $n = 13$ for 24 h post-MI, and $n = 10$ for 72 h post-MI in both ZT groups; ZT5 versus ZT13: * $P = 0.0364$ (24 h MI).
- D Flow cytometric analysis of neutrophils in hearts and bone marrow under inverted light cycle conditions. Two-way ANOVA followed by Bonferroni *post hoc* test; $n = 3$ mice for no MI in both ZT groups, $n = 5$ for ZT5 and $n = 6$ for ZT13 at 24 h post-MI; ZT5 versus ZT13: * $P = 0.0147$ (24 h MI).
- E Representative gating strategy for GMPs in the bone marrow, identified as lineage negative (CD11b $^-$, Gr1 $^-$, B220 $^-$, CD3 $^-$, and Ter119 $^-$) and Sca-1 $^-$, c-kit $^+$, CD16/32 $^+$, and CD34 $^+$. Flow cytometric quantification of GMP in the bone marrow. Two-way ANOVA followed by Bonferroni *post hoc* test; $n = 4$ mice for no MI and 24 h post-MI in both groups; ZT5 versus ZT13: * $P = 0.0077$ (no MI), * $P = 0.0013$ (24 h MI).
- F CXCL12 levels in bone marrow lavage. Two-way ANOVA followed by Bonferroni *post hoc* test; $n = 7$ mice for no MI and $n = 6$ for 24 h post-MI in both groups; ZT5 versus ZT13: * $P = 0.0077$ (no MI), * $P = 0.0013$ (24 h MI).
- G Plasma levels of pro-inflammatory cytokines and chemokines. Two-way ANOVA followed by Bonferroni *post hoc* test; $n = 11$ mice for no MI in both ZT groups, $n = 7$ for ZT5 and $n = 8$ for ZT13 at 24 h post-MI; ZT5 versus ZT13: * $P = 0.0271$ (CXCL12, no MI), * $P = 0.0108$ (TNF- α , 24 h MI), * $P = 0.001$ (G-CSF, 24 h MI), * $P = 0.005$ (CXCL1, 24 h MI), * $P = 0.0005$ (CXCL2, 24 h MI), * $P = 0.0016$ (CCL3 24 h MI), * $P = 0.0144$ (CCL5, 24 h MI).

Data information: All data are expressed as mean \pm SEM.

**Figure 3. MI during active phase (ZT13) leads to infarct expansion and reduced cardiac function.**

- A Permanent LAD occlusion was performed at ZT5 or ZT13. TTC staining (white, infarct; red, vital myocardium) and quantification of infarct size normalized to the left ventricle (LV). Student's *t*-test; $n = 4$ mice for ZT5 and $n = 5$ for ZT13 MI; * $P = 0.0041$.
- B Plasma troponin I levels 24 h after MI. Student's *t*-test; $n = 4$ mice for ZT5 and $n = 5$ for ZT13 MI; * $P = 0.0007$.
- C Flow cytometric analysis of dead cardiomyocytes (CD45⁻, Zombie⁺) 24 h after MI. Student's *t*-test; $n = 3$ mice in both groups; * $P = 0.0072$.
- D Survival rates after MI and cause of death. Log-rank test; $n = 87$ mice in both groups; * $P = 0.0006$.
- E Myofibroblasts within infarcts were quantified by alpha-smooth muscle actin (α SMA) staining as ratio between stained and total area of random fields. Student's *t*-test; $n = 4$ mice in both groups; * $P = 0.0134$.
- F Masson's trichrome staining of fibrosis (blue, collagen; red, vital myocardium) and quantification relative to total LV (* $P = 0.0095$) as well as LV anterior wall thickness (* $P = 0.0068$) 7 days after MI. Student's *t*-test; $n = 6$ mice for ZT5 and $n = 7$ for ZT13 MI.
- G Analysis of relative collagen type I content identified by Sirius Red staining 7 days after MI. Student's *t*-test; $n = 4$ mice for ZT5 and $n = 5$ for ZT13 MI; * $P = 0.0175$.
- H Echocardiographic assessment of ejection fraction (EF), end-systolic volume (ESV), and end-diastolic volume (EDV). Two-way ANOVA; $n = 6$ mice for no MI for both groups, $n = 6$ for ZT5 and $n = 9$ for ZT13 at 72 h post-MI, $n = 8$ for both groups at 7 days post-MI, and $n = 7$ for ZT5 and $n = 5$ for ZT13 at 14 days post-MI; ZT5 versus ZT13: * $P = 0.0001$ (EF, 3 days), * $P = 0.0042$ (EF, 7 days), * $P = 0.0121$ (EF, 14 days); * $P = 0.0253$ (ESV, 3 days), * $P = 0.0421$ (ESV, 7 days), * $P = 0.0005$ (ESV, 14 days); * $P = 0.0053$ (EDV, 14 days).

Data information: All data are expressed as mean \pm SEM.

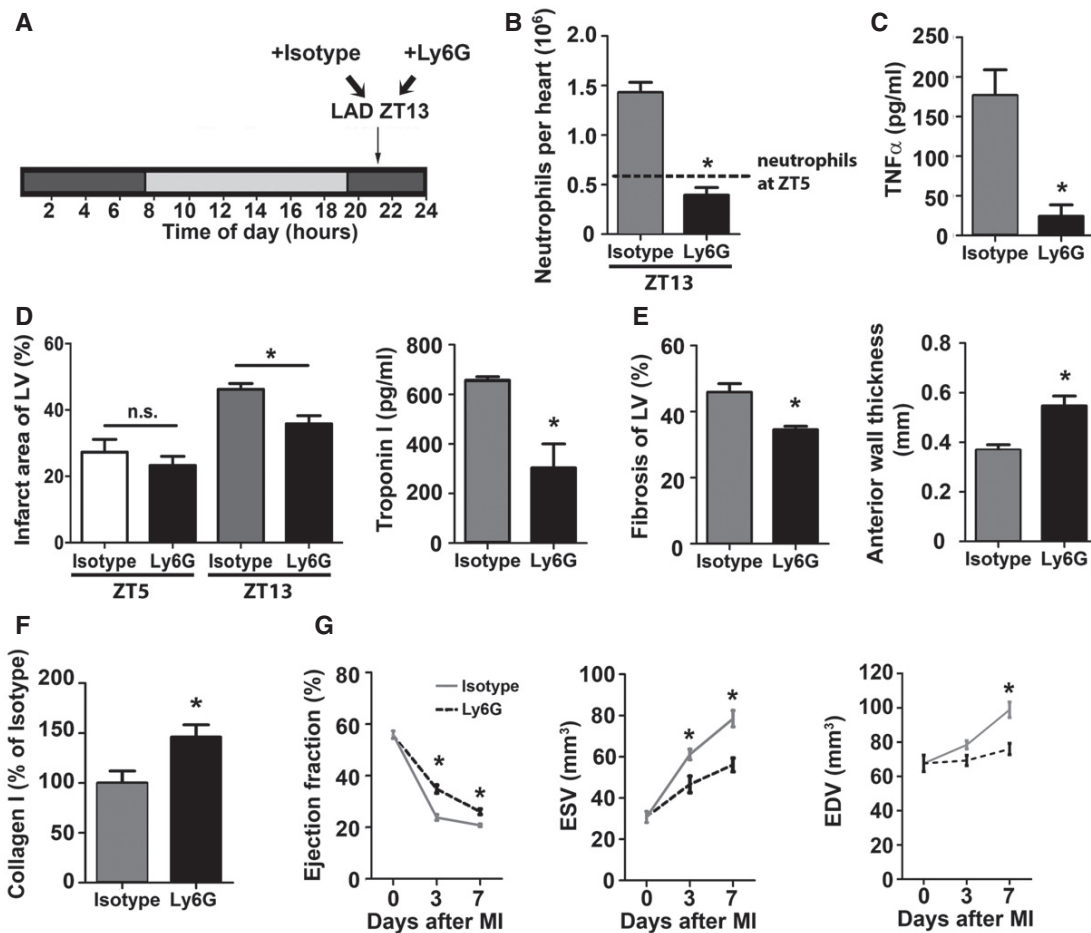


Figure 4. Limiting neutrophilic inflammation during active phase (ZT13) reduces MI damage.

- A Permanent LAD occlusion was performed at ZT13 followed by injection of isotype or Ly6G antibody 45 min after surgery and then every 24 h.
- B Flow cytometric analysis of cardiac neutrophils 24 h after ZT13 MI. The dotted line indicates cardiac neutrophil counts 24 h after ZT5 MI, as shown in Fig 2A. Student's *t*-test; $n = 3$ mice for isotype and $n = 5$ for Ly6G injected mice; * $P = 0.0004$.
- C Plasma TNF- α levels 24 h after ZT13 MI. Student's *t*-test; $n = 8$ independent samples for isotype and $n = 6$ for Ly6G injected mice; * $P = 0.0019$.
- D Infarct size relative to left ventricular area (LV) and plasma troponin I levels 24 h after ZT5 or ZT13 MI. Student's *t*-test; for infarct size, $n = 3$ mice in both groups for ZT5 and $n = 4$ mice for isotype and $n = 3$ mice for Ly6G at ZT13; isotype versus Ly6G: * $P = 0.0158$ (ZT13). For troponin levels, $n = 8$ mice for isotype and $n = 6$ mice for Ly6G with ZT13 MI; * $P = 0.0012$.
- E Masson's trichrome staining of fibrosis (blue, collagen; red, vital myocardium) and quantification relative to total area of the LV (* $P = 0.0084$); morphometric quantification of the LV anterior wall thickness (* $P = 0.0027$) 7 days after ZT13 MI. Student's *t*-test; $n = 5$ mice for isotype and $n = 4$ mice for Ly6G.
- F Analysis of collagen type I fibers within infarcts identified by Sirius Red staining 7 days after ZT13 MI. Student's *t*-test; $n = 5$ mice for isotype and $n = 4$ mice for Ly6G; * $P = 0.0375$.
- G Echocardiographic measurement of ejection fraction (EF), end-systolic volume (ESV) and end-diastolic volume (EDV) before and after ZT13 MI. Two-way ANOVA; $n = 6$ mice for no MI in both groups, $n = 9$ for isotype and $n = 5$ for Ly6G at 72 h post-MI, and $n = 8$ for isotype and $n = 4$ for Ly6G at 7 days post-MI. Isotype versus Ly6G: * $P = 0.0001$ (EF, 3 days), * $P = 0.0227$ (EF, 7 days); MI * $P = 0.0133$ (ESV, 3 days), * $P = 0.0004$ (ESV, 7 days); * $P = 0.0017$ (EDV, 7 days).

Data information: All data are expressed as mean \pm SEM.

myocardium, we did functional blocking experiments with CXCR2 antagonist SB225002. CXCR2 antagonism induced a massive reduction in CXCR2 hi -expressing blood neutrophils in mice with ZT13 MI (Fig 5C). Remarkably, the percentages of CXCR2 hi blood neutrophils in the ZT5 MI group remained unchanged after SB225002 treatment (Fig 5C). Likewise, the CXCR2 antagonist did not affect neutrophil numbers in bone marrow and heart of mice with ZT5 MI (Fig 5D and E), whereas cardiac neutrophil recruitment

in ZT13 infarcts was significantly inhibited by CXCR2 antagonism (Fig 5D). This was paralleled by reduced mobilization from the bone marrow in these mice (Fig 5E).

To validate the role of CXCR2 in circadian rhythm-dependent cardiac neutrophil recruitment, we performed additional experiments with lethally irradiated wild-type mice transplanted with Mrp8-Cre-CXCR2flox bone marrow. Transplantation with bone marrow from CXCR2flox littermates served as wild-type control. We

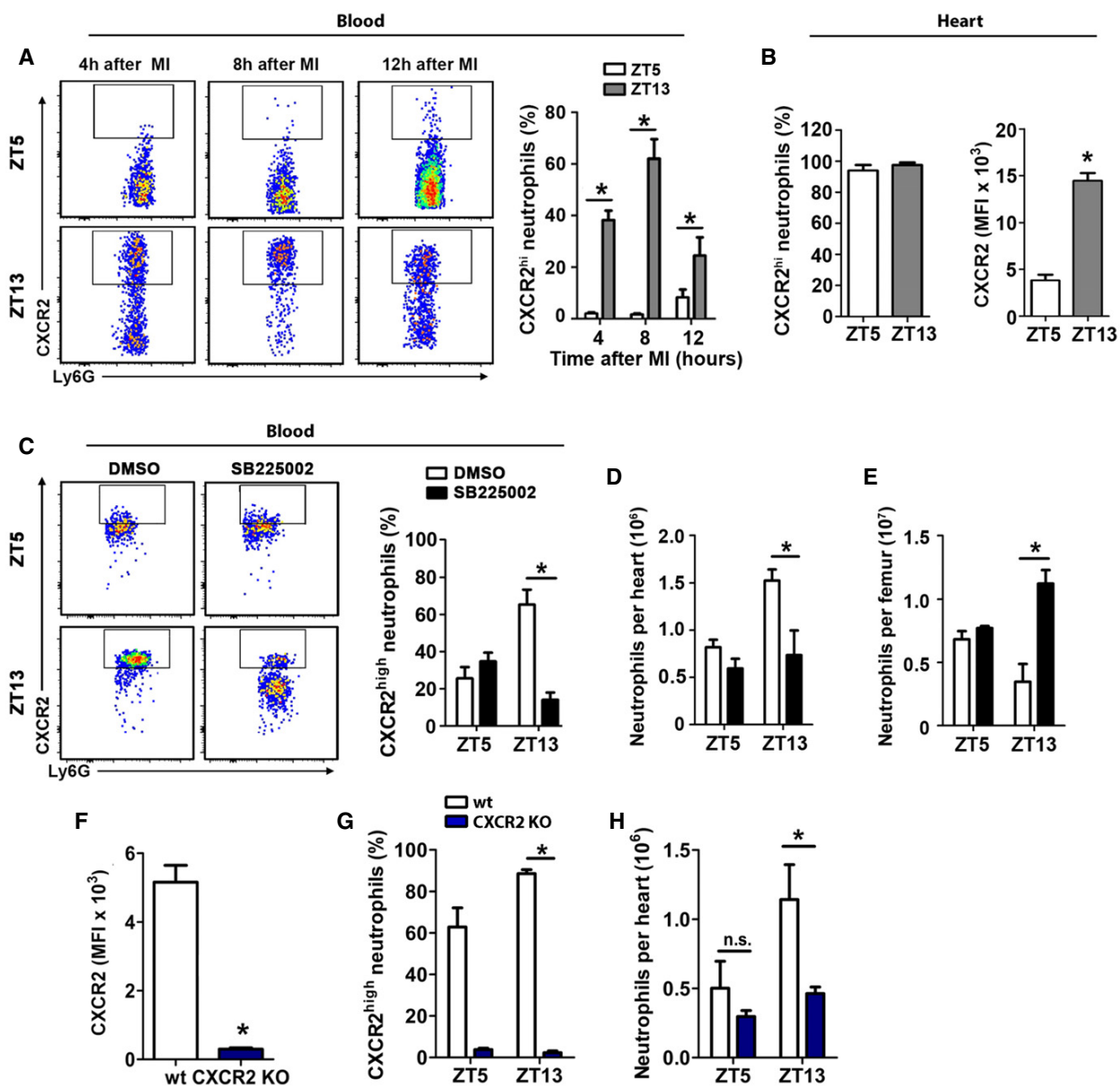


Figure 5. Antagonism or deficiency of CXCR2 inhibits enhanced cardiac neutrophil accumulation during active phase (ZT13).

- A Representative flow cytometric analysis and quantification of CXCR2^{high} neutrophils in the blood after ZT5 and ZT13 MI. Two-way ANOVA followed by Bonferroni post hoc test; $n = 4$ mice for all time points in both groups; ZT5 versus ZT13: * $P = 0.0001$ (4 h), * $P = 0.0001$ (8 h), * $P = 0.0447$ (12 h).
- B Percentage and mean fluorescence intensity (MFI) of CXCR2 expression by cardiac neutrophils 12 h post-MI after ZT5 and ZT13 MI. Student's t-test; $n = 4$ mice in both groups; * $P = 0.0001$.
- C Percentage of CXCR2^{high} neutrophils in the blood 24 h after ZT5 or ZT13 MI in mice receiving CXCR2 antagonist SB225002 or vehicle. Two-way ANOVA followed by Bonferroni post hoc test; $n = 4$ mice in both groups; DMSO versus SB225002: * $P = 0.0005$ (ZT13).
- D Flow cytometric quantification of neutrophils in hearts 24 h after ZT5 or ZT13 MI in mice receiving CXCR2 antagonist SB225002 or vehicle. Two-way ANOVA followed by Bonferroni post hoc test; $n = 4$ mice in both groups; DMSO versus SB225002: * $P = 0.0079$ (ZT13).
- E Flow cytometric quantification of neutrophils in bone marrow 24 h after ZT5 or ZT13 MI in mice receiving CXCR2 antagonist SB225002 or vehicle. Two-way ANOVA followed by Bonferroni post hoc test; $n = 4$ mice in both groups; DMSO versus SB225002: * $P = 0.0002$ (ZT13).
- F MFI of CXCR2 expression at ZT5 in the blood 24 h after MI in wild-type (WT) and CXCR2 KO mice. Student's t-test; $n = 6$ mice in both groups; * $P = 0.0001$.
- G Percentage of CXCR2^{hi} blood neutrophils 24 h after ZT5 or ZT13 MI in WT and CXCR2 KO mice. Two-way ANOVA followed by Bonferroni post hoc test; for ZT5 $n = 6$ mice in both groups, for ZT13 $n = 7$ WT mice and $n = 5$ CXCR2 KO mice; WT versus CXCR2 KO: * $P = 0.0001$ (ZT13).
- H Flow cytometric quantification of neutrophils in hearts 24 h after MI in ZT5 and ZT13-operated WT and CXCR2 KO mice. Two-way ANOVA followed by Bonferroni post hoc test; for ZT5 $n = 6$ mice in both groups, for ZT13 $n = 7$ WT mice and $n = 5$ CXCR2 KO mice; WT versus CXCR2 KO: * $P = 0.0461$ (ZT13), ns = not significant.

Data information: All data are expressed as mean \pm SEM.

first validated the knockdown of CXCR2 on neutrophils (Fig 5F) and confirmed that increased numbers of CXCR2^{hi} neutrophils at ZT13 were also found in control mice transplanted with wild-type CXCR2 bone marrow, assessed 24 h after MI (Fig 5G). In agreement with the findings of pharmacological CXCR2 antagonism, neutrophil CXCR2 deficiency blunted the time-of-day-dependent differences in cardiac neutrophil counts after ZT5 and ZT13 MI (Fig 5H).

CXCR2 antagonism administered shortly before reperfusion inhibits exaggerated cardiac neutrophil recruitment at ZT13

Finally, we aimed to validate the effect of CXCR2 blockade in a clinically more relevant scenario and therefore subjected mice to transient LAD occlusion (Fig 6A). Similar to the effects observed in the permanent occlusion model, we found a higher percentage of CXCR2^{hi} blood neutrophils at ZT13 compared to ZT5, assessed 24 h after reperfusion (Fig 6B). Moreover, vehicle-treated mice 24 h after ZT13 MI had significantly higher neutrophil counts in the myocardium than ZT5 infarcted mice, as well as enhanced mobilization from the bone marrow (Fig 6C and D). Administration of the CXCR2 antagonist after LAD occlusion 5 min before reopening the vessel prevented excessive neutrophil recruitment at ZT13 (Fig 6C and D), suggesting a potential clinical benefit for targeting this receptor.

Discussion

In this study, we provide evidence that the time-of-day determines the severity of MI damage and outcome. This is due to oscillations of cardiac neutrophil recruitment regulated by modulation of their CXCR2 receptor expression levels. Our findings thereby reveal a

potential explanation for the poorer outcomes in subjects with MI in the early morning hours.

Circadian oscillations of leukocytes between blood and peripheral tissue have been previously reported, peaking at ZT5 in the blood of mice and at ZT13 in skeletal muscle (Scheiermann *et al*, 2013). As humans have an opposing sleep–wake cycle, the peak of blood neutrophils is around 8:30 pm (Sennels *et al*, 2011). Here, we extended these findings to the murine myocardium: At baseline, we found twofold higher numbers of neutrophils in the heart at ZT13 compared with ZT5. This is facilitated by enhanced cardiac expression of adhesion molecules and neutrophil chemoattractants, that is, CXCL1, CXCL2, CXCL5, CCL3, and CCL5 at this time point. Interestingly, the circadian modulation of chemokine expression was only detectable in the heart, but not systemically, suggesting a local clock regulating chemokine expression in the myocardium. A similar mechanism has been recently highlighted by Gibbs *et al* who identified a local pulmonary epithelial cell clock controlling neutrophil recruitment to the lung under inflammatory conditions (Gibbs *et al*, 2014). Consequently, if an infarct occurs at ZT13, more leukocytes are present in the heart to respond locally to the ischemic injury by releasing pro-inflammatory mediators in order to attract more inflammatory cells into the infarcted area. This might contribute to the enhanced inflammatory response observed in ZT13 infarcts.

Blood neutrophils follow rhythmic cycles of release and migration back to the bone marrow, maintained by circadian changes in bone marrow stromal CXCL12 production and upregulation of CXCR4 by aged neutrophils for their clearance (Casanova-Acebes *et al*, 2013). These aged CXCR4^{hi} neutrophils concomitantly decrease L-selectin (CD62L) (Casanova-Acebes *et al*, 2013). Aged neutrophils are thought to exhibit different migratory and pro-inflammatory properties (Whyte *et al*, 1993); however, more recent data reported enhanced pro-inflammatory activity of *in vivo* aged

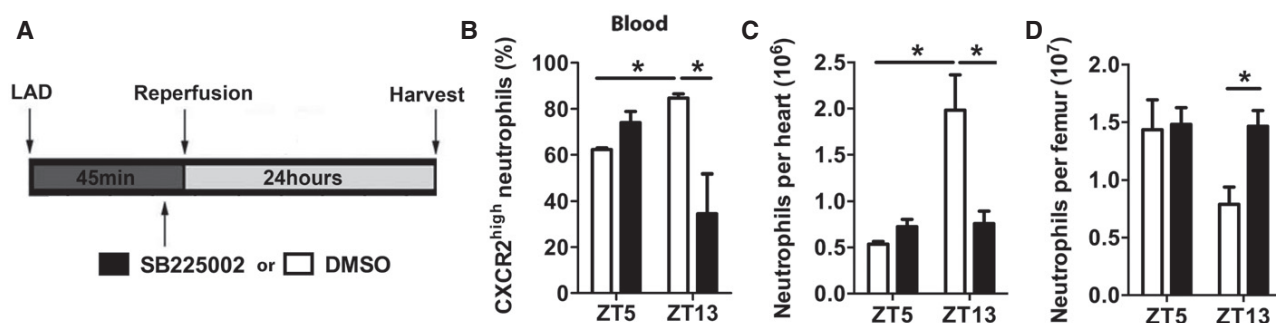


Figure 6. Antagonism of CXCR2 inhibits enhanced cardiac neutrophil accumulation after ischemia/reperfusion during active phase (ZT13).

- A Schematic representation of transient ischemia and reperfusion protocol, performed at ZT5 and ZT13. The CXCR2 antagonist SB225002 or vehicle was injected 5 min before reopening the LAD.
- B Percentage of CXCR2^{hi} neutrophils in the blood 24 h after ZT5 or ZT13 MI in mice receiving CXCR2 antagonist SB225002 or vehicle. Two-way ANOVA followed by Bonferroni post hoc test; $n = 5$ mice in both groups at ZT5, $n = 5$ mice for vehicle, and $n = 6$ mice for SB225002 at ZT13; DMSO versus SB225002: $*P = 0.0046$ (ZT13); ZT5 versus ZT13: $*P = 0.0153$ (DMSO).
- C Flow cytometric quantification of cardiac neutrophils 24 h after ZT5 or ZT13 MI in mice receiving CXCR2 antagonist SB225002 or vehicle. Two-way ANOVA; $n = 5$ mice in both groups at ZT5, $n = 5$ mice for vehicle, and $n = 6$ mice for SB225002 at ZT13; DMSO versus SB225002: $*P = 0.0006$ (ZT13); ZT5 versus ZT13: $*P = 0.0001$ (DMSO).
- D Flow cytometric quantification of neutrophils in bone marrow 24 h after ZT5 or ZT13 MI in mice receiving CXCR2 antagonist SB225002 or vehicle. Two-way ANOVA followed by Bonferroni post hoc test; $n = 5$ mice in both groups at ZT5, $n = 5$ mice for vehicle, and $n = 6$ mice for SB225002 at ZT13; DMSO versus SB225002: $*P = 0.0486$ (ZT13).

Data information: All data are expressed as mean \pm SEM.

neutrophils (Zhang *et al.*, 2015). In support of reduced migratory capacity of aged neutrophils, we found a low percentage of circulating CXCR2^{hi} neutrophils at ZT5 at steady state, when high numbers of aged CXCR4^{hi} CD62L^{lo} neutrophils are present in the circulation (Casanova-Acebes *et al.*, 2013). Conversely, circulating neutrophils at ZT13 MI, the time point with lowest numbers of aged neutrophils in the blood, were mostly CXCR2^{hi} positive. Similar patterns were observed after MI. Our blocking and genetic knockout experiments demonstrated the requirement of CXCR2 for enhanced cardiac neutrophil recruitment at the beginning of the active phase. Of note, CXCR2 antagonism or neutrophil-specific knockout did not generally block neutrophil recruitment at both time points, but only prevented the accelerated infiltration into the myocardium at ZT13 compared to ZT5. Accordingly, it was previously described that bone marrow CXCR2 deficiency did not affect neutrophil infiltration after ischemia/reperfusion (Liehn *et al.*, 2013). Thus, additional neutrophil chemoattractants and receptors seem to be involved in cardiac neutrophil recruitment in a circadian-independent manner, whereas the CXCR2 ligand/receptor axis follows rhythmic cycles of expression levels in the myocardium or circulating neutrophils, respectively.

Under homeostatic conditions, we found that GMP numbers increased in the bone marrow at ZT13, which is in agreement with previous findings revealing a rhythmic modulation of the hematopoietic niche (Smaaland *et al.*, 1992; Mendez-Ferrer *et al.*, 2008). Aged neutrophils return from the circulation back into the bone marrow and are eliminated, thereby providing a signal for regulating the homeostatic release of their own precursors (Casanova-Acebes *et al.*, 2013).

The retention and release of neutrophils is tightly regulated by chemokines and their cognate receptors (Kolaczkowska & Kubes, 2013). Bone marrow stromal cells produce CXCL12, which provides a retention signal for hematopoietic cells expressing high levels of CXCR4. Circadian reductions in CXCL12 in the bone marrow correlate with oscillations of hematopoietic progenitor cells in the circulation (Mendez-Ferrer *et al.*, 2008). G-CSF, which is upregulated after MI, is known to decrease CXCL12 in the bone marrow in order to facilitate neutrophil mobilization. Surprisingly, there was no further decrease in CXCL12 levels after ZT13 MI despite massive upregulation of G-CSF. A possible explanation is that the CXCL12 levels reach lowest levels at ZT13; thus, no additional decrease in a post-MI inflammatory situation may occur. Instead, the massive release of neutrophils from the bone marrow 24 h after ZT13 MI might be explained by the strong increase in chemokine levels in the plasma.

A well-balanced inflammatory response is needed, as dying cardiomyocytes must be removed by phagocytes and replaced by fibrous tissue, since mammals cannot regenerate cardiac tissue (Frangogiannis, 2012). In addition to monocytes/macrophages (Nahrendorf *et al.*, 2010), a sufficient number of neutrophils is certainly needed for favorable MI healing (Frangogiannis, 2012). In support of this hypothesis, we have recently found that neutrophils improve cardiac healing after MI by influencing macrophage polarization toward a “reparative” phenotype (Horckmans *et al.*, 2016). However, an exaggerated neutrophilic inflammation, as observed after ZT13 MI, generates an environment in which a physiological and beneficial wound healing is impaired. The consequence is an insufficient stabilization of the infarct area by collagen fibers, elevated risk for ventricular rupture and worsening of cardiac function.

Finally, we may speculate that oscillations of pro-inflammatory Ly6C^{hi} monocytes (Nguyen *et al.*, 2013) contribute to the enhanced inflammatory response after ZT13 MI. Indeed, we found elevated numbers of monocytes in the blood and heart at ZT13 compared to ZT5 under homeostatic conditions; however, monocyte numbers significantly increased only 3 days after MI (data not shown). Neutrophils represent the predominant innate immune cell population that massively infiltrate the infarcted myocardium within the first hours, and we found that limiting neutrophil influx with depleting antibody was successful to prevent excessive cardiac damage at ZT13.

Our observations in this mouse model have certain limitations as permanent coronary ligation does not reflect the predominant situation in acute MI patients, in which catheter treatment is the gold standard. Therefore, we repeated a key experiment in the ischemia/reperfusion model, thereby confirming a potential clinical relevance for targeting CXCR2 in situations of exaggerated neutrophil infiltration. Our data may provide an explanation for the worse outcomes found in patients suffering an acute MI in the early morning hours.

In conclusion, our findings suggest that the time-of-day of ischemia onset is a critical determinant when considering anti-inflammatory treatments targeting neutrophils for improving MI outcome.

Materials and Methods

Animal model of myocardial infarction

Adult (8–10 week old) female C57BL/6J wild-type mice (Janvier Labs, France) were housed for at least 2 weeks under controlled conditions in a 12-h light/12-h dark cycle with lights on at 7:30 am (ZT0) and lights off at 7:30 pm (ZT12). Littermates were randomized and subjected to permanent ligation of the left anterior descending coronary artery (LAD) at ZT5 (12:30 pm) or ZT13 (8:30 pm). Mice were anesthetized with midazolam (5 mg/kg), medetomidine (0.5 mg/kg), and fentanyl (0.05 mg/kg), intubated, and ventilated with a MiniVent mouse ventilator (Harvard Apparatus). A left thoracotomy was performed in the 4th left intercostal space, and the pericardium was incised. MI was induced by permanent ligation of the LAD proximal to its bifurcation from the main stem with monofilament nylon 8-0 sutures (Ethicon, Somerville, USA). The chest wall and skin were closed with 5-0 nylon sutures (Ethicon). After surgery, naloxone (1.2 mg/kg), flumazenil (0.5 mg/kg), and atipamezolehydrochloride (2.5 mg/kg) were injected to reverse the effect of anesthesia. Postoperative analgesia (buprenorphine, 0.1 mg/kg) was given subcutaneously for the first 12 h after surgery. Sham-operated animals were submitted to the same surgical protocol as described but without LAD occlusion. For inducing changes in light regime, mice were placed in a light cycler (Park Bioservices) for a minimum of 2 weeks to completely establish a 12-h inverted light cycle. Under these conditions, ZT5 corresponded to 8:30 pm and ZT13 to 12:30 pm. In additional experiments, mice subjected to MI at ZT13 were randomized in two groups to receive monoclonal neutrophil-depleting antibody (clone 1A8; 50 µg; BioXcell) or isotype by intraperitoneal (i.p.) injection 30 min after LAD occlusion and then every 24 h for up to 7 days. In other experiments, mice received i.p. injection of CXCR2 antagonist SB 225002 (Tocris, 1 mg/kg) or vehicle 5 min before LAD occlusion. Further experiments were performed in which mice were subjected to transient 45-min

ischemia followed by 24 h of reperfusion. Five min before reopening the occluded LAD, mice received an i.p. injection of SB 225002 (1 mg/kg) or vehicle. All animal experimental procedures were performed in strict accordance with the Guide for the Care and Use of Laboratory Animals published by the US National Institutes of Health (NIH publication No. 85-23, revised 1996) and were approved by the local ethical committee (District Government of Upper Bavaria).

Conditional inactivation of CXCR2 in mice and generation of bone marrow chimeras

We induced homologous recombination in embryonic stem (ES) cells using a construct containing 4.9 kb of gDNA, including exon 1 and part of intron 1–2, an IRES-LacZ cassette and Neo Cassette were inserted in between Frt sites, a loxP-site was introduced in 5' direction to the Neo cassette, and 2.9 kb of gDNA, including CXCR2 exons 2 and 3, was flanked by loxP sites (floxed). The construct was finished by introducing a 3.5-kb fragment of gDNA serving as 3' recombination arm (Appendix Fig S3). Correctly targeted ES cell clones were injected into blastocysts to produce a chimeric mouse that transmitted the modified allele through the germ line. A male heterozygous for the targeted allele was bred with a female expressing ubiquitous Flippase (Flp) transgene to ultimately produce animals that had deleted the IRES-LacZ and Neo cassettes, preserving the loxP sites flanking exons 2 and 3. Those homozygous animals were bred with mice expressing a MRP8-Cre transgene (Passegue *et al.*, 2004) to ultimately produce animals that had deleted CXCR2 coding exons into neutrophils.

C57BL/6J wild-type mice (Janvier) underwent lethally whole body irradiation (2×5 Gy). Donor bone marrow cells were obtained from Mrp8-CreCXCR2flox or CXCR2flox mice (littermates). After flushing bones (femur, tibia, humerus), cells were washed, filtered, and intravenously injected (4×10^6 cells/mouse) in sterile saline into recipient mice 1 day after irradiation. Post-transplantation, recipient mice were reconstituted for another 6 weeks before undergoing LAD occlusion surgical procedure.

Echocardiography

Transthoracic echocardiography was performed on mildly anesthetized spontaneously breathing mice (sedated by inhalation of 1% isoflurane, 1 l/min oxygen), using a Vevo[®] 2100 High Resolution Imaging system equipped with a 40-MHz transducer (VisualSonics, Toronto, Canada). The mice were placed on a heated ECG platform. Left parasternal long-axis view and left mid-papillary, apical and basal short-axis views were acquired. End-diastolic volume, end-systolic volume, and ejection fraction were evaluated on the left parasternal long-axis and parasternal short-axis view in a blinded manner.

Infarct size and cause of death

Hearts were perfused and harvested 24 h after LAD ligation and sectioned into four equal transverse slices. The slices were incubated in 2% triphenyltetrazolium chloride (TTC) solution (Sigma-Aldrich) at 37°C for 15 min and fixed overnight in 4% formalin at 4°C. For quantification of the area at risk, Evan's blue was injected

into the left ventricle to distinguish between perfused cardiac tissue stained blue and non-perfused area at risk 24 h after MI. The area at risk was calculated as the percentage relative to the left ventricle (Appendix Fig S4). Images were taken at 10× magnification, and quantification of viable (red) and infarct areas (white) was performed in a blinded manner with ImageJ software. Each mouse which died after surgery prior to organ harvest underwent thoracotomy to investigate whether there was blood inside the pericardium indicating cardiac rupture.

Histology

Four-micrometer paraffin sections were stained with Masson's trichrome (Sigma-Aldrich). Fibrosis was quantified as the relative area of blue staining (collagen) compared to the left ventricle surface, as an average of 3–4 sections per heart at the level of the papillary muscle, using ImageJ software. The anterior wall thickness of the left ventricle was measured on Masson's trichome-stained sections as an average of 3–4 sections per heart. For Sirius Red staining of collagen, 3–4 sections per heart were incubated with 0.1% Sirius Red (Sigma-Aldrich). Sections were photographed with identical exposure settings under ordinary polychromatic or polarized light microscopy. Total collagen content was evaluated under polychromatic light. Interstitial collagen subtypes were evaluated using polarized light illumination; under this condition, thicker type I collagen fibers appeared orange or red, whereas thinner type III collagen fibers were yellow or green. Quantifications were performed with LAS software (Leica). For quantification of myofibroblasts, sections were stained with an antibody against smooth muscle actin (α SMA, clone 1A4 Sigma-Aldrich, dilution 1/300). Myofibroblast density was quantified using ImageJ software by examining 10 fields per section at 20× magnification, in a blinded fashion.

Cytokine and chemokine analysis

Blood was harvested by cardiac puncture, and bone marrow supernatant was obtained by flushing femurs three times with 2 ml of saline. Troponin I levels were measured with a precoated enzyme-linked immunosorbent assay (ELISA, Biotrend Chemicals). G-CSF, CXCL5, and CXCL12 in plasma and bone marrow supernatant were quantified with ELISA DuoSets from R&D systems. All other pro-inflammatory markers were quantified with ProcartaPlexTM Multiplex Immunoassay (eBioscience).

Blood counter

Freshly obtained EDTA blood harvested by cardiac puncture was used to analyze leukocyte counts using an animal blood counter (scil Vet ABC Hematology Analyzer).

Flow cytometry of heart and bone marrow

Hearts were harvested, perfused with saline to remove peripheral cells, minced with fine scissors, and digested with collagenase I (450 U/ml), collagenase XI (125 U/ml), hyaluronidase type I-S (60 U/ml), and DNase (60 U/ml; Sigma-Aldrich and Worthington Biochemical Corporation) at 37°C for 1 h. Bone marrow cells were obtained by flushing femurs with 2 ml of saline and triturated

through 70-μm nylon mesh strainer. The resulting single cell suspensions were centrifuged, resuspended in PBS/BSA 1%, and incubated with following monoclonal antibodies for 30 min at 4°C at 1/1,000 dilution: anti-CD45.2 (clone 104, BD Biosciences), anti-CD11b (clone M1/70, BioLegend), anti-c-Kit (clone 2B8, BioLegend), anti-Sca-1 (clone E13-161.7, BioLegend), anti-CD16/32 (clone 93, BioLegend), anti-CD34 (clone MEC14.7, BioLegend), anti-Ly6G (clone 1A8, BioLegend), lineage cocktail (clone 17A2/RB6-8C5/RA3-6B2/Ter-119/M1/70, BioLegend), and isotype controls (BioLegend). Anti-CD182 (CXCR2, PerCP/Cy5.5 labeled, clone TG11/CXCR2, BioLegend) was used at 1/300 dilution. Viable cells were identified as unstained with dead cell marker Zombie Yellow™ (BioLegend) in a 1/100 dilution. Data were acquired on a FACS Canto II (BD Biosciences), and analysis was performed with FlowJo software (Ashland, USA). Neutrophils were identified as CD45⁺, CD11b⁺, and Ly6G⁺; granulocyte-monocyte progenitor cells (GMPs) were identified as lineage⁻, Sca-1⁻, c-kit⁺, CD16/32⁺, and CD34⁺ (Fig 2); and dead cardiomyocytes were identified as Zombie⁺, CD45⁻. Gating for CXCR2^{hi} was performed as shown in Appendix Fig S5.

Quantitative real-time PCR

Whole RNA from lysed hearts (TissueLyser LT, Qiagen) was extracted (RNeasy mini kit, Qiagen) and reverse-transcribed (Prime-Script™ RT reagent kit, Clontech). Real-time PCR was performed with the 7900HT Sequence Detection System (Applied Biosystems) using the KAPA PROBE FAST Universal qPCR kit (Peqlab) and predesigned primer and probe mix (TaqMan® Gene Expression Assays, Life Technologies). Messenger RNA expression of markers of interest was normalized to HPRT, and the fold induction was calculated by the comparative C_t method.

Statistical analysis

Sample size for *in vivo* experiments was calculated in order to provide a statistical power > 85% for an $\alpha < 0.05$ in detecting a population effect size > 0.8. Comparisons between two groups of normally distributed and not connected data were performed using the unpaired Student's *t*-test. Multiple group comparisons were performed by one-way analyses of variance analyses (ANOVA, for one independent variable) followed by Tukey's multiple comparison tests or two-way ANOVA (for two independent variables) followed by Bonferroni *post hoc* test. Mortality was analyzed by log-rank test. All results are expressed as mean \pm SEM. $P < 0.05$ was considered significant.

Expanded View for this article is available online.

Acknowledgements

This work was funded in part by the FoFoLe (Foerderung von Forschung und Lehre) program of the Ludwig-Maximilians-University Munich (to S.S. and M.J.S.), the Deutsche Forschungsgemeinschaft (STE-1053/5-1 to S.S.; SO876/6-1 and as part of the SFB1123 TP A6 to O.S., M.D.; B5 to O.S. and TP A1 to C.W.; Emmy-Noether grant SCHE 1645/2-1 and SFB 914 project B09), the German Centre for Cardiovascular Research (DZHK MHA VD1.2 to C.W., O.S. and doctoral fellowship to M.J.S.), the European Research Council ERC (AdG 249929 to C.W. and ERC starting grant CIRCODE to C.S.), the NWO (VIDI project 917.12.303 to O.S.), and TransCard Ph.D. Fellowship (Helmholtz International

The paper explained

Problem

Mounting evidence suggests that the outcome after myocardial infarction (MI) is time-of-day dependent. This is supported by clinical studies reporting a correlation between infarct size assessed by cardiac enzymes and the time-of-day of ischemia onset. The identification of underlying mechanisms behind this association might help developing more specialized therapies to improve prognosis after MI.

Results

We found that the heart represents an immunologically dynamic organ with circadian fluctuations of adhesion molecule and chemo-kine expression and recruited leukocytes. We observed that neutrophil production and retention in the bone marrow are time-of-day dependent and that circulating neutrophils at the beginning of the active phase have higher capacity to migrate into the myocardium due to upregulated CXCR2 expression. We conclude that MI onset during the peak phase of CXCR2^{hi}-expressing blood neutrophils and consequently cardiac neutrophil accumulation promotes an exaggerated inflammatory response. Reducing neutrophilic inflammation by blocking CXCR2 or partially depleting neutrophils prevents excessive cardiac damage after MI occurring during the active phase.

Impact

Our findings provide a mechanistic explanation for the worse outcomes in patients with MI occurring during the sleep-to-wake transition period. Limiting exaggerated neutrophil-mediated inflammation in these patients might improve their clinical outcome after MI.

Research School "Translational Cardiovascular and Metabolic Medicine" to K.N.). We thank Donato Santovito for careful revision and discussion of the manuscript and Lusine Saroyan, Orsolya Kimbu Wade, Cornelia Seidl, Yvonne Jansen, and Patricia Lemnitzer for excellent technical assistance.

Author contributions

MJS and MH performed surgical procedures and echocardiography recordings. MJS and MH performed histology, flow cytometry, plasma measurements, and gene expression analysis and analyzed data. KN performed flow cytometric measurements and analyzed data. KB generated CXCR2^{flox} mice. MD generated bone marrow chimeras. OS, JD, CS, MD, CW, and SS designed experimental approaches. OS, CW, CS, and SS provided substantial funding. All authors discussed results and commented on the manuscript. MJS and SS wrote the manuscript.

Conflict of interest

The authors declare that they have no conflict of interest.

References

- Casanova-Acebes M, Pitaval C, Weiss LA, Nombela-Arrieta C, Chevre R, N AG, Kunisaki Y, Zhang D, van Rooijen N, Silberstein LE et al (2013) Rhythmic modulation of the hematopoietic niche through neutrophil clearance. *Cell* 153: 1025–1035
- Chen L, Yang G (2015) Recent advances in circadian rhythms in cardiovascular system. *Front Pharmacol* 6: 71
- Chia S, Nagurney JT, Brown DF, Raffel OC, Bamberg F, Senatore F, Wackers FJ, Jang IK (2009) Association of leukocyte and neutrophil counts with infarct size, left ventricular function and outcomes after percutaneous coronary

- intervention for ST-elevation myocardial infarction. *Am J Cardiol* 103: 333–337
- Durgan DJ, Pulinkunnil T, Villegas-Montoya C, Garvey ME, Frangogiannis NG, Michael LH, Chow CW, Dyck JR, Young ME (2010) Short communication: ischemia/reperfusion tolerance is time-of-day-dependent: mediation by the cardiomyocyte circadian clock. *Circ Res* 106: 546–550
- Fournier S, Eeckhout E, Mangiacapra F, Trana C, Lauriers N, Beggah AT, Monney P, Cook S, Bardy D, Vogt P et al (2012) Circadian variations of ischemic burden among patients with myocardial infarction undergoing primary percutaneous coronary intervention. *Am Heart J* 163: 208–213
- Frangogiannis NG (2012) Regulation of the inflammatory response in cardiac repair. *Circ Res* 110: 159–173
- Gibbs J, Ince L, Matthews L, Mei J, Bell T, Yang N, Saer B, Begley N, Poolman T, Pariolla M et al (2014) An epithelial circadian clock controls pulmonary inflammation and glucocorticoid action. *Nat Med* 20: 919–926
- Horckmans M, Ring L, Duchene J, Santovito D, Schloss MJ, Drechsler M, Weber C, Soehnlein O, Steffens S (2016) Neutrophils orchestrate post-myocardial infarction healing by polarizing macrophages towards a reparative phenotype. *Eur Heart J* doi:10.1093/euroheartj/ehw002
- Kolaczkowska E, Kubes P (2013) Neutrophil recruitment and function in health and inflammation. *Nat Rev Immunol* 13: 159–175
- Kyne L, Hausdorff JM, Knight E, Dukas L, Azhar G, Wei JY (2000) Neutrophilia and congestive heart failure after acute myocardial infarction. *Am Heart J* 139: 94–100
- Liehn EA, Kanzler I, Konschalla S, Kroh A, Simsekilmaz S, Sonmez TT, Bucala R, Bernhagen J, Weber C (2013) Compartmentalized protective and detrimental effects of endogenous macrophage migration-inhibitory factor mediated by CXCR2 in a mouse model of myocardial ischemia/reperfusion. *Arterioscler Thromb Vasc Biol* 33: 2180–2186
- Litt MR, Jeremy RW, Weisman HF, Winkelstein JA, Becker LC (1989) Neutrophil depletion limited to reperfusion reduces myocardial infarct size after 90 minutes of ischemia. Evidence for neutrophil-mediated reperfusion injury. *Circulation* 80: 1816–1827
- Mendez-Ferrer S, Lucas D, Battista M, Frenette PS (2008) Haematopoietic stem cell release is regulated by circadian oscillations. *Nature* 452: 442–447
- Muller JE, Ludmer PL, Willich SN, Tofler GH, Aylmer G, Klangos I, Stone PH (1987a) Circadian variation in the frequency of sudden cardiac death. *Circulation* 75: 131–138
- Muller JE, Tofler GH, Willich SN, Stone PH (1987b) Circadian variation of cardiovascular disease and sympathetic activity. *J Cardiovasc Pharmacol* 10 (Suppl 2): S104–S109; discussion S110–101
- Nahrendorf M, Pittet MJ, Swirski FK (2010) Monocytes: protagonists of infarct inflammation and repair after myocardial infarction. *Circulation* 121: 2437–2445
- Nguyen KD, Fentress SJ, Qiu Y, Yun K, Cox JS, Chawla A (2013) Circadian gene Bmal1 regulates diurnal oscillations of Ly6C(hi) inflammatory monocytes. *Science* 341: 1483–1488
- Passegue E, Wagner EF, Weissman IL (2004) JunB deficiency leads to a myeloproliferative disorder arising from hematopoietic stem cells. *Cell* 119: 431–443
- Reiter R, Swingen C, Moore L, Henry TD, Traverse JH (2012) Circadian dependence of infarct size and left ventricular function after ST elevation myocardial infarction. *Circ Res* 110: 105–110
- Romson JL, Hook BG, Kunkel SL, Abrams GD, Schork MA, Lucchesi BR (1983) Reduction of the extent of ischemic myocardial injury by neutrophil depletion in the dog. *Circulation* 67: 1016–1023
- Scheiermann C, Kunisaki Y, Lucas D, Chow A, Jang JE, Zhang D, Hashimoto D, Merad M, Frenette PS (2012) Adrenergic nerves govern circadian leukocyte recruitment to tissues. *Immunity* 37: 290–301
- Scheiermann C, Kunisaki Y, Frenette PS (2013) Circadian control of the immune system. *Nat Rev Immunol* 13: 190–198
- Sennels HP, Jorgensen HL, Hansen AL, Goetze JP, Fahrenkrug J (2011) Diurnal variation of hematology parameters in healthy young males: the Bispebjerg study of diurnal variations. *Scand J Clin Lab Invest* 71: 532–541
- Smaaland R, Laerum OD, Sothern RB, Sletvold O, Bjerknes R, Lote K (1992) Colony-forming unit-granulocyte-macrophage and DNA synthesis of human bone marrow are circadian stage-dependent and show covariation. *Blood* 79: 2281–2287
- Suarez-Barrientos A, Lopez-Romero P, Vivas D, Castro-Ferreira F, Nunez-Gil I, Franco E, Ruiz-Mateos B, Garcia-Rubira JC, Fernandez-Ortiz A, Macaya C et al (2011) Circadian variations of infarct size in acute myocardial infarction. *Heart* 97: 970–976
- Tofler GH, Brezinski D, Schafer AI, Czeisler CA, Rutherford JD, Willrich SN, Gleason RE, Williams GH, Muller JE (1987) Concurrent morning increase in platelet aggregability and the risk of myocardial infarction and sudden cardiac death. *N Engl J Med* 316: 1514–1518
- Whyte MK, Meagher LC, MacDermot J, Haslett C (1993) Impairment of function in aging neutrophils is associated with apoptosis. *J Immunol* 150: 5124–5134
- Zhang D, Chen G, Manwani D, Mortha A, Xu C, Faith JJ, Burk RD, Kunisaki Y, Jang JE, Scheiermann C et al (2015) Neutrophil ageing is regulated by the microbiome. *Nature* 525: 528–532

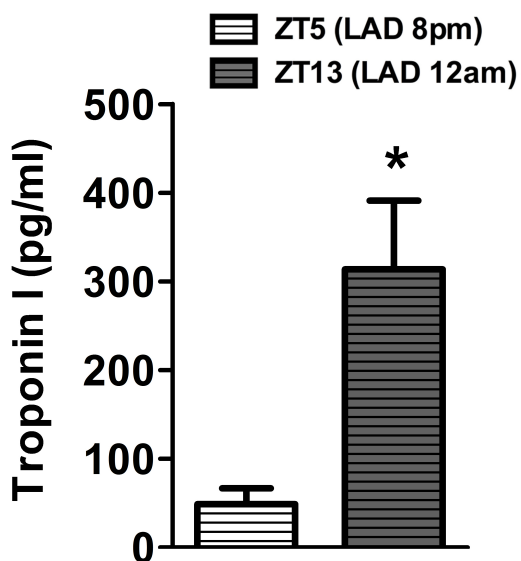


License: This is an open access article under the terms of the Creative Commons Attribution 4.0 License, which permits use, distribution and reproduction in any medium, provided the original work is properly cited.

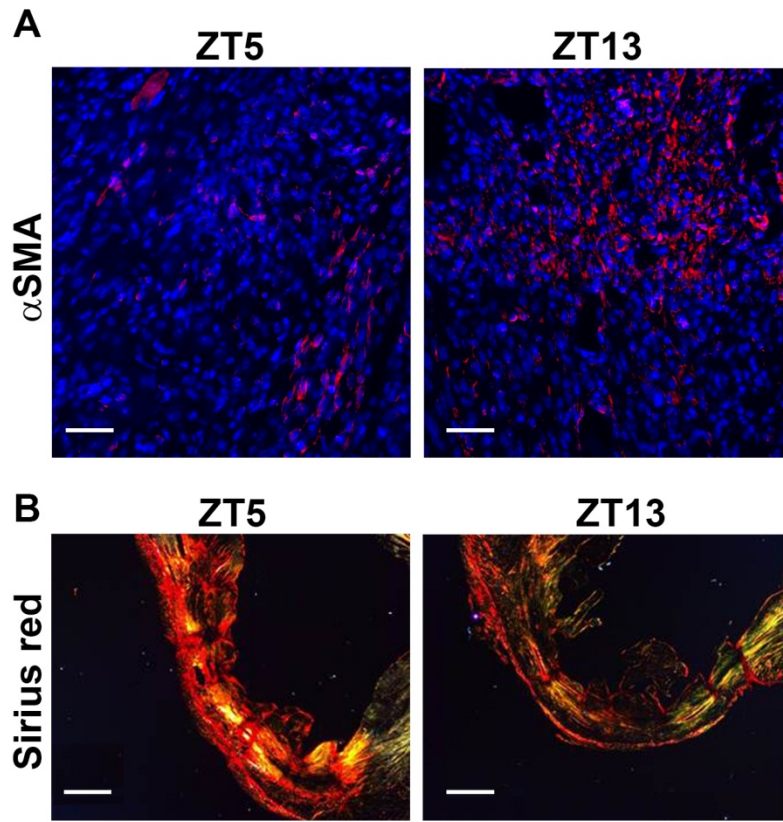
Appendix

The time of day of ischemia onset affects myocardial infarction healing and heart function through oscillations in neutrophil mobilization

Maximilian J. Schloss, cand. med.; Michael Horckmans, PhD; Katrin Nitz, MSc; Johan Duchene, PhD; ; Maik Drechsler, PhD^{1,3}; Kiril Bidzhekov, PhD¹; Christoph Scheiermann, PhD; Christian Weber, MD; Oliver Soehnlein, MD, PhD; Sabine Steffens, PhD

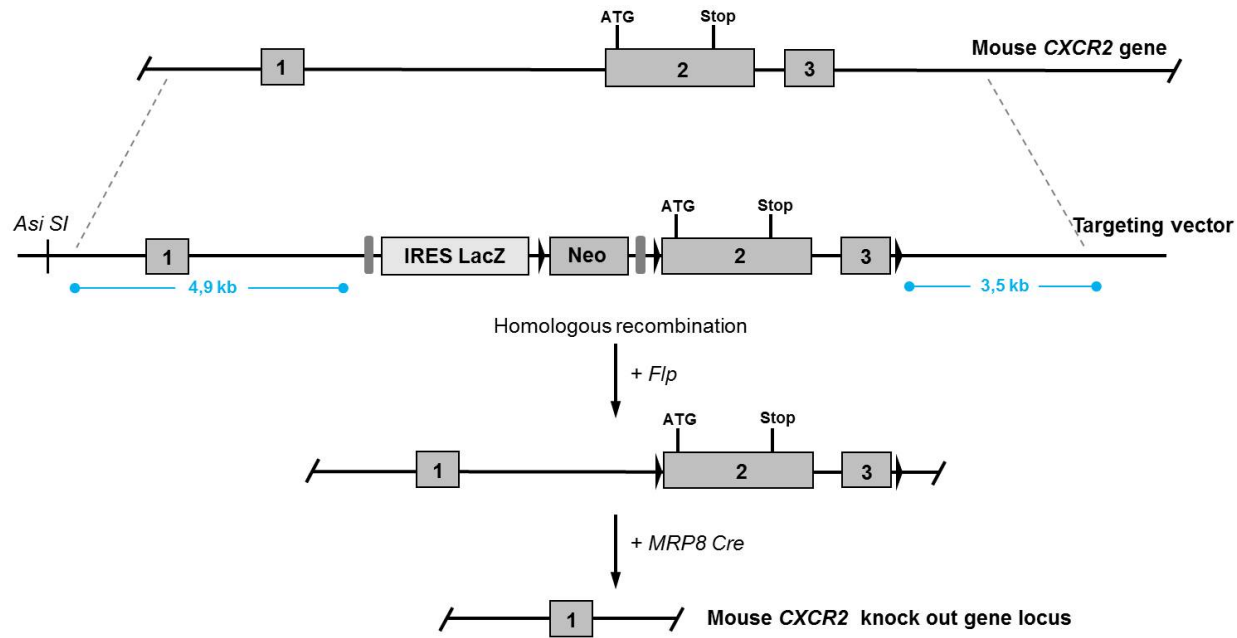


Appendix Figure S1: ZT13 MI leads to significantly increased cardiac damage compared to ZT5 MI in mice entrained to a shifted light cycle. Plasma troponin I levels 24 hours after MI. Student's t-test; $N = 5$ for ZT5 MI and $n = 6$ for ZT13 MI; * $P=0,0144$.

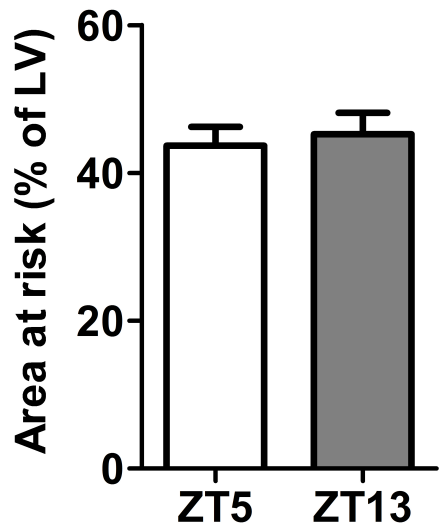


Appendix Figure S2: Histological analysis of myofibroblasts and collagen. MI was induced at ZT5 and ZT13 and hearts were harvested 7 days after ligation of LAD. **A**, Representative picture of myofibroblast staining within the infarct area using anti- alpha smooth muscle actin (SMA, positive red fluorescence) and 4',6-Diamidin-2-phenylindol (DAPI) staining of nuclei (blue fluorescence); 20x magnification; Scale bar 50 μ m. **B**, Representative Image of Sirius-Red staining identifying collagen type I fibers as red fibers within the infarct area; 2.5x magnification; Scale bar 400 μ m.

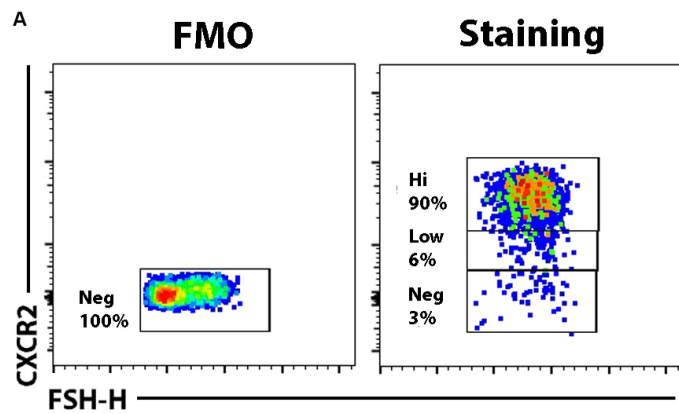
CXCR2 Knock out strategy



Appendix Figure S3: Generation of CXCR2-MRP8 Cre knockout mice. Schematic diagram of the generation of CXCR2 knockout mice. The exon-intron structure of the mouse CXCR2 locus is shown at the top. The targeting vector has a 4.9 kb 5' arm including exon 1 and intron 1-2, the IRES-LacZ coding sequence, and a Neo selection cassette, both flanked by FRT sites (gray bars). The loxP sites (black triangles) flanking exons 2-3 (the coding part of CXCR2 gene) and the Neo gene. The 3' recombination arm spanned 3.5 kb from the gDNA.



Appendix Figure S4: The area at risk is independent of the time of day of LAD ligation. Evan's blue was injected into the left ventricle to distinguish between perfused cardiac tissue stained blue and non-perfused area at risk 24h after MI. The area at risk was calculated as the percentage relative to the left ventricle. $N = 4$ per group.



Appendix Figure S5: Gating strategy for CXCR2⁺ neutrophils in blood. The representative dot plots shows the gating strategy for CXCR2 expression on blood neutrophils (identified as CD45+Ly6G+CD11b+) at baseline (ZT5) gated as CXCR2^{high}, CXCR2^{low} and CXCR2^{neg} neutrophils.

7. Literaturverzeichnis

1. Nathan C. Points of control in inflammation. *Nature*. 2002;420(6917):846-52.
2. LeBien TW, Tedder TF. B lymphocytes: how they develop and function. *Blood*. 2008;112(5):1570-80.
3. Gasteiger G, Rudensky AY. Interactions between innate and adaptive lymphocytes. *Nat Rev Immunol*. 2014;14(9):631-9.
4. Lahoz-Beneytez J, Elemans M, Zhang Y, Ahmed R, Salam A, Block M, et al. Human neutrophil kinetics: modeling of stable isotope labeling data supports short blood neutrophil half-lives. *Blood*. 2016;127(26):3431-8.
5. Furze RC, Rankin SM. Neutrophil mobilization and clearance in the bone marrow. *Immunology*. 2008;125(3):281-8.
6. Amulic B, Cazalet C, Hayes GL, Metzler KD, Zychlinsky A. Neutrophil function: from mechanisms to disease. *Annu Rev Immunol*. 2012;30:459-89.
7. Martin C, Burdon PC, Bridger G, Gutierrez-Ramos JC, Williams TJ, Rankin SM. Chemokines acting via CXCR2 and CXCR4 control the release of neutrophils from the bone marrow and their return following senescence. *Immunity*. 2003;19(4):583-93.
8. Eash KJ, Greenbaum AM, Gopalan PK, Link DC. CXCR2 and CXCR4 antagonistically regulate neutrophil trafficking from murine bone marrow. *J Clin Invest*. 2010;120(7):2423-31.
9. Weiss SJ. Tissue destruction by neutrophils. *N Engl J Med*. 1989;320(6):365-76.
10. Henson PM, Johnston RB, Jr. Tissue injury in inflammation. Oxidants, proteinases, and cationic proteins. *J Clin Invest*. 1987;79(3):669-74.
11. Zawrotniak M, Rapala-Kozik M. Neutrophil extracellular traps (NETs) - formation and implications. *Acta Biochim Pol*. 2013;60(3):277-84.
12. Leavy O. Innate immunity: Multitasking NET makers. *Nat Rev Immunol*. 2012;12(10):684-5.
13. Soehnlein O, Lindbom L, Weber C. Mechanisms underlying neutrophil-mediated monocyte recruitment. *Blood*. 2009;114(21):4613-23.
14. Soehnlein O, Zernecke A, Eriksson EE, Rothfuchs AG, Pham CT, Herwald H, et al. Neutrophil secretion products pave the way for inflammatory monocytes. *Blood*. 2008;112(4):1461-71.
15. Bentzon JF, Otsuka F, Virmani R, Falk E. Mechanisms of plaque formation and rupture. *Circulation research*. 2014;114(12):1852-66.
16. Fishbein MC, Siegel RJ. How big are coronary atherosclerotic plaques that rupture? *Circulation*. 1996;94(10):2662-6.
17. Nahrendorf M, Swirski FK, Aikawa E, Stangenberg L, Wurdinger T, Figueiredo JL, et al. The healing myocardium sequentially mobilizes two monocyte subsets with divergent and complementary functions. *J Exp Med*. 2007;204(12):3037-47.
18. Hofmann U, Frantz S. Role of lymphocytes in myocardial injury, healing, and remodeling after myocardial infarction. *Circulation research*. 2015;116(2):354-67.
19. Hofmann U, Beyersdorf N, Weirather J, Podolskaya A, Bauersachs J, Ertl G, et al. Activation of CD4+ T lymphocytes improves wound healing and survival after experimental myocardial infarction in mice. *Circulation*. 2012;125(13):1652-63.
20. Swirski FK. Inflammation and repair in the ischaemic myocardium. *Hamostaseologie*. 2015;35(1):34-6.
21. Yan X, Shichita T, Katsumata Y, Matsuhashi T, Ito H, Ito K, et al. Deleterious effect of the IL-23/IL-17A axis and gammadeltaT cells on left ventricular remodeling after myocardial infarction. *J Am Heart Assoc*. 2012;1(5):e004408.

22. Frangogiannis NG. Regulation of the inflammatory response in cardiac repair. *Circulation research*. 2012;110(1):159-73.
23. Frangogiannis NG. The role of the chemokines in myocardial ischemia and reperfusion. *Curr Vasc Pharmacol*. 2004;2(2):163-74.
24. Lei ZB, Zhang Z, Jing Q, Qin YW, Pei G, Cao BZ, et al. OxLDL upregulates CXCR2 expression in monocytes via scavenger receptors and activation of p38 mitogen-activated protein kinase. *Cardiovasc Res*. 2002;53(2):524-32.
25. Matsui Y, Morimoto J, Uede T. Role of matricellular proteins in cardiac tissue remodeling after myocardial infarction. *World J Biol Chem*. 2010;1(5):69-80.
26. Kyne L, Hausdorff JM, Knight E, Dukas L, Azhar G, Wei JY. Neutrophilia and congestive heart failure after acute myocardial infarction. *Am Heart J*. 2000;139(1 Pt 1):94-100.
27. Turner NA, Porter KE. Function and fate of myofibroblasts after myocardial infarction. *Fibrogenesis Tissue Repair*. 2013;6(1):5.
28. Giugliano GR, Giugliano RP, Gibson CM, Kuntz RE. Meta-analysis of corticosteroid treatment in acute myocardial infarction. *Am J Cardiol*. 2003;91(9):1055-9.
29. Romson JL, Hook BG, Kunkel SL, Abrams GD, Schork MA, Lucchesi BR. Reduction of the extent of ischemic myocardial injury by neutrophil depletion in the dog. *Circulation*. 1983;67(5):1016-23.
30. Litt MR, Jeremy RW, Weisman HF, Winkelstein JA, Becker LC. Neutrophil depletion limited to reperfusion reduces myocardial infarct size after 90 minutes of ischemia. Evidence for neutrophil-mediated reperfusion injury. *Circulation*. 1989;80(6):1816-27.
31. Horckmans M, Ring L, Duchene J, Santovito D, Schloss MJ, Drechsler M, et al. Neutrophils orchestrate post-myocardial infarction healing by polarizing macrophages towards a reparative phenotype. *Eur Heart J*. 2016.
32. Repert SM, Weaver DR. Coordination of circadian timing in mammals. *Nature*. 2002;418(6901):935-41.
33. Moreno-Risueno MA, Benfey PN. Time-based patterning in development: The role of oscillating gene expression. *Transcription*. 2011;2(3):124-9.
34. Zhang R, Lahens NF, Ballance HI, Hughes ME, Hogenesch JB. A circadian gene expression atlas in mammals: implications for biology and medicine. *Proc Natl Acad Sci U S A*. 2014;111(45):16219-24.
35. Scheiermann C, Kunisaki Y, Lucas D, Chow A, Jang JE, Zhang D, et al. Adrenergic nerves govern circadian leukocyte recruitment to tissues. *Immunity*. 2012;37(2):290-301.
36. Scheiermann C, Kunisaki Y, Frenette PS. Circadian control of the immune system. *Nat Rev Immunol*. 2013;13(3):190-8.
37. Oster H, Challet E, Ott V, Arvat E, de Kloet ER, Dijk DJ, et al. The functional and clinical significance of the 24-h rhythm of circulating glucocorticoids. *Endocr Rev*. 2016;er20151080.
38. Silver AC, Arjona A, Walker WE, Fikrig E. The circadian clock controls toll-like receptor 9-mediated innate and adaptive immunity. *Immunity*. 2012;36(2):251-61.
39. Logan RW, Sarkar DK. Circadian nature of immune function. *Mol Cell Endocrinol*. 2012;349(1):82-90.
40. Hriscu ML. Modulatory factors of circadian phagocytic activity. *Ann N Y Acad Sci*. 2005;1057:403-30.
41. Arjona A, Sarkar DK. Circadian oscillations of clock genes, cytolytic factors, and cytokines in rat NK cells. *J Immunol*. 2005;174(12):7618-24.
42. Sennels HP, Jorgensen HL, Hansen AL, Goetze JP, Fahrenkrug J. Diurnal variation of hematology parameters in healthy young males: the Bispebjerg study of diurnal variations. *Scand J Clin Lab Invest*. 2011;71(7):532-41.

43. Haus E, Smolensky MH. Biologic rhythms in the immune system. *Chronobiol Int*. 1999;16(5):581-622.
44. Lee JE, Edery I. Circadian regulation in the ability of *Drosophila* to combat pathogenic infections. *Curr Biol*. 2008;18(3):195-9.
45. Schmid-Hempel P. Evolutionary ecology of insect immune defenses. *Annu Rev Entomol*. 2005;50:529-51.
46. Mendez-Ferrer S, Lucas D, Battista M, Frenette PS. Haematopoietic stem cell release is regulated by circadian oscillations. *Nature*. 2008;452(7186):442-7.
47. Chen L, Yang G. Recent advances in circadian rhythms in cardiovascular system. *Front Pharmacol*. 2015;6:71.
48. Tofler GH, Brezinski D, Schafer AI, Czeisler CA, Rutherford JD, Willich SN, et al. Concurrent morning increase in platelet aggregability and the risk of myocardial infarction and sudden cardiac death. *N Engl J Med*. 1987;316(24):1514-8.
49. Muller JE, Ludmer PL, Willich SN, Tofler GH, Aylmer G, Klangos I, et al. Circadian variation in the frequency of sudden cardiac death. *Circulation*. 1987;75(1):131-8.
50. Muller JE, Tofler GH, Willich SN, Stone PH. Circadian variation of cardiovascular disease and sympathetic activity. *J Cardiovasc Pharmacol*. 1987;10 Suppl 2:S104-9; discussion S10-1.
51. Suarez-Barrientos A, Lopez-Romero P, Vivas D, Castro-Ferreira F, Nunez-Gil I, Franco E, et al. Circadian variations of infarct size in acute myocardial infarction. *Heart*. 2011;97(12):970-6.
52. Fournier S, Eeckhout E, Mangiacapra F, Trana C, Lauriers N, Beggah AT, et al. Circadian variations of ischemic burden among patients with myocardial infarction undergoing primary percutaneous coronary intervention. *Am Heart J*. 2012;163(2):208-13.
53. Reiter R, Swingen C, Moore L, Henry TD, Traverse JH. Circadian dependence of infarct size and left ventricular function after ST elevation myocardial infarction. *Circulation research*. 2012;110(1):105-10.
54. Castanon-Cervantes O, Wu M, Ehlen JC, Paul K, Gamble KL, Johnson RL, et al. Dysregulation of inflammatory responses by chronic circadian disruption. *J Immunol*. 2010;185(10):5796-805.
55. Feigin RD, San Joaquin VH, Haymond MW, Wyatt RG. Daily periodicity of susceptibility of mice to pneumococcal infection. *Nature*. 1969;224(5217):379-80.
56. Gibbs JE, Blaikley J, Beesley S, Matthews L, Simpson KD, Boyce SH, et al. The nuclear receptor REV-ERBalpha mediates circadian regulation of innate immunity through selective regulation of inflammatory cytokines. *Proc Natl Acad Sci U S A*. 2012;109(2):582-7.
57. Durgan DJ, Pulinkunnil T, Villegas-Montoya C, Garvey ME, Frangogiannis NG, Michael LH, et al. Short communication: ischemia/reperfusion tolerance is time-of-day-dependent: mediation by the cardiomyocyte circadian clock. *Circulation research*. 2010;106(3):546-50.
58. Schloss MJ, Horckmans M, Nitz K, Duchene J, Drechsler M, Bidzhekov K, et al. The time-of-day of myocardial infarction onset affects healing through oscillations in cardiac neutrophil recruitment. *EMBO Mol Med*. 2016;8(8):937-48.
59. Swirski FK, Nahrendorf M. Leukocyte behavior in atherosclerosis, myocardial infarction, and heart failure. *Science*. 2013;339(6116):161-6.

8. Danksagung

Ich möchte mich herzlich bei meiner Doktormutter, Frau Professor Dr. rer. nat. Sabine Steffens, für die Überlassung des Themas, die persönliche Betreuung und die intensive Unterstützung bedanken. Herrn Dr. Michael Horckmans (PhD) möchte ich für die Ausbildung in den verschiedenen wissenschaftlichen Methoden danken. Mein Dank gilt auch Frau Dr. rer. nat. Katrin Nitz und Herrn Dr. Johan Duchene (PhD), die Ihr exzellentes Fachwissen mit mir teilten.

Ein großer Dank gilt meinen Eltern, die mich während des Studiums und der Promotion immer unterstützt haben.